2018

DIRECT MEASUREMENT OF CROSSTIE-BALLAST INTERFACE PRESSURES USING GRANULAR MATERIAL PRESSURE CELLS

Travis James Watts
University of Kentucky, travis.watts95@gmail.com
Digital Object Identifier: https://doi.org/10.13023/etd.2018.440

STUDENT AGREEMENT:

I represent that my thesis or dissertation and abstract are my original work. Proper attribution has been given to all outside sources. I understand that I am solely responsible for obtaining any needed copyright permissions. I have obtained needed written permission statement(s) from the owner(s) of each third-party copyrighted matter to be included in my work, allowing electronic distribution (if such use is not permitted by the fair use doctrine) which will be submitted to UKnowledge as Additional File.

I hereby grant to The University of Kentucky and its agents the irrevocable, non-exclusive, and royalty-free license to archive and make accessible my work in whole or in part in all forms of media, now or hereafter known. I agree that the document mentioned above may be made available immediately for worldwide access unless an embargo applies.

I retain all other ownership rights to the copyright of my work. I also retain the right to use in future works (such as articles or books) all or part of my work. I understand that I am free to register the copyright to my work.

REVIEW, APPROVAL AND ACCEPTANCE

The document mentioned above has been reviewed and accepted by the student's advisor, on behalf of the advisory committee, and by the Director of Graduate Studies (DGS), on behalf of the program; we verify that this is the final, approved version of the student's thesis including all changes required by the advisory committee. The undersigned agree to abide by the statements above.

Travis James Watts, Student

Dr. Jerry G. Rose, Major Professor

Dr. Timothy Taylor, Director of Graduate Studies

DIRECT MEASUREMENT OF CROSSTIE-BALLAST INTERFACE PRESSURES USING GRANULAR MATERIAL PRESSURE CELLS

THESIS

A thesis submitted in partial fulfillment of the requirements for the degree of Master of Science in Civil Engineering in the College of Engineering at the University of Kentucky

By

Travis James Watts

Nicholasville, KY

Director: Dr. Jerry G. Rose, Professor of Civil Engineering

Lexington, KY

2018

ABSTRACT OF THESIS

DIRECT MEASUREMENT OF CROSSTIE-BALLAST INTERFACE PRESSURES USING GRANULAR MATERIAL PRESSURE CELLS

The magnitudes and relative pressure distributions transmitted to the crosstie-ballast interface of railroad track significantly influences the subsequent behavior and performance of the overall track structure. If the track structure is not properly designed to distribute the heavy-axle loads of freight cars and locomotives, deficiencies and inherent failures of the crossties, ballast, or underlying support layers can occur, requiring substantial and frequent maintenance activities to achieve requisite track geometrical standards. Incorporating an understanding of the pressure distribution at the crosstie-ballast interface, appropriate designs can be applied to adequately provide a high performing and long-lasting railroad track. Although this can be considered a simple concept, the magnitudes and distributions of pressures at the crosstie-ballast interface have historically proven to be difficult to quantifiably measure and assess over the years.

This document describes the development and application of a method to measure average railroad track crosstie-ballast interfacial pressures using timber crossties and pressure cells specifically designed for granular materials. A procedure was specifically developed for recessing the cells in the bottoms of timber crossties. The validity of the test method was initially verified with a series of laboratory tests. These tests used controlled loads applied to sections of trackbed constructed in specifically designed resilient frames. The prototype trackbed section was intended to simulate typical in-track loading conditions and ballast response.

Cells were subsequently installed at a test site on an NS Railway well-maintained mainline just east of Knoxville, TN. Six successive crossties were fitted with pressure cells at the ballast interface below the rail seat. Pressure cells were also installed at the center of two crossties where the ballast is typically not tamped or consolidated. Trackbed pressures at the crosstie-ballast interface were periodically measured for numerous revenue freight trains during a period of twenty-one months. After raising and surfacing the track, the ballast was permitted to further consolidate under normal train traffic before again measuring pressures. Having the ballast tightly and uniformly compacted under crossties is important to ensuring representative and reproducible pressure measurements.

Measured maximum pressures under the rail at the crosstie-ballast interface ranged from 20 to 30 psi (140 to 210 kPa) for locomotives and loaded freight cars with smooth wheels

producing negligible wheel/rail impacts. Crosstie-ballast interface pressures were typically 3 psi (20 kPa) maximum for empty freight cars with smooth wheels. Heavily loaded articulated intermodal car pressures for shared trucks tended to reach nearly 40 psi (280 kPa), actually higher than locomotive-produced pressures. The recorded pressures under the center of the ties were normally negligible, less than 1 psi (7 kPa) for locomotives and loaded freight cars.

Wheel-Rail force parameters measured by nearby wheel-impact load detectors (WILD) were compared to crosstie-ballast pressure data for the same trains traversing the test site. Increases in peak WILD forces, either due to heavier wheel loads or increased impacts, were determined to relate favorably to increases in recorded trackbed pressures with a power relationship. The ratios between the peak and nominal wheel forces and trackbed pressures also have strong relationships.

KEYWORDS: Granular Material Pressure Cells, Crosstie-Ballast Interface Pressure, Railroad Ballast, Railroad Crossties, Trackbed Pressure, Wheel Impact Load Detector (WILD)

Travis James Watts

November 2018

DIRECT MEASUREMENT OF CROSSTIE-BALLAST INTERFACE PRESSURES USING GRANULAR MATERIAL PRESSURE CELLS

By

Travis James Watts

Dr. Jerry G. Rose

Director of Thesis

Dr. Timothy Taylor

Director of Graduate Studies

ACKNOWLEDGEMENTS

First and foremost, I would like to thank my faculty advisor, Dr. Jerry G. Rose, for the continued support, patience, and for inspiring my interest in the railroad industry. Thank you for sharing your wealth of knowledge and expertise in railway engineering with me.

I would also like to thank Dr. Reginal Souleyrette, Dr. L. Sebastian Bryson, Mr. Floyd Taylor and Dr. Terrance Conners in the Departments of Civil Engineering, Mechanical Engineering and Forestry for their guidance and technical support with this research. I am grateful for the relationships we've developed during my time at the University of Kentucky.

I would also like to acknowledge undergraduate research assistant, Ethan Russell; his patience with spreadsheet data entry is greatly appreciated. My gratitude also goes to graduate research assistant, Macy Purcell, and visiting scholar Qinglie Liu (East China Jiaotong University) for their work in the early stages of this study.

I am very grateful for the financial support I have received in the form of Research/Teaching Assistantships through the Nichols Foundation, CSX Transportation Research Endowments and the UK Graduate School, but I am also very grateful for the support by College of Engineering via the Aubrey Donald May Scholarship during my 1st-year of graduate school. Additional support was provided by the National University Rail Center (NURail), a U.S. DOT OST Tier 1 University Transportation Center. The support for my education, and the research activities I've had the opportunity to be a part of have been led me to have a greater appreciation and understanding of the Civil Engineering

practice. In addition, this work has led to the advancement of technology in the railway industry in regards to dynamic measurement systems.

Additional acknowledgement goes to Norfolk Southern Corporation for their logistical, financial, and technical support during this research study. Mr. Les Hall, Track Supervisor in the Knoxville, TN area, deserves much acknowledgement for his assistance and expertise during the in-track test sequence. Furthermore, I am very grateful for the Maintenance-of-Way internship opportunity that was offered to me during the Summer of 2018.

Above all, I would like to thank my mother, Saundra, and my father, James. You both taught me at an early age to value education and to follow my dreams. Thank you, as well, to my sister, Andrea. Your success in post-secondary education has motivated me to follow the same pursuit. Without the love and support of my family, I would not be where I am today.

TABLE OF CONTENTS

LIST OF TABLES

LIST OF FIGURES

CHAPTER 1. INTRODUCTION

Railroad Track Overview

Railroad Track, in its conventional form, is described as a structure comprised of two steel rails, 56 1/2-inches (1.43 m) apart, supported by timber, concrete, steel, or composite crossties, resting on rock ballast and subballast, which in turn rests on the subgrade (Armstrong, 2008). Figure 1.1 shows the typical cross-section of the conventional railroad track structure described.

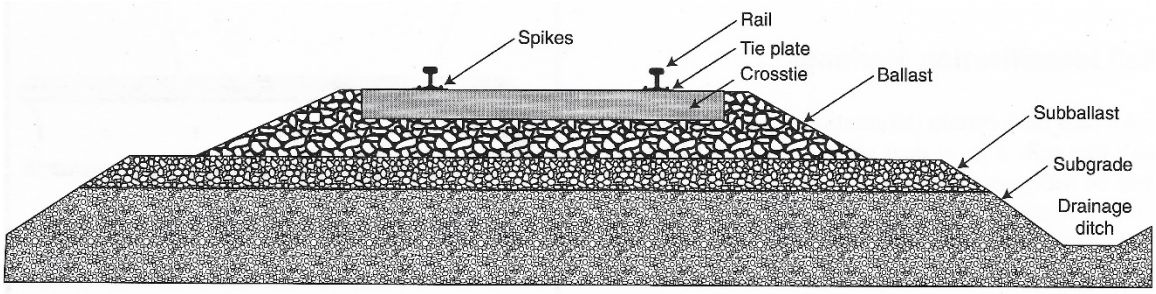

Figure 1.1 Conventional Railroad Track Structure *(REB, 2000)*

Subgrade

No matter the wheel-axle load, or how that load is distributed, the final support structure in railroad track is the subgrade. As for what the subgrade provides to the track structure, the subgrade (Hay, 1982):

1. Bears and distributes loading from the ballast/subballast,
2. Facilitates drainage, and
3. Provides a smooth platform at an established grade for which the ballast, crossties, and rail can be placed.

In order to provide an adequate subgrade for railroad construction, an understanding of the behavior of subgrade soils is essential, as soil is a material with variable composition and performance (Hay, 1982). To determine those properties for a specific soil type, several tests and classification systems are utilized, such as the Unified Soil Classification System (USCS) and compressive/shear tests. The American Railway Engineering and Maintenance-of-Way Association (AREMA) recommends a methodology similar to ASTM D 2487T to classify the predicted performance of a subgrade (AREMA, 2018). With an understanding of the engineering properties of subgrade soils, proper treatment such as lime and/or cement stabilization and mechanical compaction can be used if a weak soil/slope exists. Common soils seen in the subgrade and addressed in the railroad track structure are silts, clays, sand, and gravel (unless shallow bedrock is available).

In addition to the ASTM D 2487T recommendation set by AREMA, there are several other laboratory and in-situ test methods available for determining the strength/behavioral properties of a subgrade soil. Some of the most common laboratory tests are ASTM D2166 (Unconfined Compression Strength Test), ASTM D3080 (Direct Shear), ASTM D1883 (California Bearing Ratio), and ASTM D3999 (Cyclic Triaxial) to name a few. As for in-situ tests, ASTM D1196 (Plate Load Test), ASTM D1586 (Standard Penetration Test), ASTM D3441/D5778 (Cone Penetration Test), and ASTM D4694 (Falling Weight Deflectometer) are very common tests for determining strength and behavioral properties of subgrade soils. Details for each of these testing procedures and several other experimental domestic and international practices can be found in a Kentucky

Transportation Center publication cited at the end of this document (McHenry & Rose, 2012).

Ballast

Similar to the subgrade, the ballast layer is a critical element of the track structure. The railroad term, *ballast*, has been suggested to be a term carried over from the sand and gravel ballast, that was formerly use for stability in cargo ships (Hay, 1982). For the railroad however, ballast refers to permeable, granular materials such as sand, gravel, crushed rock or slag, or cinders placed around and under the crossties to provide track stability. When the use of crossties was first introduced, crossties were positioned directly against the subgrade, but heavy loads led to subgrade failure. The addition of ballast allowed the track to support heavier axle loads, which in turn increased operating efficiency and serviceability.

As for utility, ballast serves the following purposes (Hay, 1982):

1. Transfers and distributes tolerable loading from the crossties to the underlying subballast and subgrade,
2. Provides longitudinal and lateral track support to resist vehicle loading and rail thermal stress,
3. Provides drainage through and away from the track structure,
4. Allows for crosstie and rail adjustment (by the means of tamping, shovel packing, stone blowing, etc.) to achieve proper surface alignment,
5. Prevents the growth of vegetation, and
6. Reduces the occurrence of frost heave.

In order for ballast to perform these functions, ballast should be tough, hard, angular, and resistant to chemical and environmental weathering (Kerr, 2003). Common mainline ballast used today on Class I railroads are typically crushed granite, quartzite, or trap rock. AREMA recommends that ballast should be made in accordance to the sieve analysis described in ASTM C 136 (AREMA, 2018). Figure 1.2 shows typical mainline ballast. Table 1 provides the gradation recommended for railroad ballast.

Figure 1.2 Typical Mainline Ballast

Table 1.1 Recommended Ballast Gradation (AREMA, 2018)

Sieve No.	Nominal Size Square Opening	Percent Passing									
		3”	2 1/2”	2”	1 1/2”	1”	3/4”	1/2”	d”	No.4	No.8
24	2 1/2” - 3/4”	100	90-100		25-60		0-10	0-5	-	-	-
25	2 1/2” - d”	100	80-100	60-85	50-70	25-50	-	5-20	0-10	0-3	-
3	2” - 1”	-	100	95-100	35-70	0-15	-	0-5	-	-	-
4A	2” - 3/4”	-	100	90-100	60-90	10-35	0-10	-	0-3	-	-
4	1 1/2” - 3/4”	-	-	100	90-100	20-55	0-15	-	0-5	-	-
5	1” - d”	-	-	-	100	90-100	40-75	15-35	0-15	0-5	-
57	1” - No.4	-	-	-	100	95-10	-	25-60	-	0-10	0-5

Note: Gradation Numbers 24, 25, 3, 4A, and 4 are main line ballast materials. Gradation Numbers 5 and 57 are yard ballast materials.

1” = 1-inch = 2.54 cm

Although ballast serves as a great material to promote drainage and to discourage frost heave, and inherent limitation occurs when an excess of fine material (< No. 200 sieve) fills the void space within ballast, resulting in the state called “fouled” ballast.

When a ballast layer becomes “fouled”, the performance of that layer is compromised, contributing to the degradation of track geometry, and resulting in the need for additional maintenance. Fouled ballast, as described in the literature, is caused by one of the following sources (Hay, 1982):

1. External Intrusion, by the means of wind-blown particles and locomotive sanders,
2. Subgrade Intrusion, and
3. Internal Abrasion and Weathering.

Typical maintenance practices used to address this issue include track undercutting, shoulder cleaning, sledding, and plowing which assist in providing a cleaner and more stable ballast layer. Figure 1.3 shows an example of typical fouled ballast.

Figure 1.3 Example of Fouled Ballast

In order to schedule and prioritize maintenance practices, fouling can be measured by quantifying the amount of fine material (smaller than a specified grain size) present in

a particular volume of ballast. A typical relationship used to quantify the amount of fouling is presented in Selig and Water (1994), defined as the Fouling Index (FI):

$$FI = (\%\ Passing\ No.4\ Sieve) + (\%\ Passing\ No.200\ Sieve)$$

Equation 1.1 Fouling Index (Selig and Waters, 1994)

With a higher fouling index, a greater need for maintenance to address fouling is indicated. Fouled ballast is typically attributed to 17-34% fine material passing the No. sieve, and 40-50% passing the No. 200 sieve. This corresponds to a Fouling Index between 20 and 40 (Selig & Waters, 1994).

Crossties

The crosstie, or tie (also referred to as a sleeper outside of the US), is typically a 9-inch by 7-inch (22.9 cm by 17.9 cm) (width and thickness) by 102-inch (259.1 cm) (length) rectangular structure fastened to the rail, which interfaces the rail and ballast. In addition, the crosstie serves the following purposes (Hay, 1982):

1. Secures two lines of rail transversely, holding the desired gage,
2. Transmits a reduced pressure to the ballast layer below, and
3. Restricts the movement of the rail in the lateral, longitudinal and vertical directions.

Common materials used for crossties include wood (timber), concrete, steel, and composite materials. In the United States however, timber and concrete crossties make up the majority of crossties in service. AREMA recommends species such as oaks, maples, spruces, and ashes that do not have defects that would compromise the strength of the timber tie. As for the concrete tie, a 28-day compressive strength of 7,000 psi, determined

by the methodology explained in ASTM C 39 is recommended. Metal and wire strand reinforcement within concrete ties should adhere to ASTM A 416 or ASTM A 886, and ASTM 421 (AREMA, 2018). Although not commonly used on mainline track, steel crossties are also used, but utilized mostly in a non-signalized track, such as yard tracks. AREMA presents guidelines for the minimum characteristics for proper steel crosstie performance in Chapter 30, Part 6 of the Manual for Railway Engineering. Figure 1.4 shows the typical types and dimensions of crossties used in the United States.

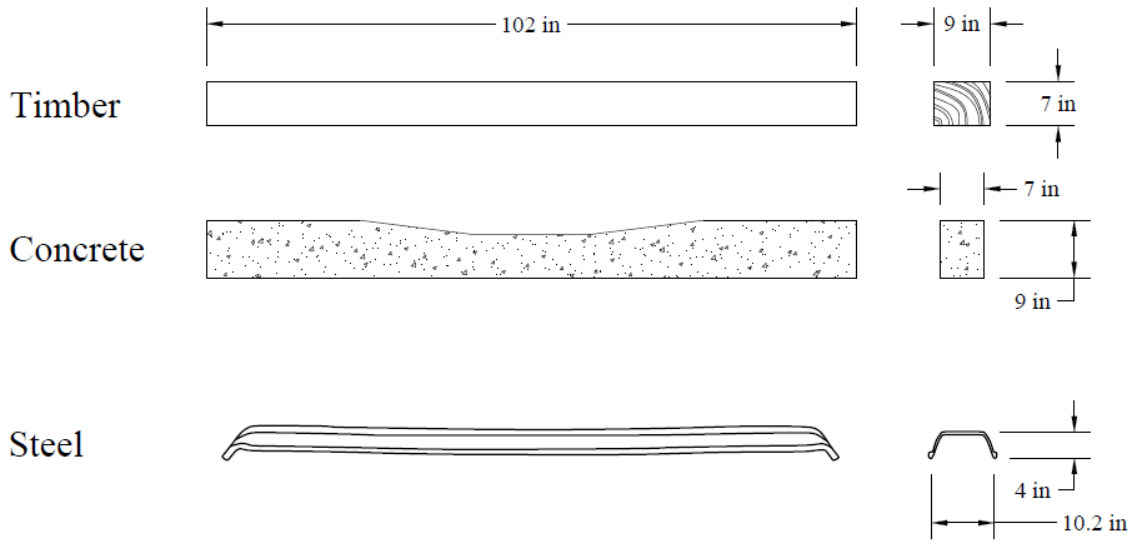

Figure 1.4 Typical Crossties in the United States

Composite crossties are also becoming a more viable and attractive substitute based on their improved life-cycle cost and mechanical properties. Although not commonly used by Class 1 Freight Railroads, the United States Army Corps of Engineers (USACE) and several Transit Agencies (e.g. Chicago Transit Authority (CTA)) have deployed and experimented with composites in recent years, particularly in special trackwork (Lampo, 2014). AREMA has guidelines for the minimum performance properties that composite crossties must adhere to in Chapter 30, Part 5 of the Manual for Railway Engineering.

Although crossties provide exceptional support, timber crossties can fail over time due to decay and service wear. Typical actions to prevent these two failure modes include preservation treatment of the crossties, by the use of either creosote or copper naphthenate, and tamping/surfacing (T&S) of the ballast. In particular interest to this study, service wear, in regards to the effect of center binding(cracking) failure of a crosstie over time will be addressed. Center-binding is a result of excessive negative bending of the crosstie at or near the centerline of the track due to the lack of support at each end of the crosstie (shown in Figure 1.5a). To prevent center-binding from occurring, maintenance-of-way crews can typically tamp the track to provide more support at each rail seat. Consequently however, instead of failing in negative bending, the crosstie can then fail due to positive flexural cracking (as shown in Figure 1.5b) after maintenance has been performed. This phenomenon is described as “end-bounding” a crosstie (Hay, 1982). Although not common, concrete crossties have been known to be prone to this type of rail seat failure in addition to typical rail seat abrasion.

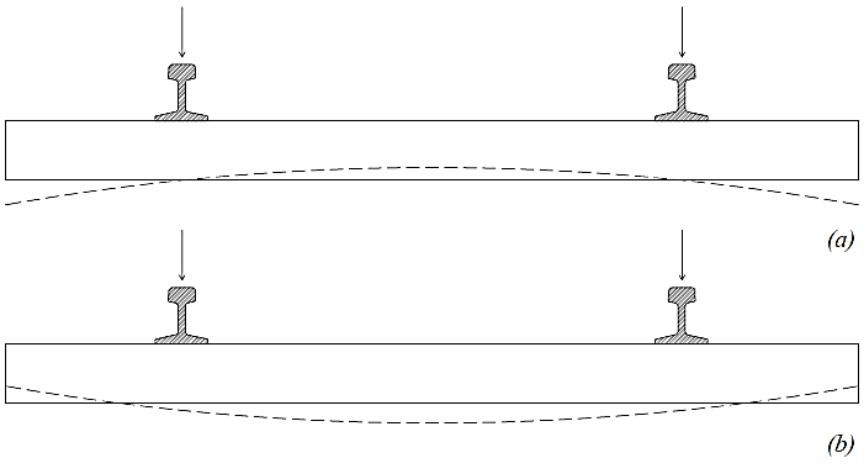

Figure 1.5 Crosstie Failure Mode (similar to Hay, 1982)

Crosstie-Ballast Interface

Within the track structure, there are several critical areas/interfaces of concern addressed by designers of railroad facilities. Those being the interface between the wheel and the rail to reduce impacts, the interface between the rail and the crosstie to protect against mechanical wear, the interface between the crosstie and the ballast to provide track stability and structural support, and the interface between the ballast/subballast and the subgrade to prevent subgrade failure. Each interface requires particular attention to perform adequately. This study in particular will focus on the vital interface located between the bottom of the crosstie and the top of the ballast, referred to as the crosstie-ballast interface. As alluded to previously, the crosstie-ballast interface serves an important role within the track structure. Specifically, the crosstie-ballast interface serves the following purposes (McHenry M. T., 2013):

1. Transmits a reduced distribution of pressure through the ballast layer,
2. Allows for adjustment of track geometry, and
3. Provides frictional resistance for lateral and longitudinal movement.

For this interface to serve its intended purpose, the proper physical characterization and structural behavior of the crosstie and the ballast, described previously, must be adhered to. In addition to material properties, the levelness and surface contact between the ballast and the crosstie can significantly change the loads/pressures exhibited at the crosstie-ballast interface. With low contact and resulting high pressures between the crosstie and ballast, ballast particle breakage, ballast fouling, differential track settlement, and tie failure can occur.

Significance of Directly Measuring Crosstie-Ballast Pressure

With increasing traffic and axle loads, rail transportation is becoming an increasingly economical and attractive mode of transport. As a result, rail traffic has increased substantially in recent years, specifically in the intermodal market. With increased traffic and axle loads however, high quality and low maintenance railroad track structures are becoming more essential to deter accelerated track degradation.

Just like any other product or component, failure in the track structure occurs when it experiences loads that it cannot support properly. To achieve higher performing and low maintenance railways, the behavior of the track structure and the inherent transmission of pressures needs to be measured. A thorough understanding of the pressures exhibited at the crosstie-ballast interface under various support conditions is critical to better understand the issues that adversely affect track quality (such as ballast degradation, tie failure, and the loss of track geometry). With this type of understanding, advances in track structure predictive modeling, design, policy making, and maintenance strategies can be enhanced.

Problem Statement

Based on typical design practices, the crosstie-ballast pressure assumed to be present, and designed for is 65 psi for timber crossties and 85 psi for concrete (AREMA, 2018). This assumption is based on a crosstie-ballast contact surface footprint that encompasses two-thirds of the entire crosstie (the outer third of each end of the crosstie). It is also assumed that approximately forty-percent of the wheel load is carried by the tie directly below the wheel load, and that an impact factor scales the pressure based on typical speed and wheel diameters (AREMA, 2018). This analysis, however, makes no allowance

for any variations in regard to the transmitted pressures along the effective length of the crosstie, and the early work that proposed this relationship lacked the use of high performing instrumentation and numerical models to validate these assumptions (Talbot, 1940). Furthermore, the data was obtained using jointed rail rather than continuously-welded rail (CWR) used today.

Objectives and Methodology

To update the current standards-of-practice, and to better understand the actual loading conditions and magnitudes of pressure at the crosstie-ballast interface, it is desirable to directly measure these variables in simulated laboratory and in-service trackbeds.

Current technology, namely Geokon Granular Material Pressure Cells, provides a reliable, simple, and durable method to attain these variables at the crosstie-ballast interface. The following objectives have been identified for this research:

1. Develop a methodology to adequately attain consistent crosstie-ballast measurements for in-service revenue train operations,
2. Quantify typical crosstie-ballast pressures for locomotives and various car types,
3. Provide a typical crosstie-ballast pressure distribution based on laboratory and in-service tests,
4. Quantify the effect of wheel imperfection and speed, and
5. Propose recommendations and suggestions for future research and applications of such data.

Content of Thesis

Chapter 2 provides a review of the literature as it pertains to the crosstie-ballast interface. Chapter 3 discusses the theory behind and utility of Granular Material Pressure Cells, and their installation in the track structure. Chapter 4 presents the preliminary calibration procedures performed and results attained in the laboratory by the manufacturer at Geokon and at the University of Kentucky. Chapter 5 discusses the more detailed tests conducted on a laboratory simulated trackbed at the University of Kentucky, specifically in regard to the proposed distribution measured along the total length of a crosstie. In Chapter 6, the in-service track measurement procedures and results are presented and discussed. In Chapter 7, a more detailed analysis of such in-track measurements are presented in regard to correlations with wheel-rail wayside impact measurements, namely the Wheel Impact Load Detector (WILD). Lastly, Chapter 8 summarizes the findings and conclusions from this study, describes data applications, and suggests future research topics. This thesis also includes various appendices containing supplementary material to enhance the readers understanding of the content for each chapter.

CHAPTER 2. LITERATURE REVIEW

A review of the literature affirms the significance of the pressures transmitted from the crosstie to the ballast layer in railroad track. In a study published by the National University Rail Center (NURail) in 2015, the crosstie-ballast interface "impacts many functions of both the tie and the ballast including initiating pressure distribution into the ballast layer, allowing for track geometry adjustments through tamping, and provides vertical, lateral, and longitudinal track stability". In addition, "a better understanding of the fundamental properties [of the crosstie-ballast interface] … can serve as an input to track maintenance planning, ultimately leading to enhanced maintenance strategies and policies" (Rose, et al., 2015).

Previous Pressure Measurement Studies

For several years, studies have been undertaken to determine the pressures exhibited in the track structure. Several of the early studies focused on determining the typical distribution of pressures along the crosstie and their potential transmitted pressures through the ballast layer. These studies were needed so railroad engineers could design more adequate structures, track components, and be able to incorporate such information into industry recommended practices. Although impressive in its time, many of those studies utilized instrumentation far outdated compared to current technology. The following review will outline those early studies to determine track stresses, but also include more recent studies that provide insight into new stress measuring technology.

Early Track Structure Pressure Research

As chairman of the Special Committee on Stresses in Railroad Track from 1918-1940 for the American Railroad Engineering Association (AREA), A.N. Talbot is credited with much of the early technical work published that brought forth insight into the behavior and variations of stresses in the track structure. Of the four progress reports Talbot and his committee published during that time period, the first and second reports prove to be of particular interest to this study. Specifically, in the Second Progress Report Talbot discusses the challenges faced by his committee in regard to properly and accurately measuring pressures at the crosstie-ballast interface. Talbot explains the inherent issues of variable support conditions from one crosstie to the next, which ultimately has a significant effect on measurement results. He also cites the measurement problems induced by the installation of the instrumentation under the crossties, and the excessive amount of pressure capsule instruments needed to cover the effective length of the crosstie. All of which inhibited his committee from directly measuring the stresses exhibited at the crosstie-ballast interface (Talbot, 1940).

Although Talbot cites numerous instruments used to measure trackbed stresses, the device referenced to be the most accurate in this early study was of the pressure capsule variety. These pressure capsules used a method of measuring the elastic deflection in the center of a thin harden steel diaphragm with a micrometer, this micrometer reading in turn was converted to a pressure from the material properties of the harden steel and the active area of the pressure capsule. In this case, the active area was 5 square inches (32.3 cm^2). These pressure capsules were also favored because they required little to no calibration or correction factors to induce a zero reading before an installation or test. This is because the

micrometer could be re-set for each subsequent test (Talbot, 1940). A schematic of the pressure capsules and their installed locations are shown in Figure 2.1.

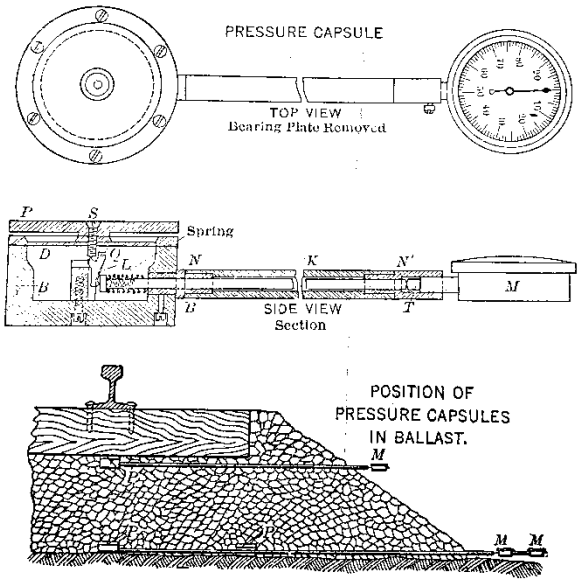

Figure 2.1 A.N Talbot Pressure Capsule *(Talbot, 1940)*

Talbot also discusses two of the various other devices attempted during this study. One such device was a similar capsule to the one shown in Figure 2.1, but was filled with water. The capsule measured the amount of pressure transmitted to the device by the amount of water forced out of the capsule into a small tube connected to the capsule. This device proved to be unreliable however, because of the effect of temperature on the water (Talbot, 1940). The other device used that Talbot discusses was a capsule that measured deflections with a spring beneath the cover of the instrument. However, the stiffness of the spring was not sensitive enough for this study. Talbot also discusses the attempt in using electrical conductivity produced in various materials under specific pressures, but mentions that unreliable results were produced (Talbot, 1940).

Although Talbot mentions the pressure capsule(s) used in this study, an indirect method was eventually used to derive crosstie-ballast pressures due to the variability in measured results. This was done by measuring the flexural curves of the ties under load. With the load relationship between flexure and the bending moment, the stress distributions could be obtained (Talbot, 1940). The higher the bending moment, the higher the stress would be at the crosstie-ballast interface. Although true, Talbot points out that the stresses at the crosstie-ballast interface are directly dependent on the conditions to which the crosstie is subjected. Unevenness of the ballast, in particular, can increase the intensity of the bearing pressure at various points along the crosstie, which also induces additional bending stress in the crosstie at those specific points (Talbot, 1940). For this specific reason, Talbot presents a series of hypothetical distributions of bearing pressure on the ballast along the effective length of the crosstie (shown in Figure 2.2). For each distribution, Talbot provides descriptions for the situations that would cause each distribution.

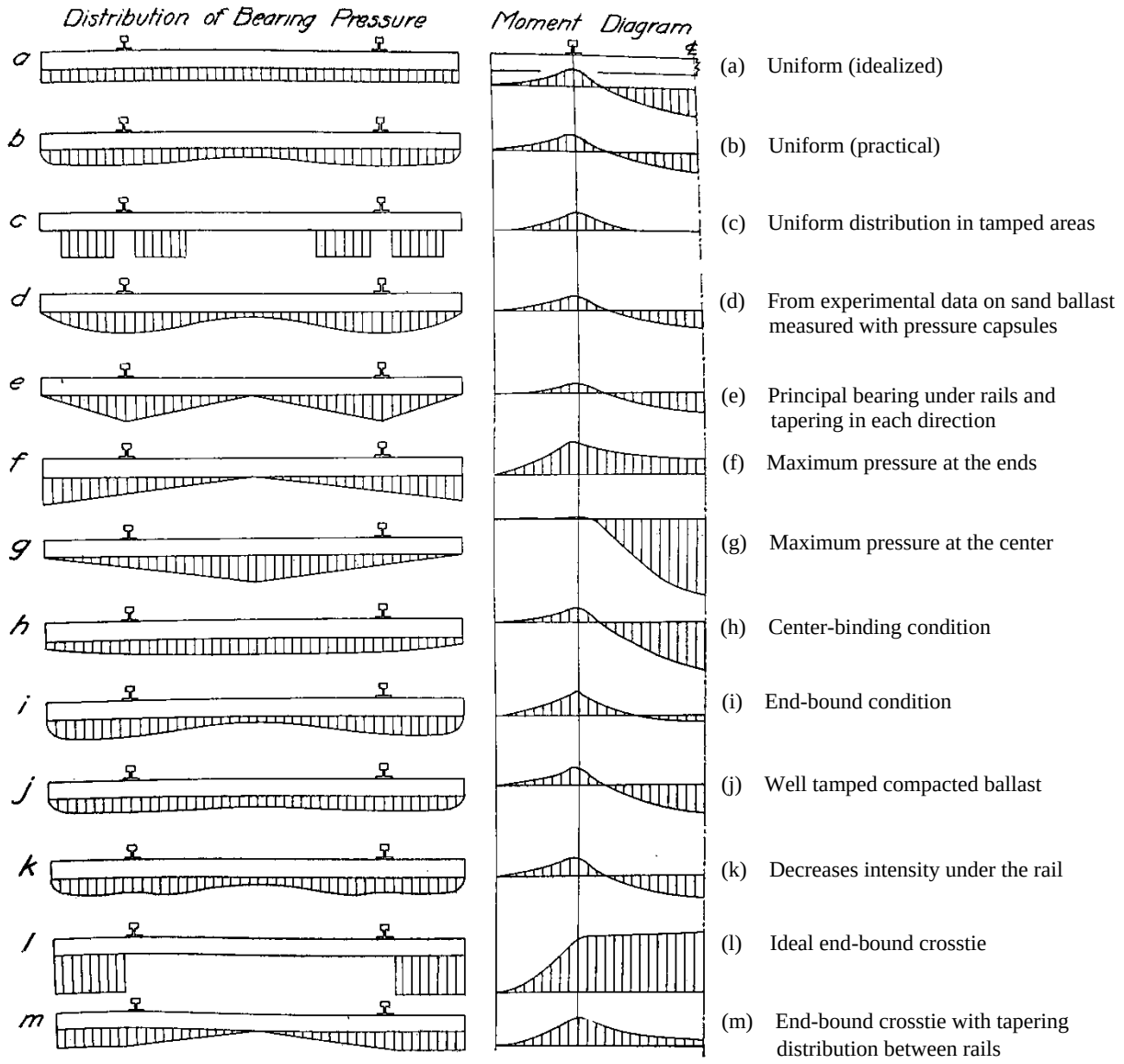

Figure 2.2 Hypothetical Distribution of Bearing Pressure and Corresponding Moment Diagrams at the Crosstie-Ballast Interface *(Talbot, 1940)*

Considering the fact that direct measurements of typical in-service crosstie-ballast interface pressures were not consistently feasible, Talbot and his committee later discuss the tests conducted in the laboratory at the University of Illinois to quantify the pressures transmitted to the subgrade from the ballast later (Talbot, 1940). Capsules were once again used, and were positioned in the track structure (at labeled location P) as shown in Figure 2.3.

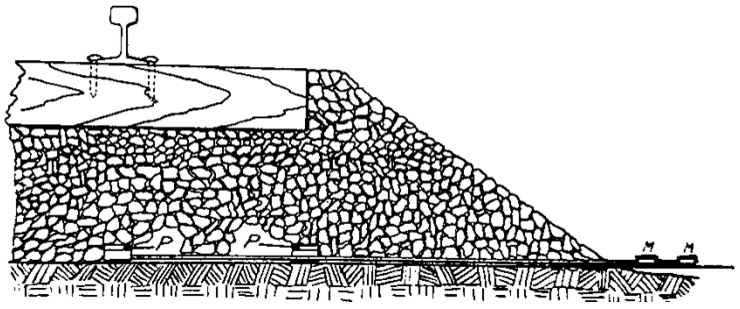

Figure 2.3 A.N. Talbot Subgrade Test Schematic *(Talbot, 1940)*

At this location in the track structure, Talbot and his committee discovered that less variability, less intense stresses, and more consistent behavior between the ballast and subgrade were apparent. As a result, more consistent results could and were measured with the pressure capsules described previously. Due to the success of their instrumentation at this interface, Talbot was able to propose the following relationship for the pressure transmitted to the subgrade, at the centerline of the track, with a specific depth of ballast.

$$p_c = \frac{16.8 p_a}{h^{1.25}}$$

Equation 2.1 A.N. Talbot Relationship for Subgrade Pressure *(Talbot, 1940)*

In Equation 2.1, p_c represents the pressure at the ballast-subgrade interface, h represents the thickness of the ballast layer, and p_a represents the pressure calculated at the crosstie-ballast interface. Although very useful for design practices, this relationship is based on the assumed crosstie-ballast pressure, p_a, that Talbot also presents in his series of progress reports (Talbot, 1940). Since direct measurements were inconsistent, the assumption for the crosstie-ballast pressure was based on a uniform support under the crosstie, and only two-thirds of the crosstie carrying load (Hay, 1982). The relationship Talbot presents for this particular interface is shown in Equation 2.2.

$$p_a = \frac{2P}{\left(\frac{2}{3}\right) bL}$$

Equation 2.2 A.N. Talbot Relationship for Crosstie-Ballast Pressure (Hay, 1982)

In Equation 2.2, p_a represents the pressure transmitted from the crosstie to the ballast layer, P represents the wheel load in pounds-force (lbf), b represents the width of the crosstie in inches (in), L represents the total length of the crosstie in inches (in), and 2/3 represents the factor for the assumed load carrying area of the crosstie mentioned previously.

This assumption however is not entirely valid, knowing the variation of support conditions cited previously in Talbot's progress reports. Thus, a need for adequate instrumentation and measurement procedures is still needed to this day, 100-years after the first progress report was published.

In an attempt to improve the pressure capsules used in the Talbot study, a study was conducted at the University of Illinois in 1966, which used a strain gauge type of pressure capsules in a statically loaded laboratory environment (Salem, 1966). Although improvement in technology had been made, the scope of the work primarily focused on determining adequate ballast depth to provide uniform distribution along the ballast-subgrade interface. Thus, the relationship is that ballast depth for uniform ballast-subgrade stress distribution is typically the tie-spacing minus three-inches (Salem, 1966). An example used described the use of eighteen-inches of ballast for twenty-one-inch crosstie spacing, compared to twenty-four-inches of ballast needed for the same spacing using the Talbot relationship. This study also found that for all cases tested, the maximum pressure

transmitted to the subgrade and within the ballast layer never exceeded the estimates presented by Talbot. Thus, the use of the Talbot relationship would be too conservative. Unfortunately, throughout this study, there was no attempt to directly measure the pressures transmitted to the ballast by the crosstie. Until more recently, there seems to have been no attempt to measure this interface since the AREA Special Committee's work back in the early 1900's. Before those more recent studies are discussed, a review of the most commonly used practices will be presented.

American Railway Engineering and Maintenance of Way Association (AREMA) Recommended Practice

The American Railway Engineering and Maintenance-of-Way Association's (AREMA) Manual for Railway Engineering serves as the most current and primary guide that many Railroad Maintainers and Engineers use for day-to-day practice. Of particular interest to this study, Chapter 1, Part 2 – Ballast, and Chapter 30 – Ties outlines the current practice for describing and designing the interaction between the crosstie and the ballast.

The relationship presented in Equation 2.3 is the current practice used by AREMA (Ch. 30, Article 1.3.6.1), but instead of the two-third footprint assumed in the Talbot procedure and in the Hay text, this relationship assumes an average pressure for the entire tie footprint. This is because AREMA acknowledges that crosstie to ballast pressures are not typically uniformly distributed along the bottom of the crosstie.

$$Average\ Ballast\ Pressure\ (ABP) = \frac{\left[2P\left(1+\frac{IF}{100}\right)\left(\frac{DF}{100}\right)\right]}{A}$$

Equation 2.3 AREMA Relationship for Ballast Pressure

In Equation 2.3, P represents the nominal Wheel Load in Pounds-force (lbf), IF, which also equals 33V/100D, represents the Impact Factor intended to estimate the dynamic forces due to wheel irregularities, V represents the known Velocity in miles-per-hour (mph), D represents the nominal Wheel Diameter in inches (in), DF represents the Distribution Factor in percent (%), and A represents the Contact area of the crosstie.

In regards to the distribution factor presented in Equation 2.3, AREMA estimates that variable by relationships of varying degrees of track modulus, crosstie type, and crosstie spacing. Figure 2.4 presents one such conventional relationship cited in the AREMA standards that provides the distribution factor needs for Equation 2.3.

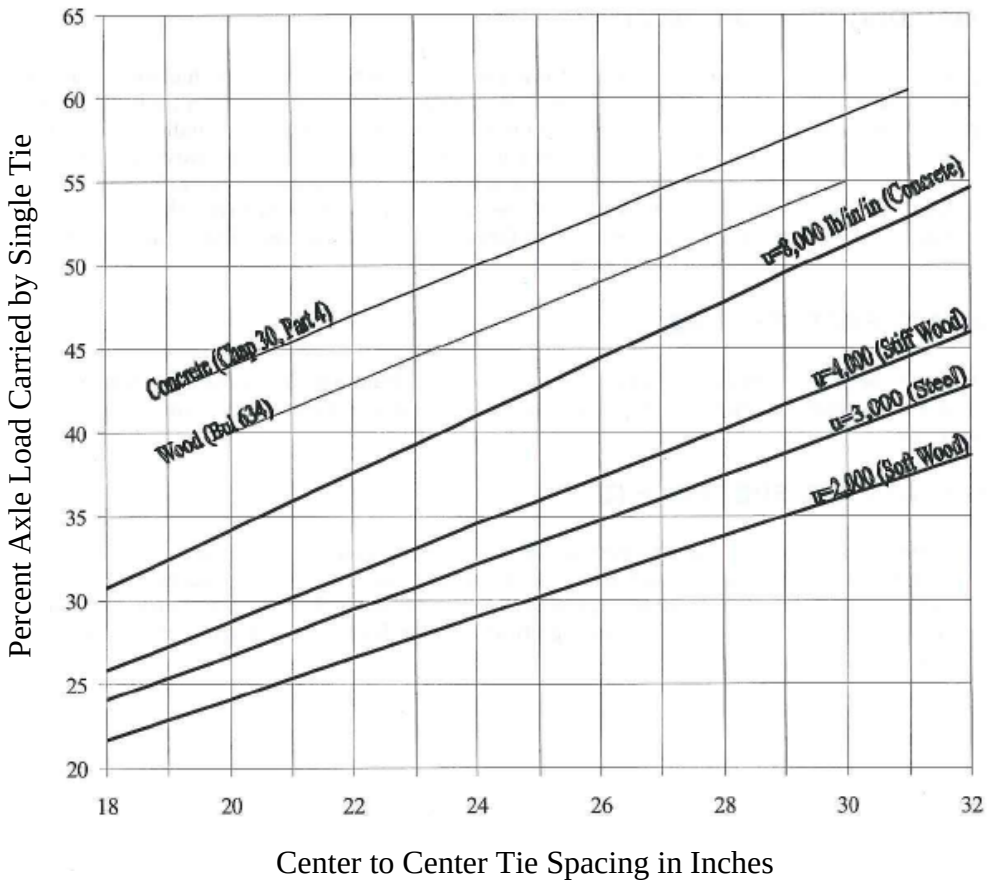

Figure 2.4 AREMA's Estimated Distribution of Loads (AREMA, 2018)

Interestingly enough however, Article 1.3.6.1 notes that there are differing methods presented in this AREMA manual for determining the area, A, used in Equation 2.3. In Chapter 30, which was just discussed, the bearing area of the crosstie appears to be the entire footprint of the crosstie. However, in Chapter 16, Part 10, Article 10.11.1, the bearing area of the crosstie is only defined as two-thirds of the crosstie footprint (as shown in Figure 2.5).

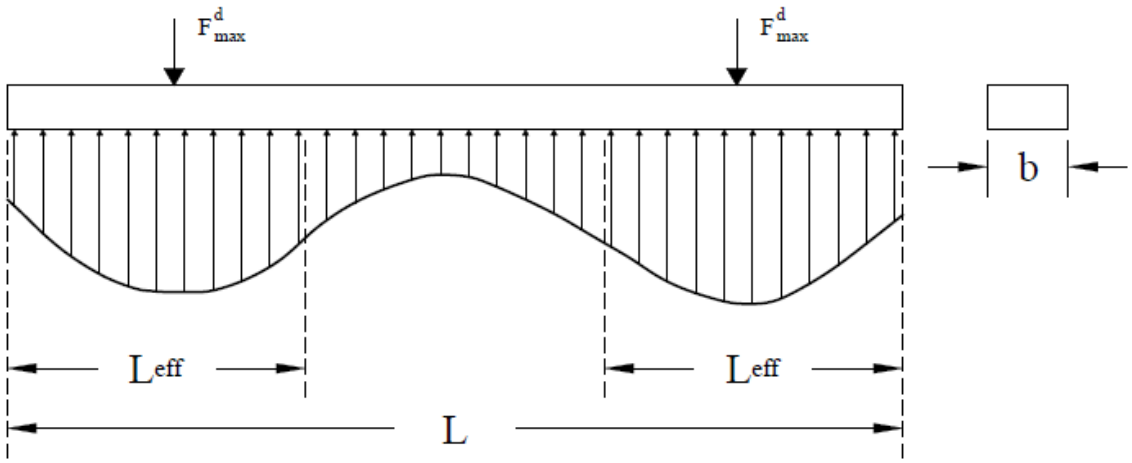

Figure 2.5 Two-Thirds Assumed Crosstie Footprint (similar to Kerr, 1989 and AREMA, 2009)

It is presumed that the two-thirds crosstie footprint cited in Chapter 16 was developed for new construction of track, whereas the recommendation for the entire tie footprint is better suited for existing track. If you consider all of the same properties, such as wheel load, tie spacing, etc., the pressure limit from Chapter 16's recommendation is effectively 50% of what would be considered a crosstie-ballast pressure limit in Chapter 30. Even with that discrepancy in mind, AREMA still cites an average crosstie-ballast pressure maximum value of 65 psi for timber ties, whereas concrete ties have a limit of 85 psi (AREMA, 2018).

Additional Design Practices & Research Attempts

While AREMA publishes its own recommended practices, several other authors/agencies have published trackbed design supplements and guidelines throughout the years. Some of the most notable being the work published by: British Railways, Japanese National Railway, United States Army Corp of Engineers, G.P Raymond, and Li & Selig.

The British Railway Method (Heath, Shenton, Sparrow, & Waters, 1972), is based on a threshold stress which protects the subgrade from potential shear failure. Based on a particular subgrade modulus, the method provides a chart (Figure 2.6) which guides the designer in selecting a granular material thickness that will support a specific axle load.

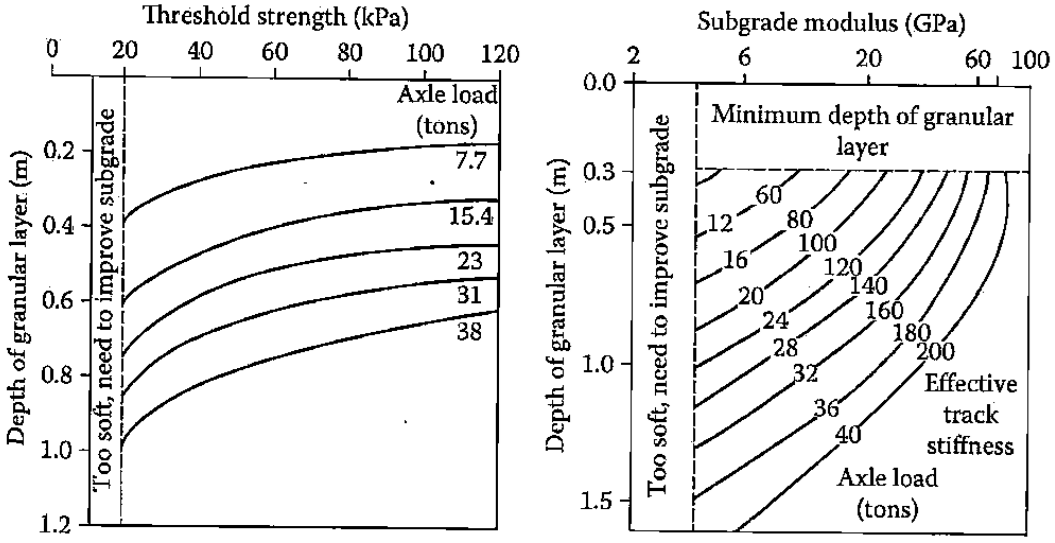

Figure 2.6 British Railway Design Charts *(Heath, Shenton, Sparrow, & Waters, 1972)*

However, it should be noted that the British Railway method assumes a single homogeneous layer encompassing the ballast/subballast and the subgrade. As a result, this

design method often gives very large granular material thicknesses due to the higher modeled stresses on the subgrade. Although this method oversimplifies the soils in the track structure, researchers with the British Railway did provide a basis for how they determined the stress dissipation below the crosstie. Based on the work Shenton presented, researchers actually used a series of pressure cells placed below the bottom of a single crosstie and measured the readings produced by a 200 kN (44. 9 kips) axle load (Heath, Shenton, Sparrow, & Waters, 1972) & (Shenton, 1975). It is unclear what type of pressure cell was used, but based on the distribution shown in Figure 2.7, it seems that a series of very small cells was utilized, similar in size to what was used in A.N. Talbot's work. As can be seen though, the results are very erratic and vary greatly from test to test. Although erratic, the method utilizes the maximum field measurement directly below the rail seat, which is in the range of 250-300 kPa (36-44 psi).

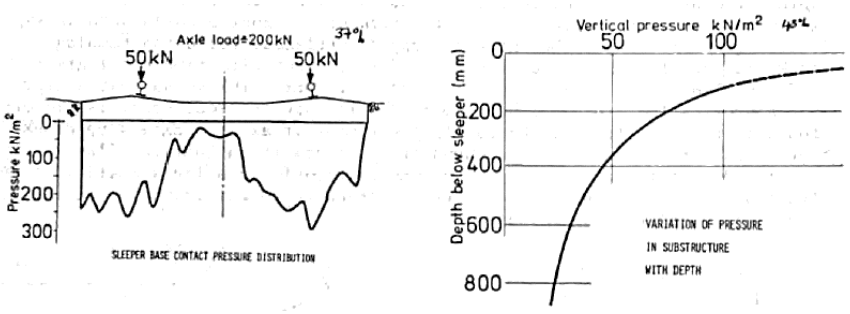

Figure 2.7 British Railway Sleeper/Ballast Contact Pressure (Shenton, 1975)

The Japanese National Railway (Atalar, Das, Shin, & Kim, 2001) also presents a method which derives the thickness of granular material with the assumption that load is applied to only the outer portions of the crosstie (similar to AREMA). Specifically, the distance from the center of the rail head to the edge of the crosstie is used (shown in Equation 2.4).

$$P_a = \left(\frac{q_r}{2aB}\right) \times F_2 \rightarrow \sigma_{zmax} = \frac{50 \times \sigma_{max}}{10 + h^{1.35}}$$

Equation 2.4 Japanese National Railway Standard

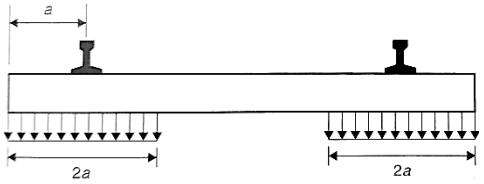

Figure 2.8 Japanese National Railway Load Distribution *(Indraratna, 2011)*

Where: $P_a = \sigma_{max}$ = average crosstie-ballast contact pressure (kPa), q_r = maximum rail seat load (kN), a = distance between the rail head center and the edge of the crosstie (cm), B = width of the crosstie (cm), F_2 = crosstie type/maintenance factor, σ_{zmax} = subgrade stress (kPa), and h = thickness of granular material (cm). It should be noted however that this method was developed for a more narrow-gauge track, thus it is not very applicable to freight railway track in the United States.

In addition to the methods presented earlier, the US Army Corps of Engineers (US Army Corps of Engineers, 2000) also provides guidance for calculating the ballast surface stress and the corresponding ballast depth for their freight operations. This method incorporates differing rail bending moments, tie size, and load coefficient factors taking vehicle dimensions into account, however, it assumes the effective bearing area is uniform across one-half of the crosstie contact surface. Although the distribution of stress is similar to the other methods presented, this assumption results in an even more conservative design.

$$p_m = \frac{q_0}{A_b} \rightarrow h = \frac{\left(50 \times \frac{p_m}{p_c} - 10\right)^{0.74}}{2.54}$$

Equation 2.5 US Army Corps of Engineers Method

Where: h = ballast thickness (in), p_m = ballast surface stress (psi), p_c = subgrade bearing capacity (psi), q_0 = maximum rail seat load (lb.), A_b = effective bearing area of one-half crosstie on ballast (in^2).

G.P. Raymond (Raymond, 1978) and Li & Selig (Li & Selig, 1998) also provide guidance in the form of chart solutions for trackbed design, but primarily focused on preventing shear failure in the subgrade based on cumulative damage, assuming plastic strain (Li, Hyslip, Sussmann, & Chrismer, 2016). Both methods also assume the AREMA recommended threshold for crosstie-ballast pressure to model their stress dissipation for various track conditions.

In India (Mundrey, 2017), some interesting design procedures exist, which are shown in Figures 2.9, and 2.10.

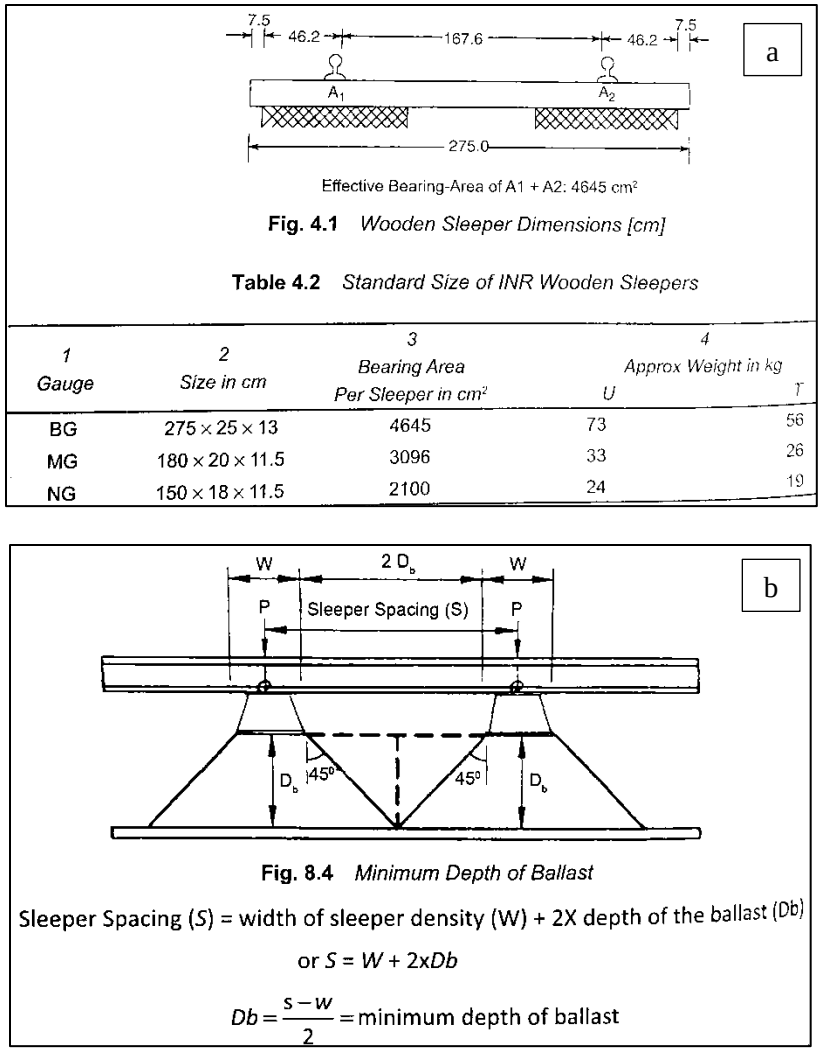

Fig. 4.1 *Wooden Sleeper Dimensions [cm]*

Table 4.2 *Standard Size of INR Wooden Sleepers*

1 Gauge	2 Size in cm	3 Bearing Area Per Sleeper in cm²	4 Approx Weight in kg U	T
BG	275 × 25 × 13	4645	73	56
MG	180 × 20 × 11.5	3096	33	26
NG	150 × 18 × 11.5	2100	24	19

Fig. 8.4 *Minimum Depth of Ballast*

Sleeper Spacing (*S*) = width of sleeper density (W) + 2X depth of the ballast (Db)

or $S = W + 2xDb$

$$Db = \frac{s - w}{2} = \text{minimum depth of ballast}$$

Figure 2.9 a) India Railways Crosstie Bearing Area, b) Minimum Depth of Ballast

In Figure 2.9a, India Railways specify the use of a uniform bearing area that encompasses about 68% of the tie footprint, which is very similar to AREMA. However, the bearing area does not include the outer 7.5 cm (2.9 inch) of the crosstie footprint (Mundrey, 2017). In addition, India Railways specifies different bearing areas for the three unique gauges in that country (Broad (1676 mm, 65.9 inch), Metre (1000 mm, 39.4 inch), and Narrow (762 mm, 30.0 inch)). Each bearing area is presented in Figure 2.9a.

India also has its own procedure for calculating minimum ballast depth, but, unlike AREMA, which bases the ballast depth calculation on the stress transmitted on the ballast and subgrade, India bases their calculation on crosstie spacing and crosstie density, as shown in Figure 2.9b (Mundrey, 2017).

Although a crosstie-ballast stress calculation does not seem to exist for India Railways in the literature, Mundrey does provide a figure (Figure 2.10) that shows the percentage of average pressure within the track structure due to an applied wheel load. The author does not provide any context for what the average stress would be in order to apply these percentages, however, recommended ballast depths are suggested based on gauge classification (≈ 200-300 mm, 8-12 inch).

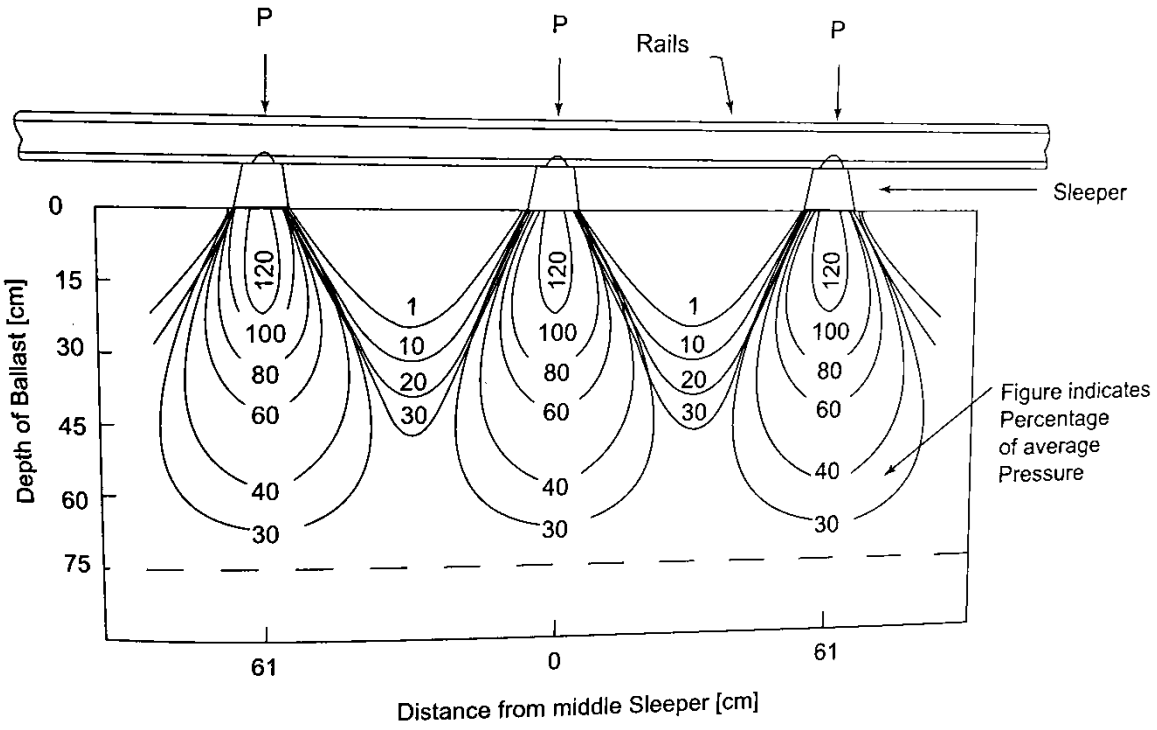

Figure 2.10 India Railways Longitudinal Pressure Distribution (Mundrey, 2017)

As a precautionary note, the methodology described previously for India Railways was based on the details provided by one singular author (Mundrey, 2017). The sources for the original research/work for each design parameter is not provided in this particular text.

Use of Earth Pressure Cells and TEKSCAN in the Early to Mid-2000s

In the early 2000s, several tests were conducted at the University of Kentucky to understand how a Hot-Mix-Asphalt (HMA) underlayments could assist in providing optimal pressure distribution in the track structure. This was achieved by using Geokon Model 3500 Earth Pressure Cells embedded above and below the asphalt mat. The pressure cells consisted of two stainless steel, nine-inch (22.86 cm) diameter cylindrical disks, which are sealed at their periphery and filled with de-aired hydraulic fluid (Walker, 2002). An image of one of the pressure cells used during this study is shown in Figure 2.11.

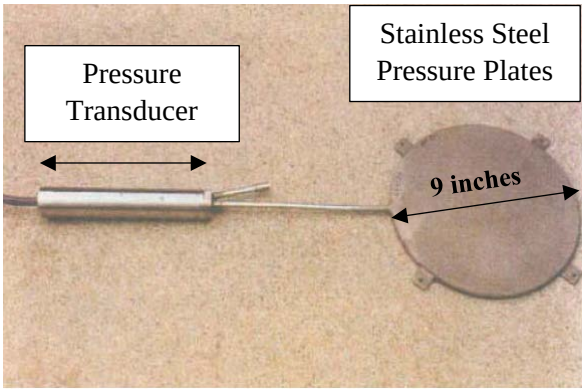

Figure 2.11 Geokon Model 3500 Earth Pressure Cell (Walker, 2002)

As pressure is applied to the pressure cell, the fluid is forced out of a tube connected to the device. The tube contains a pressure transducer, which converts the pressure of the hydraulic fluid to an electrical signal that can be translated by the computer.

A schematic of the typical testing procedure is shown in Figure 2.12.

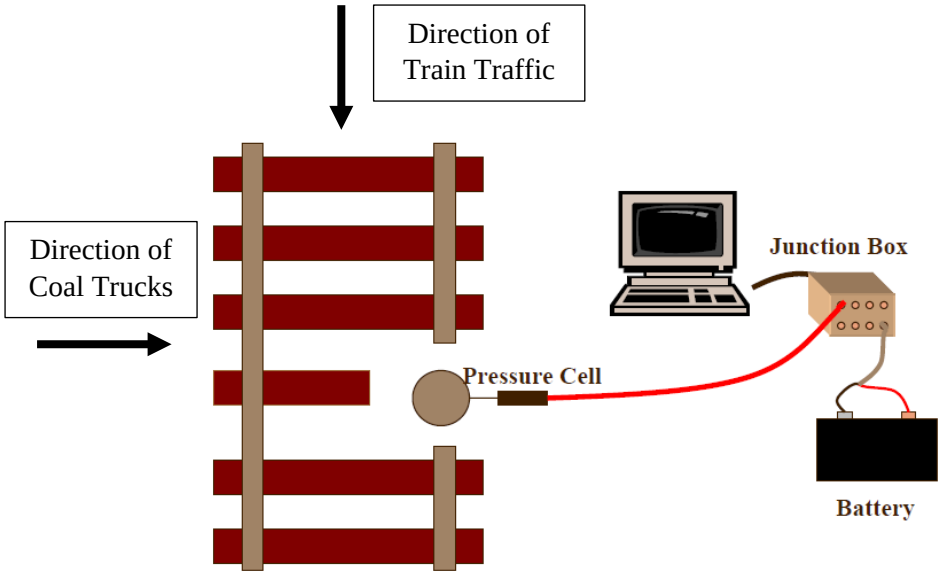

Figure 2.12 Schematic of Earth Pressure Cell Tests (Walker, 2002)

Real-time tests with these devices were conducted on both mainline heavy-haul track, and at highway at-grade crossings. The average axle peak pressure values ranged from approximately 14-17 psi (96-117 kPa) on top of the asphalt layer directly under locomotives and heavily-loaded coal cars. For heavily-loaded coal trucks traversing the same crossing, the maximum pressure transmitted on the asphalt layer was 11 psi (76 kPa) (Walker, 2002). A typical plot of a real-time pressure signature recorded during these series of tests is shown in Figure 2.13.

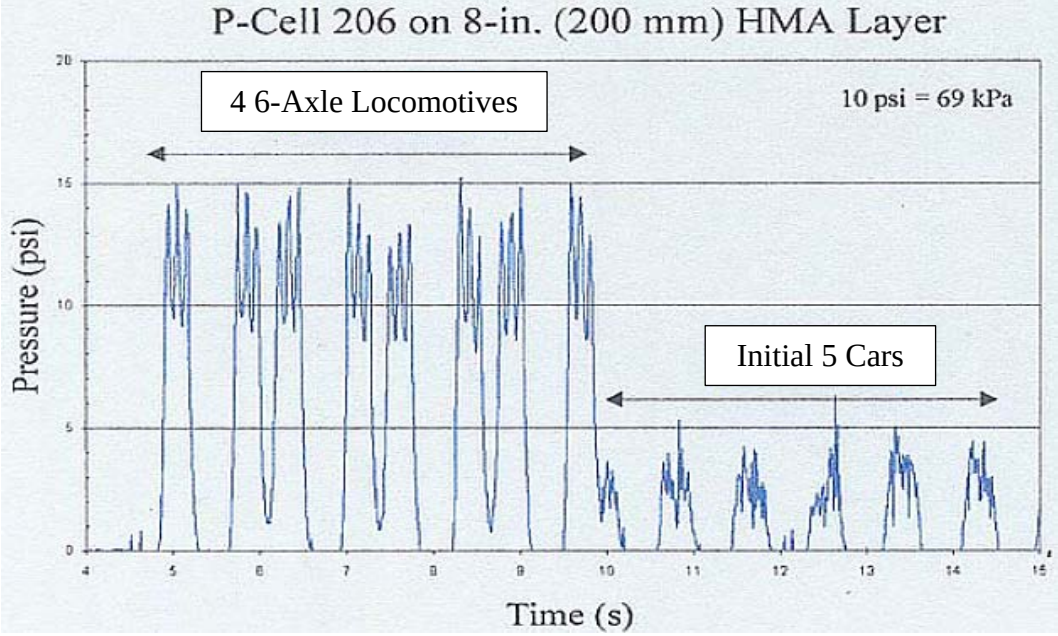

Figure 2.13 Typical Pressure Reading with Asphalt Underlayment (Walker, 2002)

As a result of this study, it was also found that pressure cells installed in the track structure could be used to detect wheel irregularities on trains. The added impact of wheel imperfections was seen to have the potential to increase the wheel load by several magnitudes for locomotives and train cars (Walker, 2002). This particular topic will be addressed further in Chapter 7.

While completing this study in regards to asphalt underlayments, it was discovered that Earth Pressure Cells were not applicable to the loading requirements for measuring pressures in higher regions of the track structure (i.e. crosstie-ballast or rail-tie interface). This was primarily due to the fact that the Earth Pressure Cells used at the time had a maximum recording range of approximately 50 psi (345 kPa), were prone to puncture with angular ballast particles, and could rupture due to high loads transmitted by the rail. Therefore, research was focused on developing a new method to measure higher level

pressures in the rack structure (Stith, 2005), (McHenry M. T., 2013), (Rose, Purcell, & Liu, 2016), & (Liu, Lei, Rose, & Purcell, 2017).

The initial method devised was the use of TEKSCAN, a matrix based sensor consisting of two flexible polyester sheets with silver electrodes printed on them (Stith, 2005). One sheet of the device has a semi-conductive "ink" printed in rows, while the other sheet has "ink" printed in perpendicular columns. By exciting one row and columns at a time, the device system was able to isolate the location of a particular force by measuring the resistivity change through a circuit (Stith, 2005). Figure 2.14 shows a schematic (a) and a photo of these TEKSCAN sensors (b).

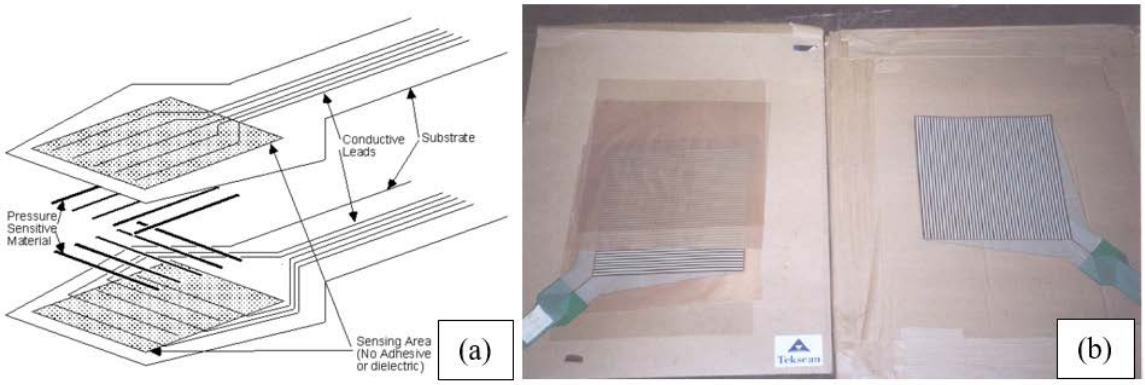

Figure 2.14 TEKSCAN Schematic and Photo (Stith, 2005)

The benefit of using such a device was apparent in the 5250 model sensor of this variety, which had the capacity to read pressures in the magnitude of 1,200 psi (8.3 MPa) (Stith, 2005). This was particularly useful for measuring pressures at the rail-crosstie interface. However, this device had not been used before in the harsh conditions of railroad track. Due to the thin design of the sensor, and the polyester material composition, real concerns of puncture and delamination by shear force were evident. Therefore, two sheets

of Teflon (0.15mm thick) and two sheets of Mylar (0.18mm thick) were used to prevent such damage (Stith, 2005).

After proper protection was provided, several series of calibration test were performed using a static loading universal testing machine to determine accuracy for this application. With just a few adjustments, a near perfect correlation between the applied load and the senor output was recorded ($\approx R^2 = 0.97$). Thus, in-track testing ensued.

In-track testing was performed initially with locomotives in a yard environment at TransKentucky Transportation Inc. (TTI) in Paris, KY. The senor was placed between the bottom of the rail and the top of the crosstie as shown in Figure 2.15.

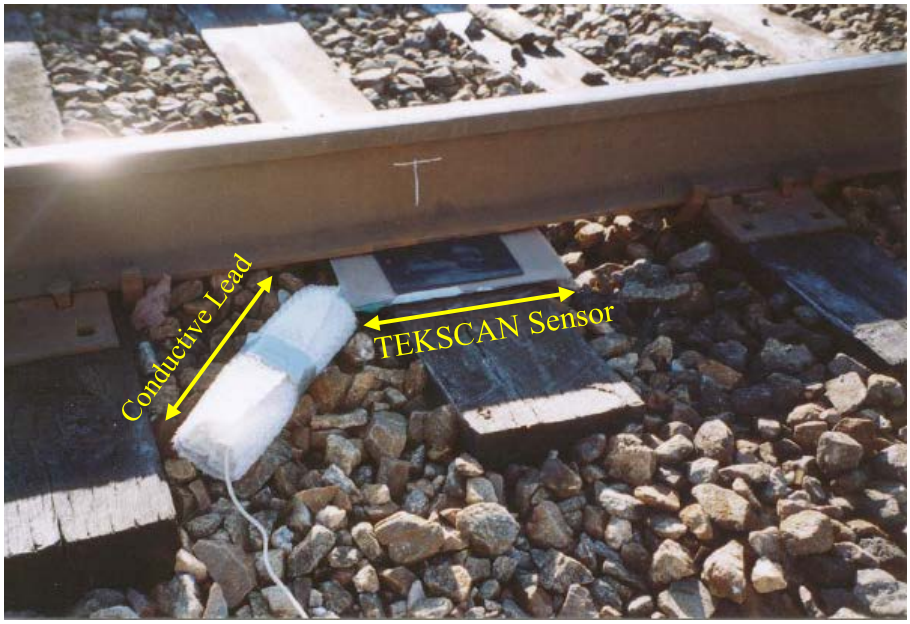

Figure 2.15 TEKSCAN In-Track Installation (Stith, 2005)

After evaluating a few different arrangement methods, the research team was able to successfully record a locomotive traversing the sensor. Based on the success at TTI, the research was then focused on measuring in-service track. This was conducted shortly after

at a site in Conway, KY, which is open to mainline traffic on CSXT. The results of one of those tests is shown in Figure 2.14.

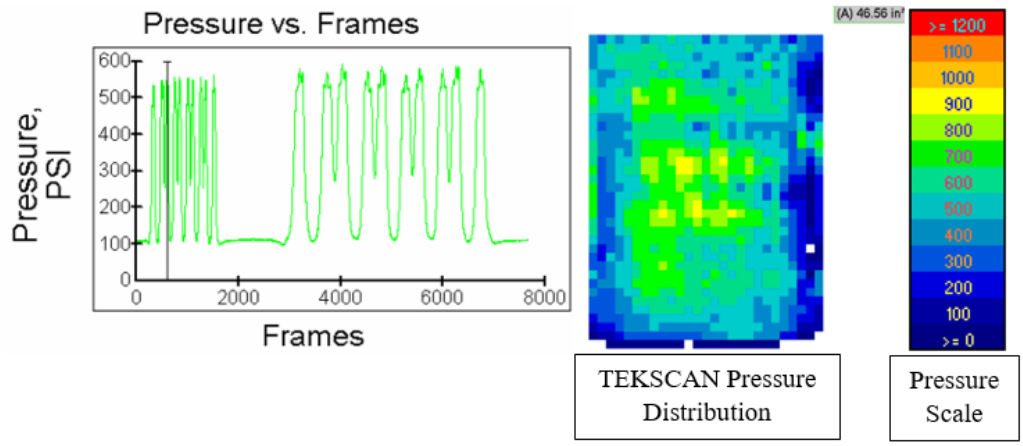

Figure 2.16 TEKSCAN In-Track Results (Stith, 2005)

As shown by example in Figure 2.16, the TEKSCAN measurement system recorded pressures at the rail-crosstie interface ranging from 200-900 psi (1.4-6.2 MPa) in real time signature of the train traversing the test site. As noted in Stith's thesis and corresponding Railway Engineering publication (Rose & Stith, 2004), the distribution of pressures were fairly consistent, and could potentially validate design practices (Stith, 2005).

Too validate the results of this measurement system further, a subsequent study was conducted to measure the contact pressure and patch with regards to the automobile-pavement interaction (Anderson, 2006).

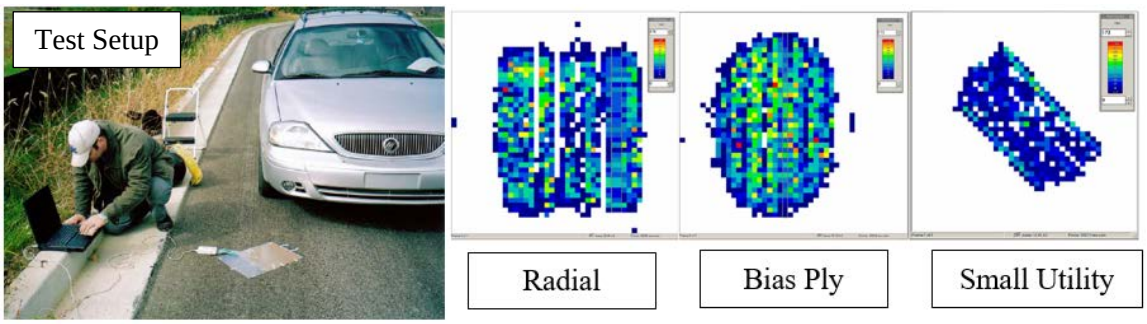

Figure 2.17 Tire-Pavement Interaction - TEKSCAN (Anderson, 2006)

The results of this study indicated that the recorded pressures on average were indeed similar to the pressures corresponding to the tire inflation pressure for cars. The contact patch varied based on the type of tire, which should be expected; verifying the sensors ability to detect the contact area. Based on this research, the results from the rail-crosstie interface could be more comfortably accepted. Furthermore, the results of this validation study brought forth motivation to measure the crosstie-ballast interface.

Recent Matrix Based Tactile Surface Sensor (MBTSS) Studies

After the rail-crosstie interface was studied to validate the TEKSCAN measuring system, the motivation to measure the crosstie-ballast interface ensued. This process is outlined in both a thesis (McHenry M. T., 2013) and a Transportation Research Record (McHenry, Brown, LoPresti, Rose, & Souleyrette, 2015).

Although the same measurement system would be used as in previous studies, a newer approach insured that this type of system could perform properly at an interface of granular material. In this case, it was decided that 3/16-inch (0.48 cm) rubber sheets should be used to protect the sensor (McHenry M. T., 2013). This sheeting would assist in the prevention of puncture and shear action, just as the Teflon and Mylar had previously.

When Stith and Rose (Rose & Stith, 2004) performed calibration tests with a universal testing machine, they were able to place the sensor directly on the crosstie and/or tie plate which proved to have consistent and reliable calibration results. However, during the calibration testing for this study, it was discovered that the re-arrangement of ballast particles under load and the inconsistent contact areas of those particles made calibration difficult under those conditions. Due to those inconsistences, McHenry tried a machined "waffle" plate would be used to consistently control the contact area (McHenry M. T., 2013). The squares on this machined plate were intended to mimic the individual contact points of the ballast surface. Figure 2.18 shows the machine plate with 0.5-inch squares used for the calibration tests and the calibration test setup.

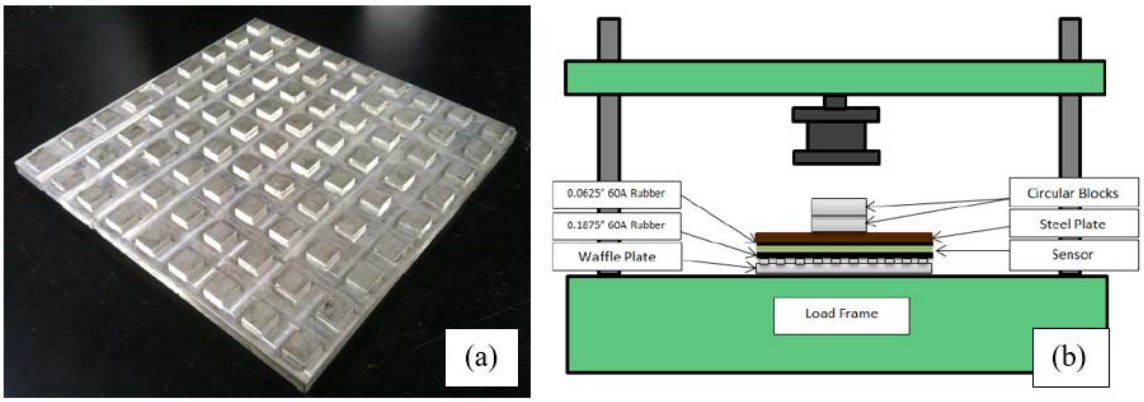

Figure 2.18 MBTSS Calibration for Crosstie-Ballast Interface (McHenry M. T., 2013)

This calibration with the waffle plate was done with respect to the plate being placed directly against the platen of the universal testing machine, and interfaced with a ballast box (as shown in Figure 2.19(a)). Both testing procedures proved to have reasonable and repeatable results. As an interesting note of the McHenry thesis, peak pressure values based on induvial and groupings of ballast particles was analyzed. An example of the shape of those peak pressures can be seen in Figure 2.19 (b).

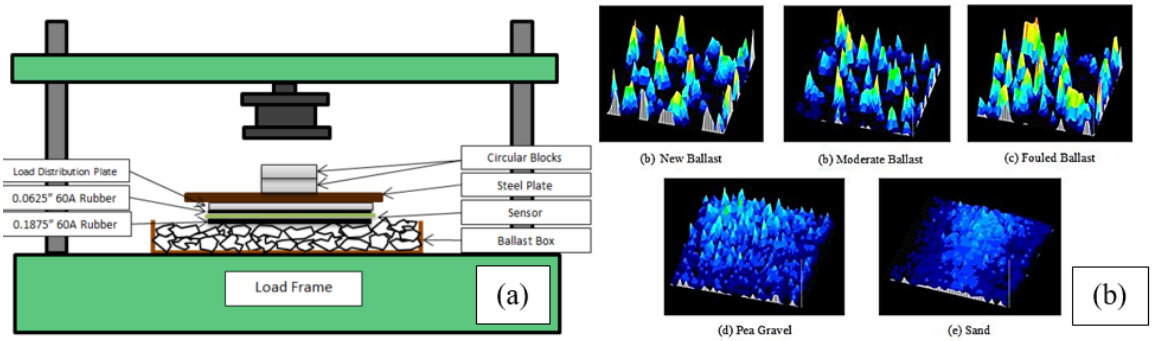

Figure 2.19 MBTSS Ballast Box Calibration (McHenry M. T., 2013)

McHenry explains that based on the calibration tests performed on different ballast materials (shown in Figure 2.19b) with resulting differences in peak pressure signatures, that both the material type, age, geography, and tie type need to taken into consideration when designing and maintaining trackbed structures. Each parameter evoked a certain amount of "roughness" that the author recommends to be considered in practice (McHenry M. T., 2013). After several tests and analytics, McHenry presents the following results for ballast type (shown in Table 3 and Figure 2.20), in terms of peak pressures, and a relationship for what is called the "Ballast-Tie Contact Index" (Equation 2.6).

Table 2.1 Peak and Theoretical Pressures by Ballast Type (McHenry M. T., 2013)

Ballast Material	Average Peak Pressure (psi)	Percent of the Theoretical Uniform Pressure (%)
Sand	283.9	399%
Peak Gravel	444.1	624%
Fouled Ballast	681.3	958%
Moderate Ballast	929.7	1307%
New Ballast	1449.9	2036%

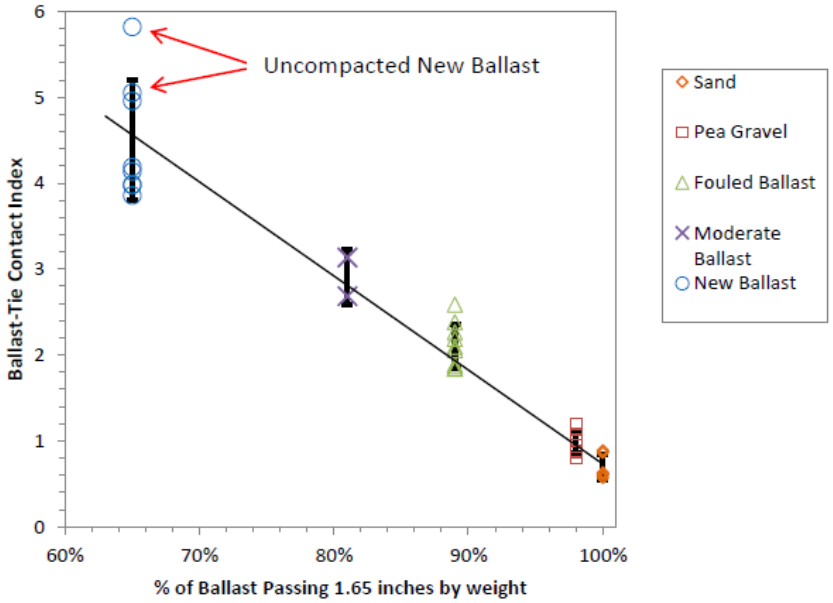

Figure 2.20 McHenry's Peak Pressures and BTCI (McHenry M. T., 2013)

$$BTCI = -11.31\left(\frac{\%\ Passing\ 1.65\ inches}{100}\right) + 12.03$$

Equation 2.6 McHenry's Ballast-Tie Contact Index (BTCI)

Following calibration tests, McHenry continued his work during an internship with TTCI where he was able to perform extensive in-track testing to measure and develop the typical distribution of pressure under a crosstie (as shown in Figure 2.21).

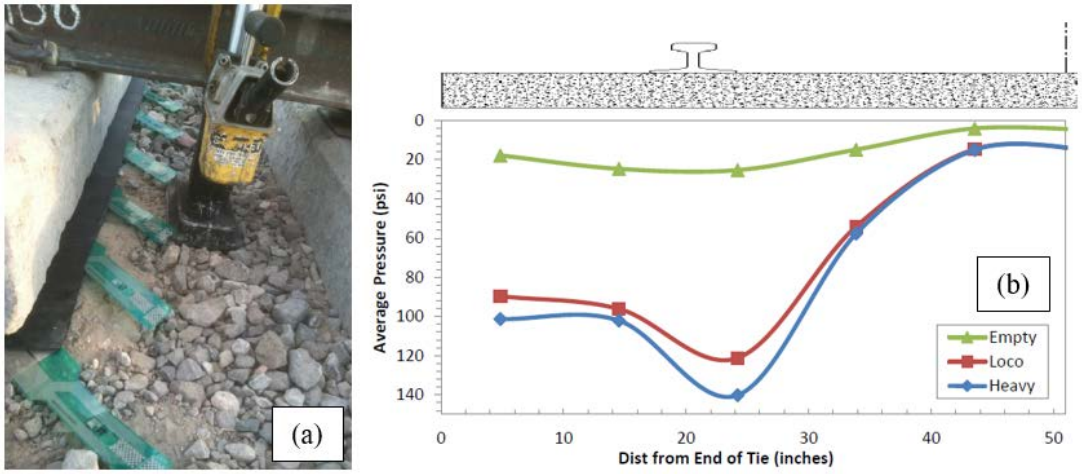

Figure 2.21 McHenry's In-Track work at TTCI (McHenry M. T., 2013)

Based on the results McHenry was able to attain at TTCI, you can see that for a typical wheel load from a locomotive traversing a track, an average pressure of approximately 120-140 psi (0.8-0.96 MPa) can be found at the crosstie-ballast interface, directly below the rail. This is an interesting point to note since the maximum average pressure recommended by AREMA is 85 psi (0.59 MPa) for concrete (analyzed here) and 65 psi (049 MPa) for timber tie track.

McHenry's work brought forth a lot of questions in regards to if changes need to be made to AREMA's Manual for Railway Engineering. As of 2018 however, changes have yet to be made to the AREMA standards. Other than some continued work by the University of Illinois in terms of under-tie pads, TEKSCAN is believed to be completely exhausted in terms of it's abilities. As cited by McHenry, these TEKSCAN sensors had a life-span of on average about 16,000 cycles, which limits it use for any type of continuous measurement study for in-service track. Thus the need for a more durable sensor.

Recent work at the University of Kentucky, 2015-2018

After McHenry completed his work in 2013, a focus on developing a more durable and reliable measurement system for the crosstie-ballast interface began. Surprisingly, this came in the form of pressure cells, similar to what had been used by Rose and Walker in 2002.

Starting in 2015, work was performed to determine if a new model of earth pressure cell was suitable for higher level loading (Rose, Purcell, & Liu, 2016). The Geokon model 3500 earth pressure cell that was used during the early 2000s work was again evaluated after developments in technology allowed the cell to record pressures up to 290 psi (2 MPa). Another, much thicker pressure cell (1-inch (2.54 cm) compared to 0.25-inch (0.635 cm) with the 3500 model) was also evaluated, which shared the same capacity as the 3500 model. These two cells were both tested in a laboratory setting using a similar ballast box procedure as McHenry and Stith explain in their respective thesis reports (shown in Figure 2.22).

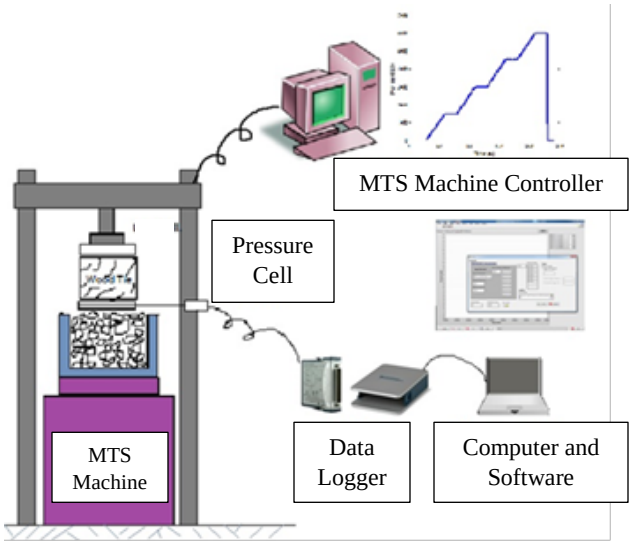

Figure 2.22 Pressure Cell Ballast Box Testing (Rose, Purcell, & Liu, 2016)

Based on the ballast box testing performed, it was determined that both types of pressure cells could be used for crosstie-ballast interface pressure testing, but it seemed that the standard 3500 model would require more protection (Rose, Purcell, & Liu, 2016). Therefore, 3515 would be adopted for in-track ballast testing.

As was conducted in the early stages of TEKSCAN, initial tests of in-track measurements were performed at the CSX/TTCI interchange in Paris, KY. Pressure cells were placed directly under the crosstie, and below the rail, after the ballast shoulder was excavated (as shown in Figure 2.23).

Figure 2.23 TTCI and Flatrock, KY In-Track Pressure Cell Installation

Several trains were then recorded to evaluate the repeatability of in-track measurements, but variability of results between 0.34 and 1.72 MPa (49 to 250 psi) were recorded (Liu, Lei, Rose, & Purcell, 2017). After this series of tests, research was moved to a tangent section on Norfolk Southern's mainline located in Flatrock, KY. Pressure cells were once again installed and positioned in the same manner as was performed in Paris, KY, and several trains traversed the test section. However, as was observed at the CSX, TTCI track, variable results ensued. After careful observations were made, it was discovered that due to the "looseness" of the ballast after installation, a gap/void would form between the crosstie and the pressure cell. Attempts were made to "shim" the cells to

bring them flush against the tie, but extremely high magnitudes of pressures were recorded as a result (Liu, Lei, Rose, & Purcell, 2017). Nominal pressures measured at Flatrock, KY however, were in the range of 0 kPa (0 psi) to 400 kPa (58 psi).

Additional details of this work at Paris, KY and Flatrock, KY can be reviewed from the Master's Research Report written by Macy L. Purcell (Purcell, 2017), whom is the predecessor of the current research.

Pressure Cell Research in Australia

In 2010, Professor Buddhima Indraratna of the University of Wollongong performed a study to assess the performance of ballasted track with and without geosynthetics (Indraratna, Nimbalkar, Christie, Rujikiatkamjorn, & Vinod, 2010). One parameter this study focused on was the effect that geosynthetic inclusion had on the horizontal and vertical stresses in the ballast layer. Interestingly enough, the author chose to use a similar pressure sensor that has been utilized in previous work by researchers at the University of Kentucky (Walker, 2002) and (Rose, Purcell, & Liu, 2016). However, the author states that the cell is 12 mm (0.5 in) thick rather than the 1 in (25.4 mm), thus it may be an experimental cell for this particular study.

The pressure measurements however were not the focus of this study. The author actually justifies much of the geosynthetic inclusion on deflection results but does mention the pressure measurement to strengthen his argument. Similar to the work at Kentucky, the cells were positioned freely within the ballast layer (see Figure 2.24), but no comments are made on whether the positioning affected measurement results.

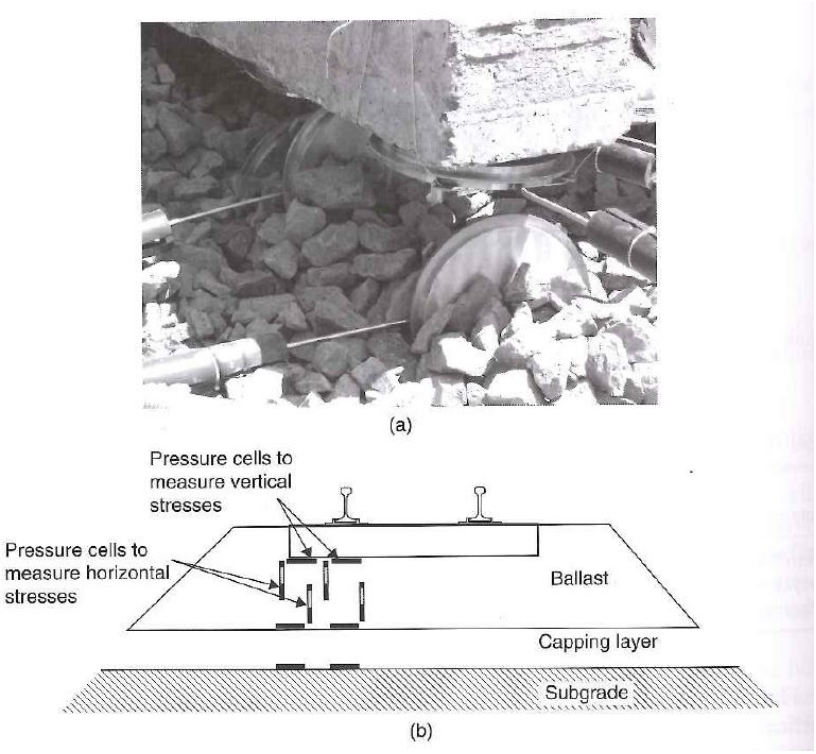

Figure 2.24 Pressure Cell Configuration: Australian Study (Indraratna, 2011)

In addition, the author presents values for typical wheel loads stresses at the crosstie-ballast interface, which tend to approximately 200 kPa (29 psi). In this case the wheel loads transmitted to the ballast were induced by a coal train. However, unlike other studies, the author identifies the magnitude increase of a possible wheel irregularity. In this case, Figure 2.25, the wheel irregularity produced a pressure of approximately 425 kPa (61.6 psi). These are very similar to the pressures recorded by researchers at UK.

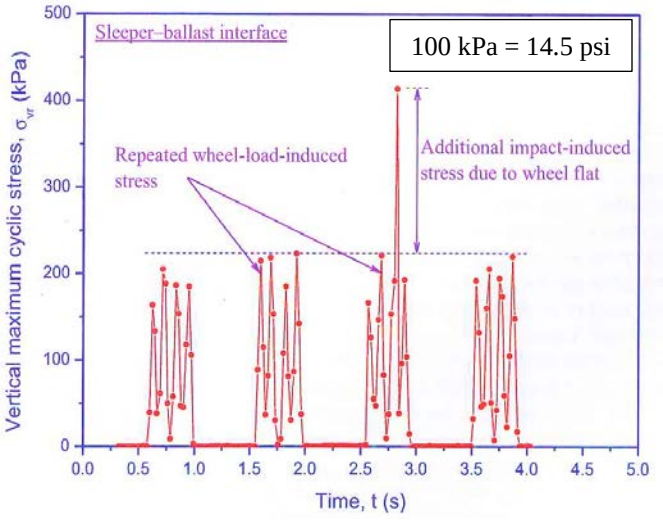

Figure 2.25 Measured Wheel Loads and Impact: Australian Study (Indraratna & Ngo, 2018)

Work has also been recently published by researchers from Queensland University and Christchurch Polytechnic (New Zealand) on the use of earth pressure cells to evaluate track structure performance (Askarinejad, Barati, Dhanasekar, & Gallage, 2018). As shown in Figure 2.26, earth pressure cells were placed directly below the centerline of the rail at the crosstie-ballast interface with tie wires to hold the cell against the bottom of the crosstie.

(a) Preparing the pressure cell (b) Fixing the pressure cell in position

Figure 2.26 Earth Pressure Cells used in Australia *(Askarinejad, Barati, Dhanasekar, & Gallage, 2018)*

Axle pressures measured by the researchers, as shown in Figure 2.27, for a 4-axle truck(bogie) were in the range of 30-40 psi (210-280 kPa). However, the author notes that over time, there is a significant decrease in pressure due to ballast consolidation. This is the same problem cited in previous work done at UK (Liu, Lei, Rose, & Purcell, 2017).

Although this work is interesting, it is not known what particular model of earth pressure cell was used (i.e. Geokon Model 3500), nor does the author explain what type of train consist traversed over the instrumented crossties.

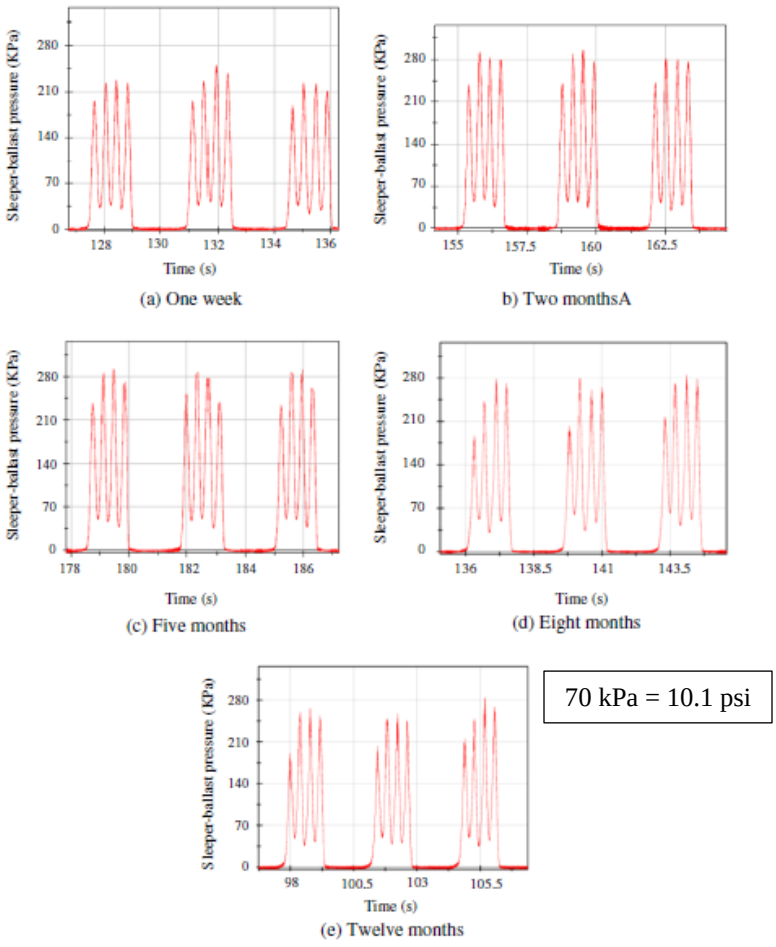

Figure 2.27 Crosstie-Ballast Pressures Measured in Australia *(Askarinejad, Barati, Dhanasekar, & Gallage, 2018)*

Recent European Trackbed Studies

Pressure cells have also been used in recent work conducted in the United Kingdom and France to assess the stresses transmitted at and below the subgrade(formation) interface.

In regards to the work performed in the United Kingdom, pressure plates were staggered along the ballast-subgrade interface in an attempt to understand subgrade deformation in heavy haul track (Grabe, Clayton, & Shaw, 2005). As shown in Figure 2.28, pressures were recorded in the range of 115-160 kPa (17-23 psi) over a 7-month period at the ballast-subgrade interface. These pressures are observed to be very similar to those measured at the ballast-HMA and HMA-subgrade interface by researcher in previous literature (Walker, 2002). However, only the pressures measured at the depth indicated by 400 mm (15.7 inches; in Figure 2.28) were directly below the centerline of the rail, where the highest pressures are assumed to exist. Thus, the results presented may underestimate the magnitude of pressure for the ballast-subgrade interface. In addition, the authors of this particular work do not indicate the particular model of pressure cell used, but it is assumed it is of the earth pressure cell variety.

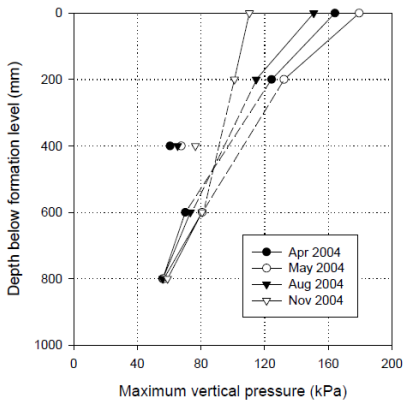

Figure 2.28 Formation Pressures over time

Work has also been done in France recently (2016), to understand the impact that train loads have on the ballast-subballast and subballast-subgrade interface (Lamas-Lopez, et al., 2016). In this study, pressure cells were placed directly below the centerline of the rail at the ballast-subballast/subballast-subgrade interface and were subject to the load of a

Locomotive (225 kN axle load, 25.3 kip wheel load) and a coach (105 kN axle load, 11.8 kip wheel load). Based on a series of tests, the researchers found that pressures at the ballast-subballast interface were in the range of 10-15 kPa (1.5-2.2 psi) and the pressures at the subballast-subgrade interface are in the range of 2.5-5 kPa (0.4-0.75 psi). These are drastically lower pressures than those recorded in previous literature (Walker, 2002) & (Grabe, Clayton, & Shaw, 2005), which questions the validity/transformation methodology of the data, especially since the ballast and subballast depths are similar to those used in the United States and un the United Kingdom. It is not known what installation procedures were used to place the cells, nor what particular model of pressure cell was used, thus it is hard to tell why such low values were measured.

Load Cells used in Iran

Load cells, instead of pressure cells or MBTSS, have also been used in an attempt to quantify the stresses transmitted to the crosstie-ballast interface. As shown in Figure 2.29, researchers in Iran were able to cast load cells firmly and flush with the bottom of concrete crossties, and installed the crossties into a test track (Sadeghi, 2008). Under what the author refers to as “type A” freight traffic (gross weight of 70-90 tons; 17.5-22.5 kip wheel load; 77.8-100 kN), the stress transmitted from an axle to the crosstie-ballast interface was in the range of 1-1.4 tons (8.9-12.5 kN). However, for design purposes, pressures over an average area are typically needed. The author in this case does not address that, and does not provide any dimensions of the load cell to calculate what the pressure might be. Based on Figure 2.29, if we were to assume a diameter of 6-inches for the load cells in questions, the pressure transmitted to the ballast would be in the range of

70-100 psi (483-690 kPa), which are very high for what is typically recommended in design for concrete crossties (AREMA, 2018).

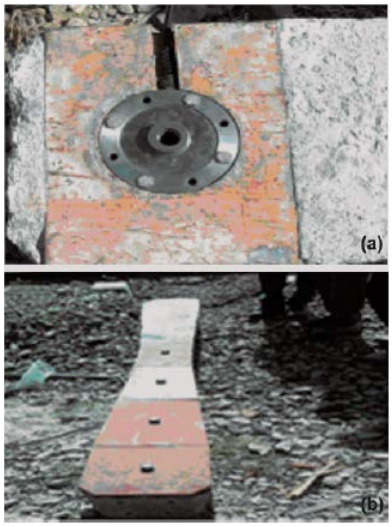

Figure 2.29 Load Cells at Crosstie-Ballast Interface

Related Work Conducted in China/Japan

A recent study by the Railway Technical Research Institute in Tokyo, Japan sought to derive relationships between the magnitudes of wheel-rail impacts and the resultant vibrations induced by the wheel-rail impacts (Aikawa, 2013). The research team performed various assessments to measure and model vibrations within the track structure, but interestingly enough, they also evaluated the magnitudes of peak forces along the footprint of a series of crossties. Figure 2.30 presents example results from a test that measured the first axle of a lead passenger coach bogie (truck) traveling at 125 km/hr. The author also states that the test section these measurements were taken from consists of 60 kg/m (40.3 lb/ft) continuously welded rail, over PC3-type concrete mono-block sleepers (crossties) on a 25 m (82 ft) tangent section of track. The track

superstructure is noted to rest on a 30 cm (11.8 in) ballast bed over “firmly tightened” sandy soil in Kyushu, Japan.

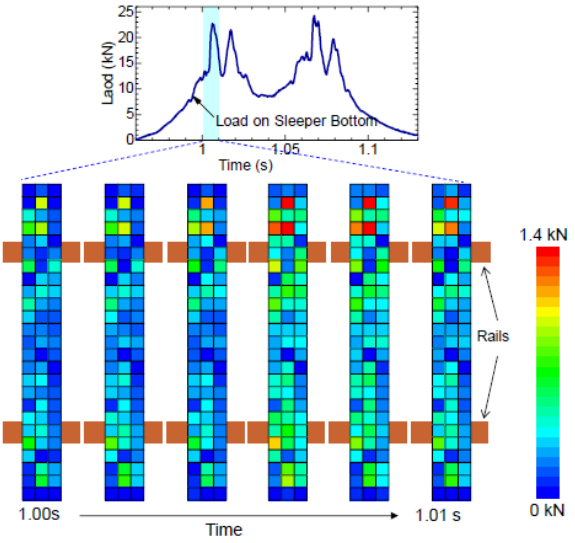

Figure 2.30 Pressures Along Sleeper: Japan

To measure these crosstie-ballast forces along the crosstie footprint, a series of “Sensing Stones” were used, which are able to quantify a particular force/pressure over a square (6 cm x 6 cm, 2.4 in x 2.4 in) contact surface (Aikawa, 2013). Figure 2.31 provides a schematic (a) and view of these “Sensing Stones” attached to the bottom of a crosstie (b).

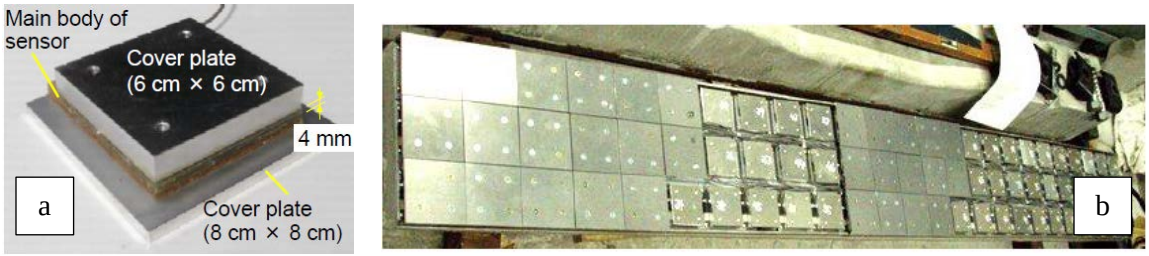

Figure 2.31 Japanese Sensing Stones

Based on the example results provided by the author, the pressure transmitted at the crosstie-ballast interface can be directly calculated based on the reported active surface of the measurement device. Therefore, it can be determined that the lead axle of a

passenger train transmits a pressure of approximately 56.4 psi (0.39 MPa) to the ballast directly between the edge of the crosstie and the rail seat. It can also be observed that a pressure between 16-32 psi (0.11-0.22 MPa) is recorded along the rest of the crosstie footprint. Most notably, the pressure is seen to increase substantially near the centerline of the track. Although the author's goal was to provide evidence to support how vibrations induced by wheel imperfections have detrimental effects on the track structure, the work presented in this article provides some interesting details on potential pressure measurement techniques that could be used in the United States. However, it should be noted that the pressures transmitted by the passenger train in this study exceed those of heavy-axle freight trains in previous studies. Thus, the measurement technique may need to be further developed.

Desirability of a New Test Procedure

Based on the literature presented to this point, several trackbed design methodologies have indicated relationships that can be used to calculated interfacial pressures and material heights based on a series of unique loading conditions. By keeping several parameters constant, such as a 33,000 lb (146.8 kN) wheel load, 40 mph (64.4 km/h) traffic, 12 inches (30.48 cm) of ballast and subballast, Figure 2.30 was created to acknowledge the differences in each design methodology. As can be noted from Figure 2.32, the Japanese National Railway and US Army Corps of Engineer's standard design procedure is much more conservative than the other methodologies accepted by AREMA.

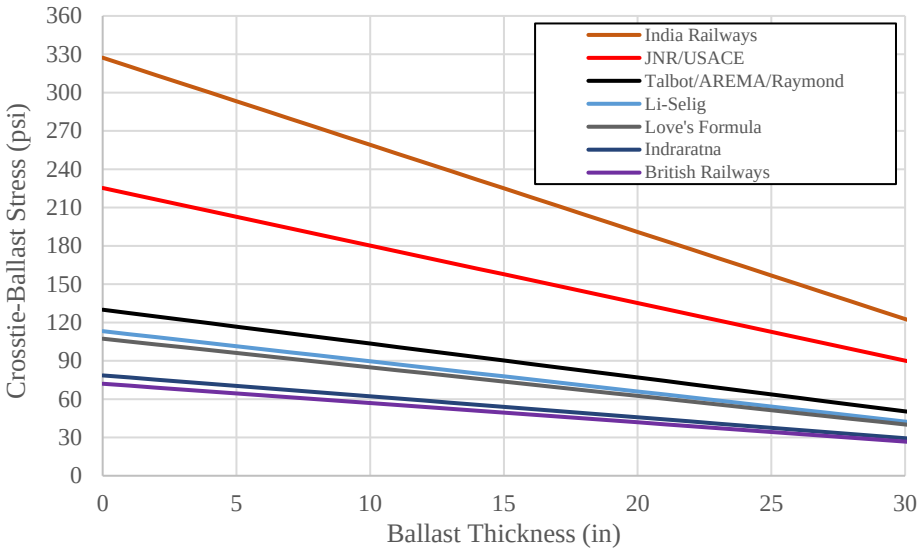

Figure 2.32 Trackbed Design Pressure Comparison

Based on the inconsistencies in measurement and analytical techniques cited in previous literature, the current research focuses on the development of a new, more-reliable, and simple method for measuring the pressures exerted within in-service trackbeds, specifically at the crosstie-ballast interface utilizing pressure cells. Special attention will be given in regard to the positioning of instrumentation in order to secure consistent and repeatable results. The following two chapters describe this new procedure.

CHAPTER 3. GRANULAR MATERIAL PRESSURE CELL MEASUREMENT SYSTEM

Granular Material Pressure Cells

In order to measure the pressures transmitted to the crosstie-ballast interface of railroad track, a durable and reliable measurement system is desirable. For this study, Geokon Model 3515 Granular Material Pressure Cells were used. Figure 3.1 is a view of this particular model of pressure cell.

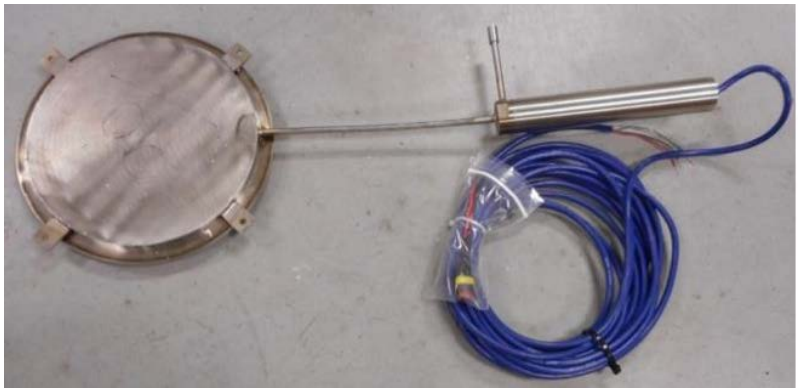

Figure 3.1 Geokon Model 3515 Granular Material Pressure Cell

In previous studies (Walker, 2002), Earth Pressure Cells (Model 3500) with a similar size and shape were used to quantify the pressures at the top and below an HMA underlayment layer, typically placed under railroad ballast. Both types of pressure cells share the same theory of operation; designed to measure the total stress/pressure applied to the active area of the device. The portion of the cell that receives the load consists of two stainless steel circular plates that are 9 inches (22.9 cm) in diameter, and welded together at their periphery. Between the two plates is a small gap (void) filled with de-aired hydraulic fluid. The earth pressure that builds on either side of the cell squeezes the two plates together, thus creating fluid pressure in the cell (Geokon, 2017).

The only differences between a typical Earth Pressure Cell, and a pressure cell of the Granular variety is the shear thickness, and the “active area” of the instrument. Typical Model 3500 Earth Pressure Cells are constructed with a total thickness of 0.25 inches (0.64 cm), whereas Granular Material Pressure Cells are typically 1 inch (2.54 cm) in thickness. This allows the plates to be sufficiently thick so that the cell does not deflect locally under a series of point loads applied by surrounding large aggregate particles. Granular Material Pressure Cells are also constructed slightly different, where an 8 inch (20.3 cm) circular extruded portion of the device serves as the “active area” or essentially the primary contact surface for measurement. Standard Earth pressure Cells however use a flat 9 inch (22.9 cm) plate surface for measurement (Geokon, 2017). A more detailed schematic showing these attributes is shown in Figure 3.2.

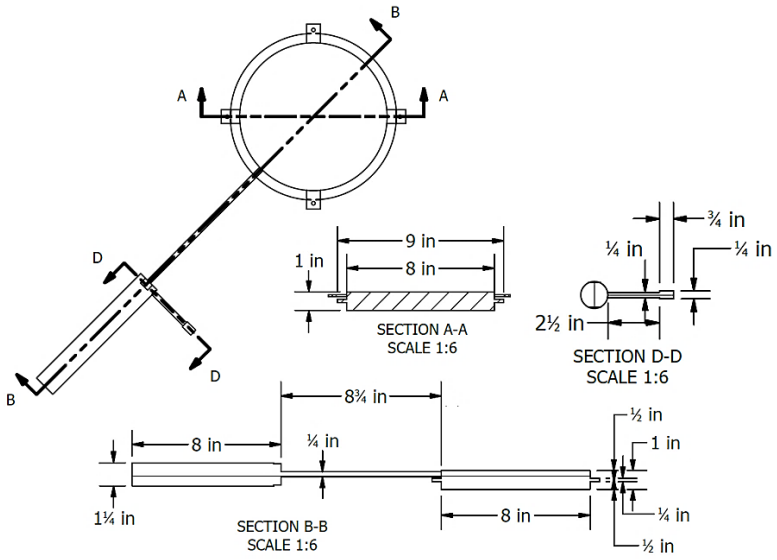

Figure 3.2 Model 3515 Pressure Cell Schematic

In order to measure the fluid pressure, the Model 3500 and 3515 Pressure Cells use a semiconductor strain gauge type of transducer, which transforms the fluid pressure into a voltage or current signal. Geokon produces a series of transducers that can have an output

of either 0-100mV, 0-5 volts or 4-20 mA, depending on the measurement intent, environment, and data acquisition systems (Geokon, 2017). A semiconductor type of transducer, rather than vibrating wire, was selected in this application because of the need to accurately measure dynamic pressures. Semiconductor type transducers are known to handle dynamic responses more effectively. Additionally, the pressure transducer has a measurement range of 0 to 362 psi (0 to 2.5 MPa), with an additional 1.5 factor of safety, which allows pressures to be recorded up to 544 psi (3.75 MPa). This is very useful for this study, as wheel irregularities may cause significant pressure increases. Additional specifications for this particular type of pressure cell is presented in Appendix A.

Derivation of Pressure

Although the transducer is able to transmit a corresponding electrical response based on earth pressure, that electrical response must be converted to a more understandable pressure value. This is done by using a linear or polynomial expression that have been provided by the manufacturer as shown in Equation 3.1 and 3.2.

$$P = G(R_1 - R_0)$$

Equation 3.1 Linear Expression for Pressure

$$P = AR_1{}^2 + BR_1 + C$$

Equation 3.2 Polynomial Expression for Pressure

Where P is the pressure value, R_1 represents the current (in progress) output reading from the transducer, R_0 represents the initial output reading, and G (also A, B and C) represents the linear or polynomial gage factor for the device (Geokon, 2017).

For better accuracy, the manufacturer recommends that the polynomial expression be used. However, this requires atmospheric pressure calibration by the user before each

and every test. Based on this, it was decided to use the linear expression instead, which only accounts for approximately 1% difference in pressure readings.

As an example, assume that the particular model of pressure cells has a linear gage factor of 0.1565 (based on an input voltage of 24 VDC). This particular pressure cell also has polynomial gage factors of 6.82E-05, 0.1549, and -0.6194, representing A, B, and C respectively. Also assume that while measuring pressure, a change was obsereved in output reading of 127.8 mA (initially -0.5mA). Using Equations 3.1 and 3.2 presented earlier, the following pressure values are obtained.

$$P = G(R_1 - R_0) = 0.1565(127.8\,mA) = 20\,psi$$

$$P = AR_1{}^2 + BR_1 + C = 6.82 \times 10^{-5}(127.3\,mA)^2 + 0.1549(127.3\,mA) - 0.6194 = 20.2\,psi$$

As can be observed from this example, the difference in measured pressures based on the polynomial and the more simplified linear expression is negligible. Thus, it is appropriate to use the more simplified expression.

The gage factors correspond to the reported factors presented on calibration reports provided by the manufacturer for each cell. An example of one of these calibration reports is shown in Appendix B. Each individual cell will have its own calibration report.

Temperature Effects

In addition to gage factors and conversion expressions, temperature also has an effect on measured pressure readings. Fluids, even hydraulic fluid, have the tendency to expand whenever their respective temperature increases. Considering that, and the added effect of the liquid being confined within a small area, the liquid may be able to deform the pressure cell body, thus causing variable pressure readings. Opposite of that, whenever the

temperature of the liquid decreases by a significant amount, fluid can respond by shrinking, thus potentially under representing pressure readings. Based on details outlined by the manufacturer, this effect can be considered minimal, especially if the pressure cell contains a fluid, such as oil or hydraulic fluid, that has a high coefficient of thermal expansion, K. However, the specifications do provide guidance if it is desirable to calculate this effect.

An expression that the manufacturer recommends to calculate this effect is shown in Equation 3.3.

$$\Delta P = \frac{1.5(E)(K)(D)}{R}$$

Equation 3.3 Temperature Effect Expression

Where ΔP is the potential change in pressure (psi) per °C, E represents the modulus of the soil media in contact with the cell (psi), K represents the coefficient of thermal expansion of the oil/hydraulic fluid (ppm/°C), D represents the oil/hydraulic fluid film thickness (in), and R represents the radius of the pressure cell (in) (Geokon, 2017).

To provide an example of this effect, consider a pressure cell (R = 9 in (22.9 cm), D = 0.060 in (1.5 mm)) interfaced with railroad ballast (E = 3,000 psi (20.7 MPa)). The thermal expansion coefficient of the oil within the cell is approximately 700 ppm/°C. Knowing this information, the potential change in pressure per °C can be calculated.

$$\Delta P = \frac{1.5(3{,}000\ psi)(700\ ppm/°C)(0.060\ in)}{9\ in} = 0.021\ psi/°C$$

Knowing the potential pressure change per °C, an estimate can be made as to the significance this will have during a typical testing day. Suppose a large temperature swing on a day beginning at a low of 10 °F (-12 °C) and rising to a high of 60 °F (15.5 °C).

$$15.5°\text{C} - (-12)°\text{C} = 27.5°\text{C}$$

$$27.5°\text{C} \times 0.021 \frac{\text{psi}}{°\text{C}} = 0.57\ psi$$

Although one-half of a psi in some scenarios may be significant, in regards to measuring pressure in the railroad track structure, one-half of a psi is not considered significant. This example also illustrated a worst case scenario, assuming the baseline temperature for normal operation was 10°F (-12 °C) (usually closer to room temperature). In Chapter 6, temperature variations and pressure measurements over time will be further analyzed.

Data Acquisition

To record the electrical response these pressure cells produce, a National Instruments Model 9203 C Series data logger was used as shown in Figure 3.3a.

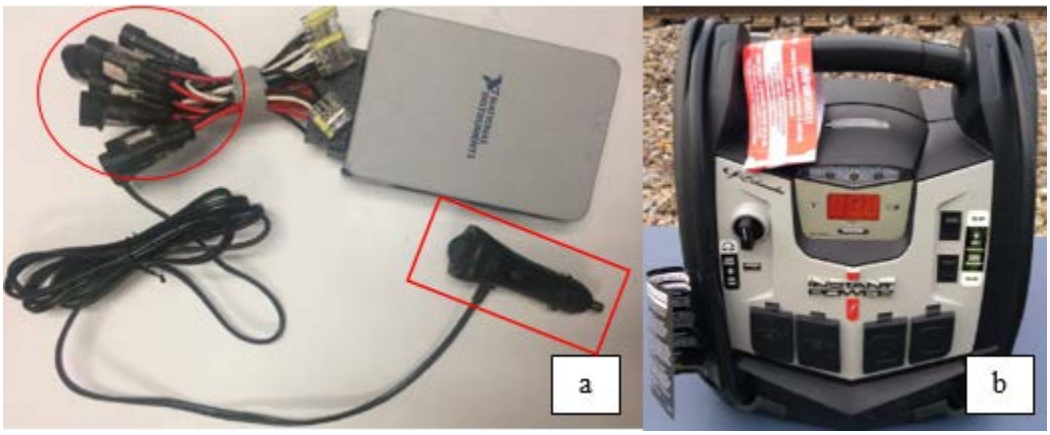

Figure 3.3 Data Logger and Power Supply; cable attachments and power connection highlighted

This particular data logger is capable of recording up to eight channels (pressure cells) concurrently, recording at a rate of 2 kHz (2000 samples/s). The data logger and pressure cells are powered by a portable 12 VDC power supply shown in Figure 3.3 b. The

data logger in this case was connected to the power supply with the connector outlined in "red" shown in Figure 3.3a.

As mentioned previously, the semiconductor transducer that produces an electrical signal, which is then converted to pressure, is manufactured to output either 100 mV, 0-5 VDC, or 4-20 mA. In this case, a 4-20 mA current option was chosen because analog signals of this variety offer increased immunity to both electrical interference and potential signal loss over long cable runs. Voltage on the other hand does not provide this type of protection. In addition, the National Instrument data logger, described earlier, was also compatible with that type of input.

To connect the cells to the data logger, a connection similar to what would be used for automobile trailer lights was used as shown in Figure 3.4. This two-wire connection is compatible to the wiring specification the manufacturer recommends. The corresponding plug for this connector is highlighted with a red circle in Figure 3.3a.

Figure 3.4 Pressure Cell Two-Wire Connector

To visualize the data during measurements and for post processing, the data logger is interfaced with a laptop computer, which has software to translate the measurements recorded by the data logger. This is shown in Figure 3.5.

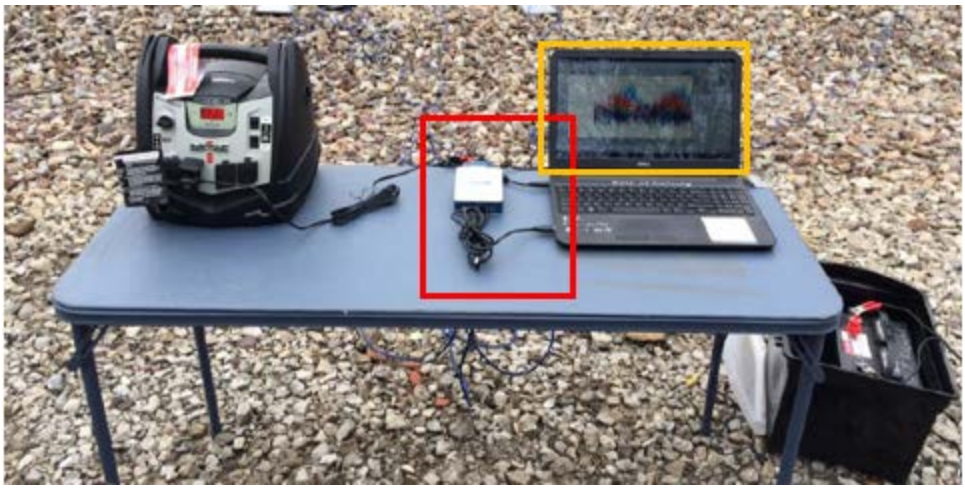

Figure 3.5 Pressure Test Setup

The data logger is interfaced with the computer, using only a simple USB connection, highlighted with red in Figure 3.5. The program used to record the pressure for each cell was written by visiting scholar Qingjie Liu using a software LabVIEW, which allows users to graphically code their desired programs in a user-friendly manner. The home screen on the software is shown in Figure 3.6 and highlighted with orange in Figure 3.5.

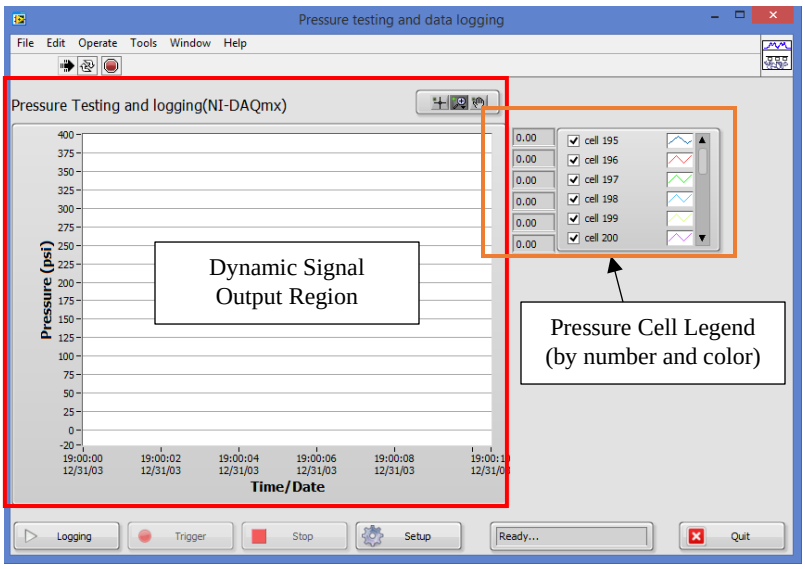

Figure 3.6 Pressure Software Home Screen

As can been seen in the home screen, the pressure signals can be plotted within the graphing area, highlighted in red, and a legend reporting the color and pressure for each pressure cell in real-time is presented in the top right of the screen, highlighted in orange. The measured data from this program is initially stored as a .TDMS file (native to National Instruments), but can easily be converted to a comma-delimitated .CSV file for use in various data processing software with a simple plug-in available through National Instruments. A code map of this program is presented in Appendix C.

Pressure Cell Installation

Special attention was also placed on the installation procedure required to embed these cells into the track structure. Previous work at the University of Kentucky (Liu, Lei, Rose, & Purcell, 2017) attempted to insert pressure cells directly under the crosstie by the use of track jacks, which raised the rail and crosstie 1.5 inches (3.8 cm) to provide sufficient space to slide the cell in place. However, over time, settlement with an additional loss of ballast support under the crosstie resulted in a dramatic decrease in the pressures recorded in the prior tests. Metal shims were then used to fill the void between the crosstie and the pressure cell, which resulted in an increase of pressure for that particular cell for the next test train. However, this fix was short-lived as pressures would typically continue to decrease during subsequent tests.

Based on these findings, a new method was developed to mount these pressure cells directly to the bottom of timber crossties, virtually nullifying the effect of settlement. This method involved the use of a CNC machine to physically route out a recess of the pressure cell, in order to mount the active surface of the cell flush within the bottom of the crosstie (Rose, Clarke, Liu, & Watts, 2018). To do this, a series of red oak timber crossties, treated

with Copper Naphthenate solution, were obtained from Norfolk Southern Corporation. With assistance from the College of Engineering Machine Shop, the ties were routed with a CNC machine to conform to the shape and dimensions of the pressure cell. The CNC has very precise tolerances, which provided a perfect fit between the cell and the crosstie. The recess of the cell typically takes approximately 45 minutes to create. Figure 3.7 shows a picture of a) routing in progress, and b) a finished product.

Figure 3.7 Routing the Pressure Cell Recess

The typical recess created on the crosstie was made to be located directly under one rail seat at the crosstie-ballast interface. However, a series of crossties were also routed to permit measurement simultaneously beneath both rail seats, and at the center of the track, as shown in Figure 3.8.

In order to route these configurations, special attention was taken to configure the CNC machine to route the pressure cell recess in the proper location. This was done by conforming to the rectangular coordinate system by which the CNC machine software operates, and by defining the locations to begin routing, at the center of the cell, based on the dimensions shown in Figure 3.8. Figure 3.9 presents a) schematic of a CNC showing

the rectangular coordinate systems, and b) a screenshot of the software that performs the routing operation.

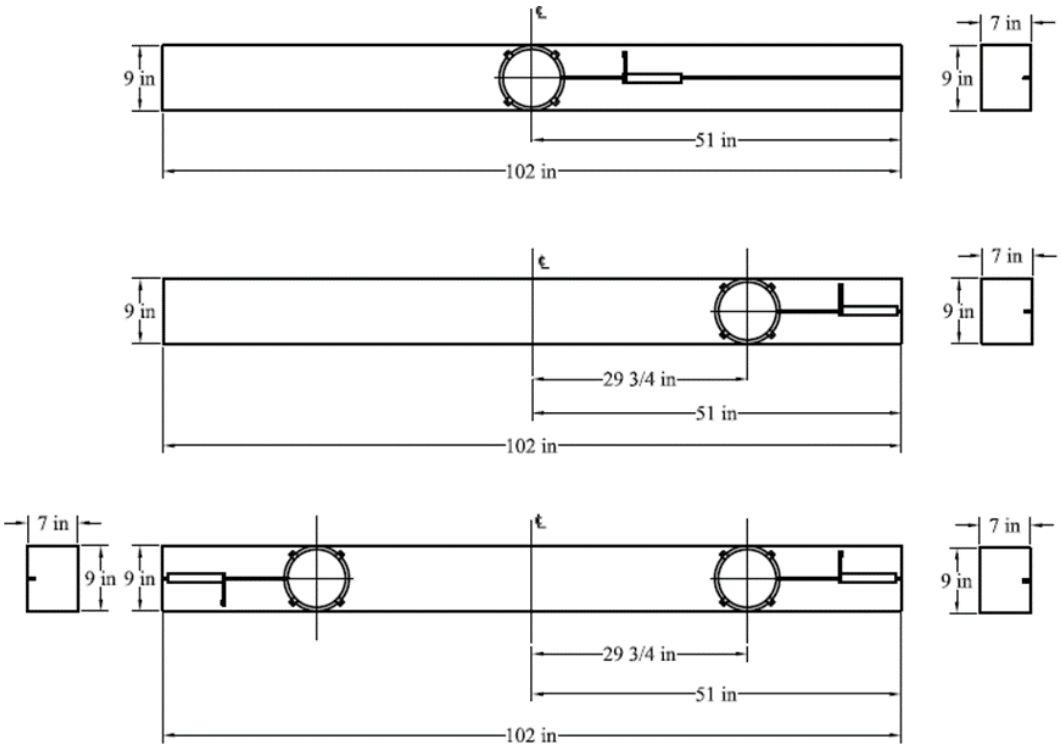

Figure 3.8 Various Routing Configurations for timber crosstie

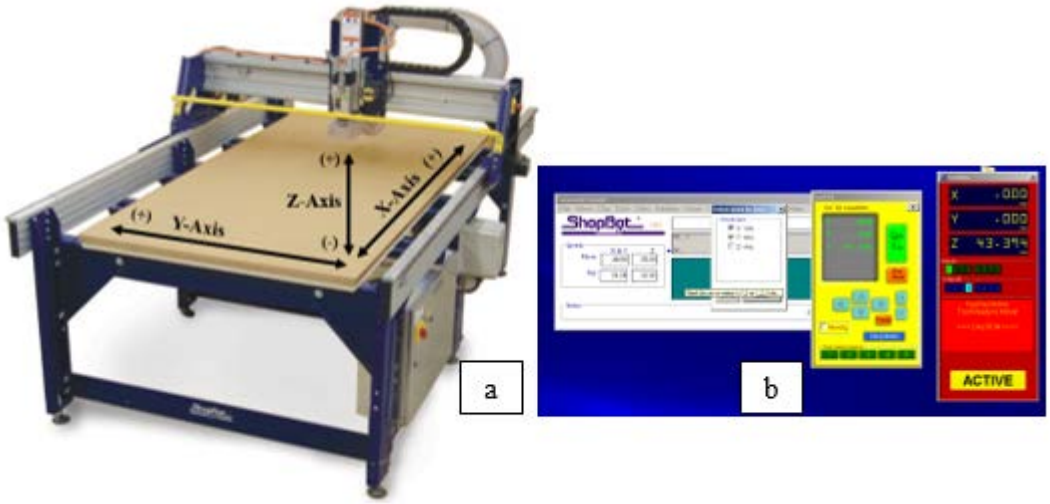

Figure 3.9 CNC Machine Configuration

In addition to routing, protection for the transducer housing and other electrical components was provided by attaching thin metal sheets with a textured surface to the bottom of the crosstie. This protected each critical component. The textured finish was necessary to restore frictional resistance between the crosstie and the ballast. A protected cell is shown in Figure 3.10.

Figure 3.10 Electrical Component Protection

Chapter 6 contains more discussion on how these pressure cells and crossties are installed in the track structure.

Although this procedure presents a major opportunity to obtain more reliable test results in the track, it is critical to verify that this procedure provides accurate and consistent measurements by evaluating this installation procedure in the laboratory. This is described in the following chapters.

CHAPTER 4. LABORATORY VERIFICATION OF PRESSURE CELLS

In order to verify that Granular Material Pressure Cells can accurately measure crosstie-ballast interfacial pressures with the installation configuration described in Chapter 3, conducting a series of laboratory calibration tests, based on controlled static loadings, are essential.

Previous Calibration Studies

Recent studies based on the early work of researchers at the University of Kentucky, indicate that the specially designed Granular Material Pressure Cells manufactured by Geokon are applicable for measuring pressures at the crosstie-ballast interface (Rose, Purcell, & Liu, 2016). The researchers found that this particular type of cell was able to measure consistent pressures under various support conditions and various aggregate types (such as new, worn, and top-size ballast material). However, this work was developed under the assumption that the pressure cells would be placed below a solid tie without constraint. As mentioned previously, this installation method in the track proved to be unsatisfactory, due to the fact that firm and consistent contact between the pressure cell and the crosstie was impossible to develop and maintain (Liu, Lei, Rose, & Purcell, 2017). Thus, the need for additional calibration.

Development of Simulated Trackbed for Calibration

To perform this calibration, the support conditions of a typical trackbed need to be simulated in the laboratory. This required developing a prototype trackbed. This particular test section incorporated a vertical resiliency so that deflections in the trackbed under typical loading would be in the range of 1/4 to 3/8 inch (0.64-0.95 cm), similar to that observed for in-service trackbeds. This deflection would inherently be achieved under

laboratory loading conditions. In addition to this, the ballast containment frame would exhibit lateral ballast confinement similar to that observed in an in-service trackbed. This was done by creating a resilient, yet expandable frame that would contain the ballast, but also provided minimal lateral support due to stress/strain produced under laboratory loading. Figure 4.1 shows a version of this testing frame used calibration.

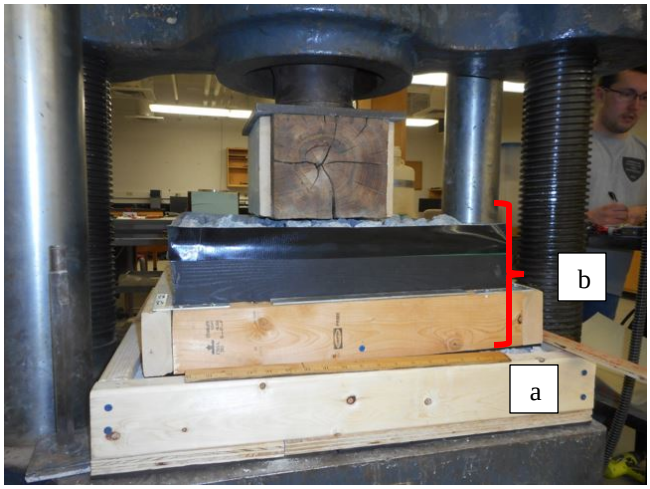

Figure 4.1 Simulated Trackbed for Calibration

In Figure 4.1, a 4-inch (10.2 cm) layer of 1 inch (2.54 cm) nominal maximum size limestone aggregate (typically used for railroad subballast and highway pavement base; locally known as dense-graded aggregate DGA), was placed in the containment frame labeled “a” to simulate typical railroad subballast. A thick layer of plywood (5/8-inch, 1.59 cm) with a 3/16-inch (4.8 mm) rubber mat was placed beneath the subballast frame to exhibit resilient behavior of the corresponding subgrade. In the area labeled “b”, a ballast mixture of new and worn ballast was placed within a frame restrained primarily by wood and lawn edging material. This lawn edging material permitted the ballast to expand laterally under load and contract whenever the load was released.

To achieve the condition of worn railroad ballast, new ballast was subjected to an LA Abrasion test to slightly round the ballast particles. Large sized ballast particles (> 1.5 inches, 3.8 cm) were removed to provide more adequate and consistent support. To interface between the ballast and subballast, a 3/16-inch (4.8 mm) layer of polyester fiber/rubber-backed floor carpet was used. Special attention was also taken to ensure that adequate and uniform compaction within each of the aggregate support layers was produced.

Timber Crosstie Section, Tie Plate, and Rail for Calibration Tests

Calibration tests also employed the use of a 9 inch (22.9 cm) wide by 7 inch (17.9 cm) thick copper naphthenate treated timber crosstie. In the interest of pressure cells calibration, an 11 inch (27.9 cm) length of crosstie was used to embed a single cell directly under the rail as shown in Figure 4.2, part a.

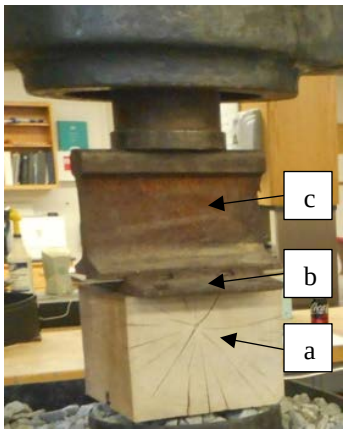

Figure 4.2 Timber Crosstie and Rail for Calibration

A standard 8 inch (20.3 cm) wide by 14 inch (35.6 cm) long steel tie plate was also positioned between the wood crosstie and rail (Figure 4.2, part b), with a 1/8 inch (3.2 mm) thick narrow spacer placed between the rail and tie plate to remove the cant. This allowed

for vertical loads to be applied uniformly through the simulated track structure. A 10 inch (25.4 cm) long section of 136-lb rail conforming to AREMA specifications, Figure 4.2 – part c, spanned the entire width of the tie plate.

Calibration Testing Equipment

To apply the laboratory loading necessary to exhibit railroad conditions, a Baldwin/Satec hydraulic universal material testing machine was used to apply static compression loads in 1,500 lbf (6.7 kN) increments to a maximum load of 6,000 lbf (26.7 kN). This range of laboratory loading provided pressures in excess of 100 psi (0.69 MPa) over an active area of 50.3-in^2 (324.5 cm^2). This range of pressure has been observed to exceed the typical pressure magnitudes of locomotives and loaded freight cars (Liu, Lei, Rose, & Purcell, 2017). In this case, the Baldwin/Satec testing machine has a test range of 300,000 lbf (1334.5 kN).

When measuring these pressure magnitudes induced by static loading, the data logger and software described in Chapter 3 are interfaced with a pressure cell and a laptop computer. Figure 4.3 shows the typical test equipment for laboratory calibration and pressure measurements.

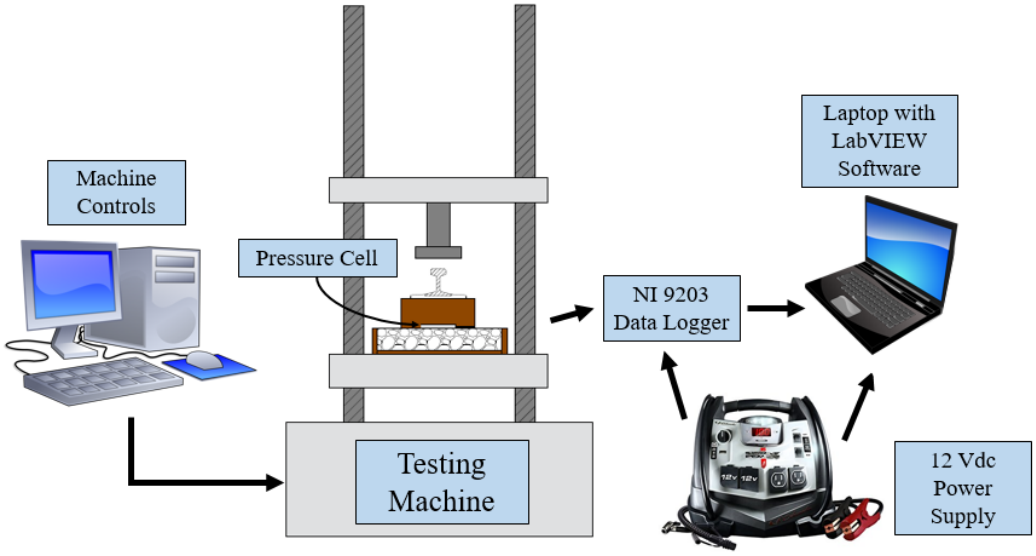

Figure 4.3 Laboratory Calibration Test Setup

Various Calibration Tests

Since the magnitude of the loading can be selected and controlled by the testing machine, a series of basic calibration-type validation tests were performed to measure the accuracy of the cells. In addition, the effects of several variables were examined to optimize installation practices used for the placement of pressure cells in the trackbed. The variables examined during these tests are the following:

- Validation of the accuracy of measurement procedure,
- Measurement repeatability within and between cells,
- Effect of cell location and position, and
- Effect of cell attachment procedures.

The first series of tests involved assessing measurement accuracy and pressure cell repeatability. Repeatability measurements employed the use of four individual cells to

evaluate if there was any inherent instrument bias. Six tests were performed for each cell, using the same loading magnitudes and routed crosstie installation method.

Figure 4.4 illustrates the relationships of machine induced stress and the corresponding cell measured pressure for each of the four cells.

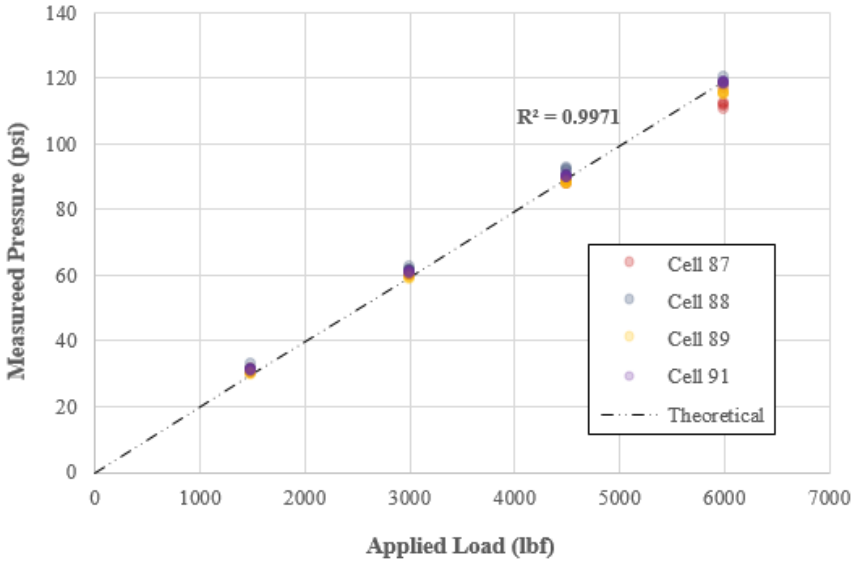

Figure 4.4 Repeated Tests for Individual Cells (Routed Tie)

Based on Figure 4.4, the results demonstrate a near-percent relationship (R^2 = 0.9971) between each cell's stress response for each machine applied load. Variations, minimal at best, are seen at higher load magnitudes, but are not considered to be significant. This test suggests that the routing procedure used to install the pressure cells is valid, but it was desirable to evaluate the effect of several other variables.

The effect of variable cell location and position was evaluated. This test evaluated whether or not there is any discrepancy between inserting the pressure cells within the recessed cavity of the crosstie, or placing the cell directly below the crosstie. Six repeated

tests were conducted with the cell placed directly below a solid 11 inch (27.4 cm) length of the crosstie, and was compared with the prior tests. Special attention was taken to make sure only the cell surface contacted the ballast. This was necessary to ensure the machine applied load was only supported by the pressure cell and excluded crosstie contact with the ballast. The comparison between each test is shown in Figure 4.5.

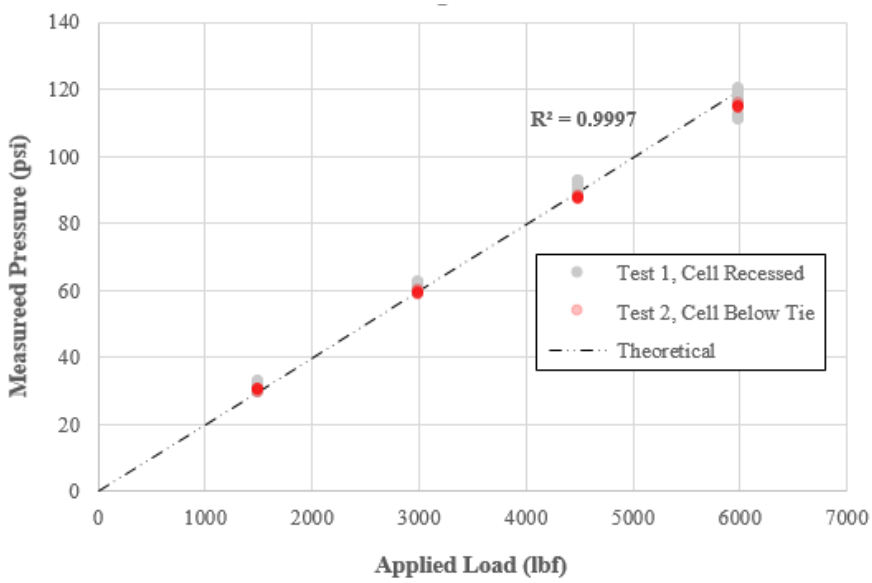

Figure 4.5 Effect of Cell Position

Based on the results of this repeated test, there seems to be no effect on the transmitted pressures between recessing the cell into the bottom of the crosstie, compared to placing the cell directly below the solid timber tie. The relationship found was, again, a near-perfect correlation between the cell's response and the machine's applied load (R^2 = 0.9997).

The preceding laboratory tests involved having the cells positioned recessed in and below the tie without any attachment method to secure the pressure cell to the tie. The cell's position for these installation procedures, without attachment, can be controlled in a

testing machine, but some type of attachment will be needed for in-track testing. Without attachment in the recessed portion of the crosstie, the cell will subsequently settle in the ballast, potentially causing the crosstie loading to “bridge” across the cell, resulting in lower pressure magnitudes than would be typical for non-instrumented ties.

Based on the need for attachment, two methods for affixing the cells to the routed cavity of the crosstie were evaluated. One method involved the use of screws through the integral brackets of the cell body. The second method used a series of small metal corner braces screwed against the tie. The corner brackets were considered to evaluate the performance of the cell when the ballast is relied upon to hold the cells in place rather than directly mounting the cell to the crosstie with screws. The attachment procedures, a) no attachment (for tests 1 & 2), b) screws, and c) corner braces, are shown in Figure 4.6.

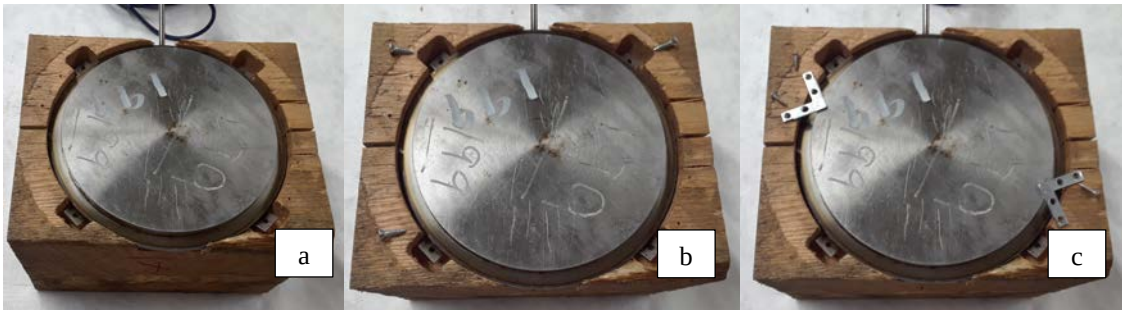

Figure 4.6 Cell Attachment Procedures

Similar to the previous calibration tests, each attachment procedure was evaluated in six repeated test sequences with the varying machine applied loading. Figure 4.7 illustrates the relationships that developed during this series of tests. Based on Figure 4.7, the test data indicates very good correlation between the cell’s pressure response and the machine’s applied loading for each attachment procedure. Screws and Corner Braces accounted for R^2 values of 0.9997 and 0.9996, respectively. Variations, minimal if any,

were less than one psi. Therefore, varying the cell attachment procedure has no effect on the transmitted pressures at the crosstie-ballast interface. However, for in-track applications, either screws or corner braces must be used.

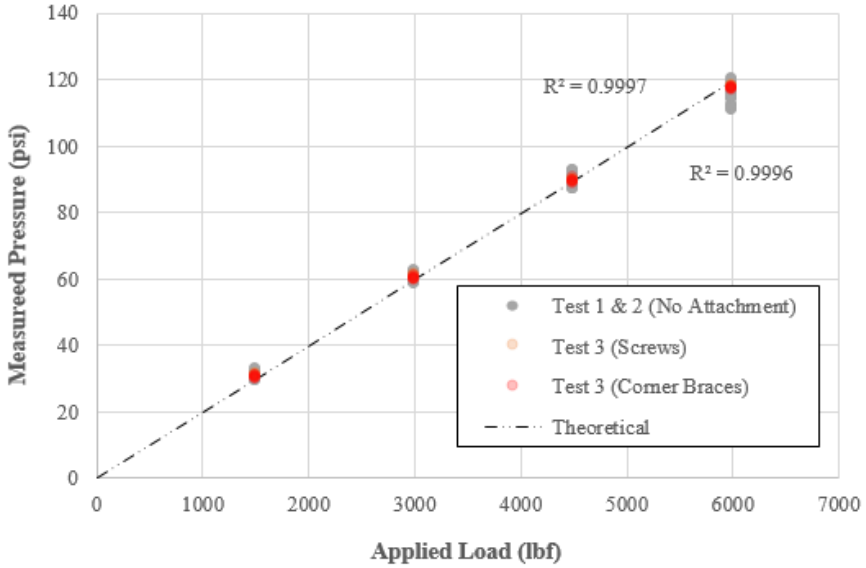

Figure 4.7 Cell Attachment Relationships

Additional Laboratory Evaluations

In addition to evaluating the effect of cell accuracy, position, and attachment, the effect of tie length on a single pressure cell was also explored. During the preceding calibration tests, a 11 inch (27.9 cm) length of timber crosstie was used. For the following test sequence, 20 inch, 30 inch, and 40 inch lengths of crosstie sections were used to evaluate the effect on the measured pressure cell response, for varying machine applied stresses.

Each test involved the use of a solid section of crosstie cut to the specific lengths. Routing did not need to be performed since the calibration testing completed prior indicated there was effectively no difference between installation procedures, thus no reason to rout

each section. The machine loading performed on each section was consistent with the loading performed during the calibration tests increments of 1,500 lbf (6.7 kN) to 6,000 lbf (26.7 kN). Figure 4.8 shows the results of these sequential tests.

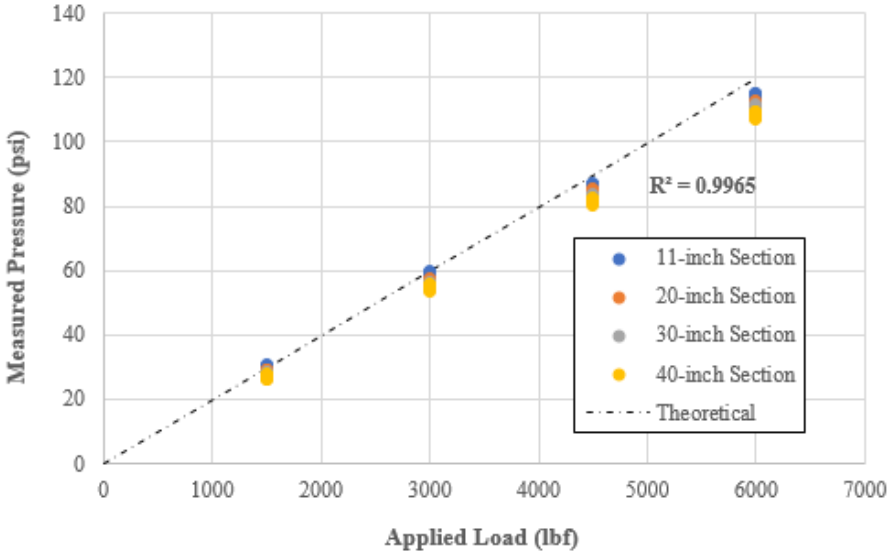

Figure 4.8 Effect of Longer Tie Sections

Based on these tests, it was apparent that there was basically no effect on a single cell's response in regard to the length of crosstie. This also served to validate the laboratory calibration procedure used in the preceding evaluations. It is interesting, however, to note the variation of the cell's pressure response at higher load magnitudes. However, the higher loading magnitudes were in excess of those existing for in-service train operations.

Tabulated data for each for the tests described in this chapter are included in Appendix D for further reference. This laboratory practice will be expanded in Chapter 5 to evaluate the distribution of pressures along the length of the crosstie transverse to the track.

CHAPTER 5. LABORATORY EVALUATION OF THE PRESSURE DISTRIBUTION AT THE CROSSTIE-BALLAST INTERFACE

Based on the successful laboratory calibration tests and evaluations, it was determined that a similar approach could be used for assessing the magnitudes and relative distributions of pressures transmitted along the crosstie-ballast interface. Knowing what this distribution is, and having a simple way to quantify it, can enhance the current understanding and applicability for design practices.

The American Railway Engineering and Maintenance-of-Way Association (AREMA) recommends that designers should consider the relative distribution of stress underneath the effective length of the crosstie to be two-thirds of the crosstie footprint. That two-thirds being the outer third of each end of the tie in bearing. Although this estimate may seem to be correct, it's important to note that this approximation was created on the basis of early analytical methods. With the current availability of accurate and durable instrumentation, it is desirable to test the validity of this standard to enhance the industry's understanding of this concept, and to optimize the current design practices. The following methodology and series of tests were performed to gain a greater understanding of the typical load distribution at the crosstie-ballast interface.

Simulated Trackbed Composition

In order to determine this distribution, the responses of a typical trackbed had to be simulated in the laboratory; similar to the information presented in Chapter 4. This was done by constructing a larger ballast bed, 55 inches (1.4 m) in length, that encompassed the length of one-half of a crosstie, as shown in Figure 5.1. A one-half length of crosstie

was chosen for this particular study because the testing machine available was only capable of applying a load at a single location, representing one rail. Also, the one-half length was more manageable for one or two persons to position and make fine adjustments to both the crosstie and the simulated trackbed. Although testing on a full length of crosstie would have been ideal, the results from one-half length testing can be converted by symmetry to represent an entire crosstie.

Figure 5.1 Simulated Trackbed for Distribution Testing

The trackbed support was similar to the calibration tests performed in Chapter 4. The support consisted of a 3/16-inch (4.7 mm) thick layer of rubber mat, which interfaced the steel platen of the testing machine to provide vertical resiliency to the trackbed. This rubber mat was then topped with a 4-inch (10.2 cm) thick compacted layer of dense-graded limestone aggregate to simulate typical subballast. The ballast layer, was a 14-inch (35.6 cm) thickness of new and worn #4A graded granite, with the >1.5-inch (38.1 mm) size

particles removed. These sizes were removed to gain more uniform and consistent compaction, and surface levelness.

As an improvement, the ballast layer was increased in thickness by 5-inches (12.7 cm), relative to what was used during the calibration tests to provide a more realistic ballast thickness normally observed in the track. This also allowed for more consistent deflection measurements in the range of 1/4-inch (6.35 mm).

As alluded to previously, the track support bed was 55-inches (1.4 m) long and used a copper naphthenate treated timber (red oak) crosstie. Along the crosstie's footprint, four critical points of the crosstie were instrumented with pressure cells to monitor the behavior at the crosstie/ballast interface. Those critical locations being the centerline to monitor any center binding effect (Cell #68), the rail seat (directly below the rail, Cell #70), the outer end of the crosstie (Cell #71), and a location equal distance between the centerline and the rail seat (Cell #69). However, in order to measure the pressures transmitted at the centerline (51-inches, 1.3 m, from the tie end) of the track, the crosstie was cut at 55-inches (1.4 m) long to provide sufficient length for an 8-inch (20.3 cm) diameter cell, as shown in Figure 5.2, to be positioned properly at the centerline. Figure 5.2 presents a schematic of the test section used for this laboratory evaluation, showing the precise locations of each pressure cell along the effective length of the tie. The more transparent portion of this figure shows the addition of the other half of the crosstie and is intended to provide scale for how this test compares to the full length of the crosstie, if it had existed.

Similar to the calibration testing procedure outline in Chapter 4, a standard 8-inch (20.3 cm) wide by 14-inch (35.6 cm) long steel tie plate was used with the AREMA

conforming 136-lb rail section. A 1/8-inch (3.2 mm) narrow spacer was also utilized to negate the cant effects of the tie plate.

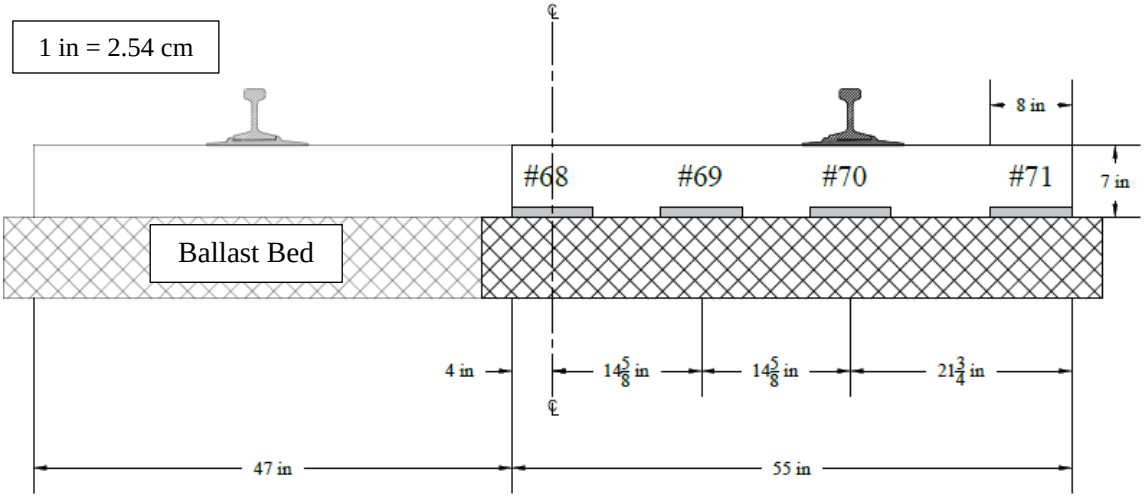

Figure 5.2 Laboratory Distribution Testing Schematic

Laboratory Test Equipment and Data Acquisition

The series of loads were applied to the crosstie with the same testing machine used during calibration. Based on the manufacturer's loading specifications for the Baldwin/Satec hydraulic universal testing machine, it was determined that this particular machine would be able to apply greatly in excess of the load required to simulate track application.

Pressures could also be recorded for all four cells simultaneously using the same measurement software and data logger as was used during calibration, as depicted in Figure 5.3. Since most, if not all, of the equipment used during calibration was used again during this phase of testing, the effect of the minor instrument deviations was negligible. Figure

5.3 provides a detailed sketch showing the data acquisition and testing equipment used during this evaluation.

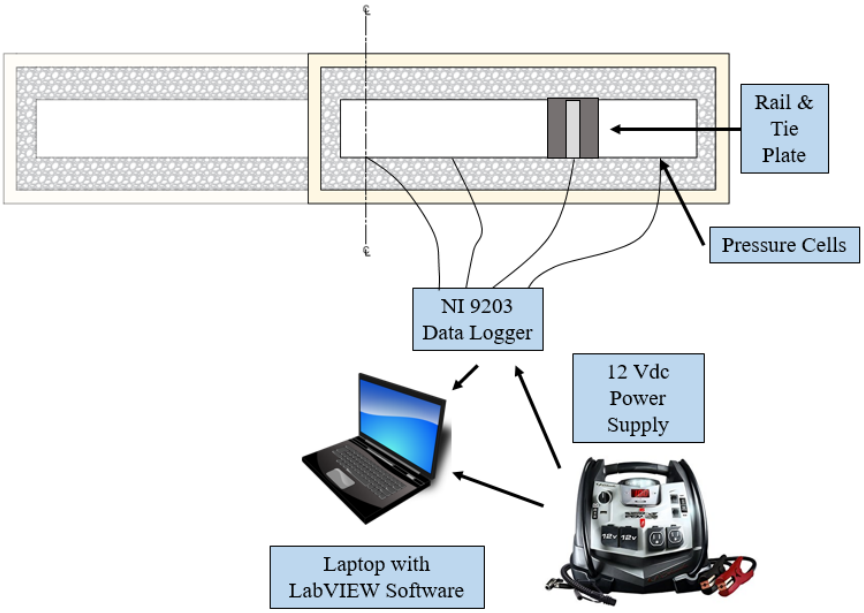

Figure 5.3 Multi-Cell Testing Data Acquisition Setup

Series of Tests to be Evaluated

Based on early observations made during preliminary laboratory testing, four different testing arrangements for measuring the transfer of loadings from the recessed cells to the ballast supporting material were selected for evaluation. These four arrangements were:

- Series #1: Ballast Contact against the Pressure Cells and the Crosstie,
- Series #2: 8-inch (20.3 cm) Spacers interfacing the Pressure Cells from the Ballast,
- Series #3: 2-inch (5.1 cm) by 10-inch (25.4 cm) Lumber Board interfacing the Crosstie from the Ballast, and

- Series #4: 8-inch (20.3 cm) Spacers interfacing the Crosstie and Cells from the 2-inch (5.1 cm) by 10-inch (25.4 cm) Board.

A visual representation of each arrangement is presented in Figure 5.4.

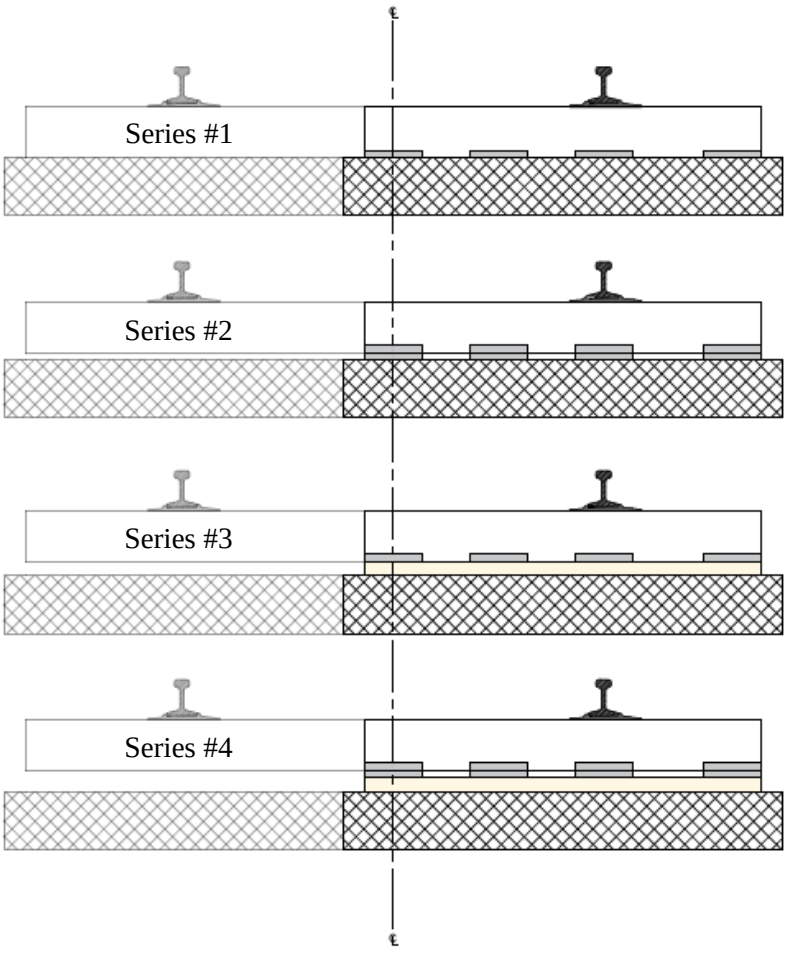

Figure 5.4 Testing Arrangements Evaluated

As shown in Figure 5.4, Series #1 involves the crosstie and the pressure cells making full contact with the ballast bed. This arrangement was chosen because it closely resembles the loading conditions that would be observed in the track. The pressure cell surfaces, in this case, accounted for approximately 40% of the crosstie footprint area,

with the remaining 60% consisting of the crosstie-ballast contact area (not routed). A series consisting of six consecutive tests were conducted at seven equal loading increments from 1,500 lbf (6.7 kN) to a maximum of 10,500 lbf (46.7 kN).

Series #2 was arranged with 8-inch (20.3 cm) diameter metal spacers between each cell, and the ballast, providing an interface for the pressure cells and the ballast bed. This arrangement was created to evaluate the distribution along the crosstie when 100% of the machine applied load was concentrated on the pressure cells.

Series #3 was a little different as a 2-inch (5.1 cm) by 10-inch (25.4 cm) board was used to interface the crosstie and cells from the ballast bed. This was done to minimize the effect of localized high and low areas on the surface of the ballast bed. The effects of those high and low spots, as will be described later in the data presentation section, greatly affected the results obtained during the Series #1 and #2 tests. This was due to the repeated static loading of the testing machine initiated settlement in the ballast bed, which had to be re-leveled for each new set of tests. With the inclusion of the wood board, less ballast manipulation between tests had to be performed.

Series #4 was evaluated for comparison with the results of Series #2. This arrangement, which minimized effect of ballast settlement, should provide an analysis of the pressure distribution with 100% of the machine applied load concentrated on the pressure cells. A complete presentation of tests performed for each series is contained in Appendix E.

Laboratory Data Consistency/Inconsistency for Each Series

The data was compiled to determine the consistencies and/or inconsistencies for each particular pressure cell for all four arrangement conditions. The data presented in Figure 5.5 to 5.17 contains the trends observed for each particular arrangement based on the applied machine loading and the pressure cell measured response (psi).

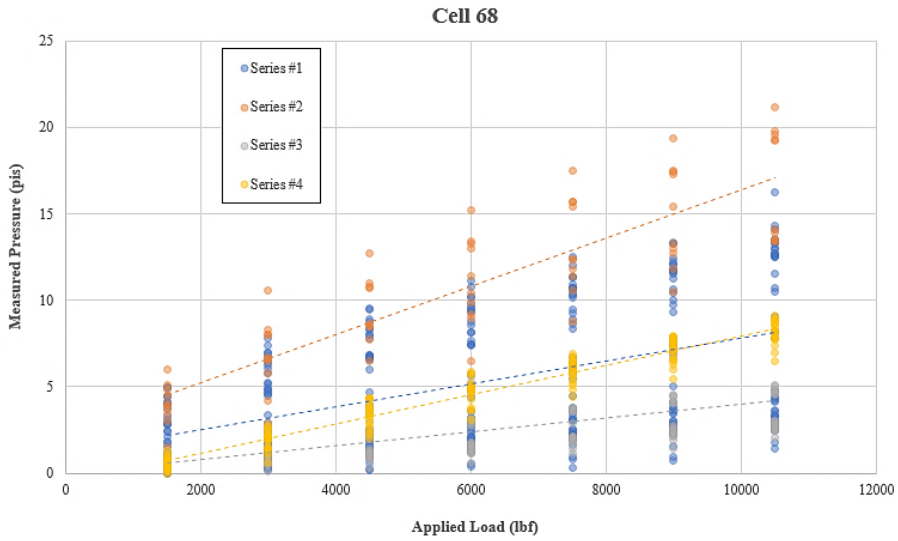

Figure 5.5 Applied Load and Measured Pressure Response for Cell 68

For pressure cell 68, which was positioned at the simulated centerline of the track, it is obvious that variations within particular arrangements and between arrangements exists, as shown in Figure 5.5. In particular, using a linear relationship it was noted that the R^2 correlative value for each series was 0.24, 0.74, 0.42, and 0.94, for series #1 through #4, respectively. Series #1, 2 and 3 in particular produced significant variations between test sequences. Based on observations during laboratory testing, this type of variation was determined to be caused by uneven concentration of compaction within the ballast bed. This was primarily due to the fact that the machine applied loading was concentrated at the rail seat, which inevitably induced localized high and low spots on the surface of the ballast.

Areas farther away from the load application, such as cell 68, did not receive the same amount of compaction. Based on these variations in compaction effort, cells in an area with less compaction inevitably had lower pressure readings. The adjoining cells in this case basically “bridged” over the surrounding ballast. Cells such as cell 70 had a much firmer contact with the ballast bed, resulting in higher pressure readings.

In an effort to address this situation, a series of smaller wood boards positioned at each desired pressure cell location, and a 2-inch (5.1 cm) by 10-inch (25.4 cm) wood beam were used in an attempt to uniformly distribute the compaction effort across the entire length of the ballast bed. As shown in Figure 5.6, the wood beam was positioned vertically to take advantage of the wood’s tangential mechanical properties as the machine load was applied through the normal increments of testing.

Figure 5.6 Ballast Bed Compaction Attempt

However, even with the considerable effort taken to uniformly distribute the compaction effort across the ballast bed, observations made, which are also reflected in the test results, indicate that the ballast bed still became uneven just after a few test sequences. Therefore, additional arrangement conditions (series #2 through #4) were conducted to address this problem.

Figure 5.7 and 5.8 illustrate the variations for cell 68 based on pressure magnitude and load percentage among all cells. As can be seen in the figure, series #1 and #3 share similar results for cell 68, as results for both arrangements were similar. Only a difference of about 2% in load percentage exists between these sets of tests, which is typically around 12-14% of the load. A similar relationship between series #2 and #4 can be seen as well, as only load percentage in comparison with the adjacent cells only varies by about 1%. These two series of tests suggest that the load transmitted at the centerline is around 3-4%. The load differential between the two similar set groupings is based entirely on the load concentration performed with the inclusion of 8-inch (20.3 cm) metal spacers, which negated any load transferring from the crosstie to the ballast.

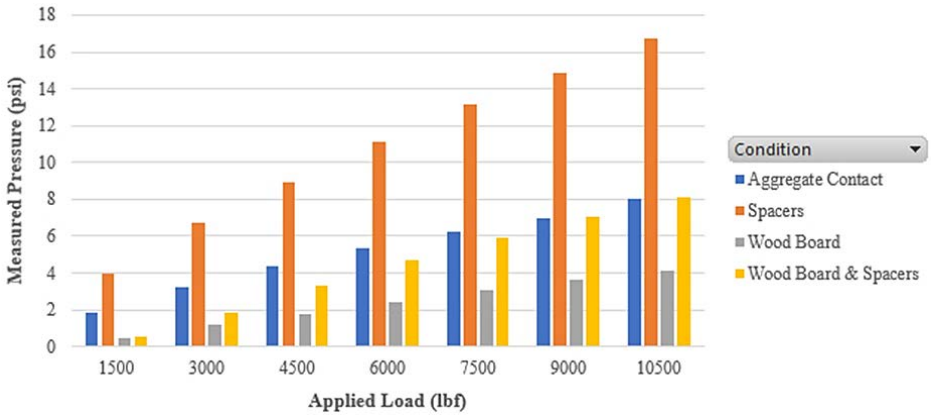

Figure 5.7 Arrangement Variations for Cell 68 via Measured Pressure

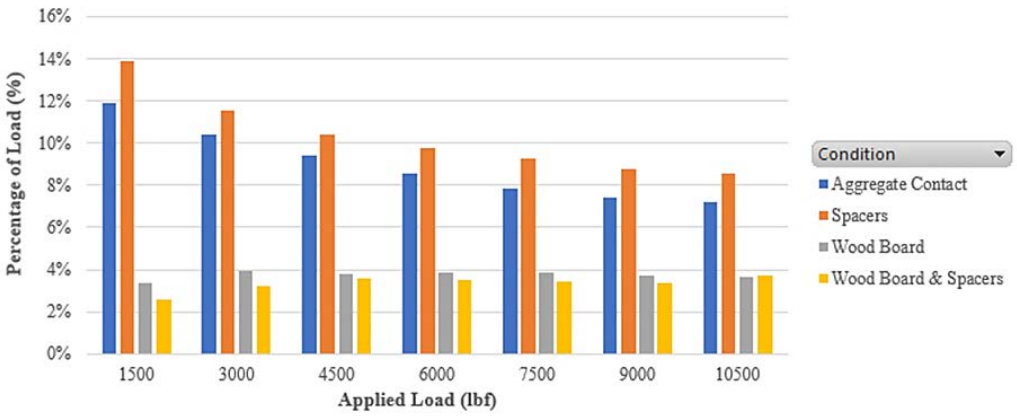

Figure 5.8 Arrangement Variations for Cell 68 via Load Percentage

A similar trend can be seen for cell 69, the midpoint between the rail seat and the centerline, where unevenness in the ballast caused minor variations within and between sets of test. However, on a percentage basis, the load carried at cell 69 is fairly constant between 20-25%. It's interesting to note that in regards to cell 69 and 68, a higher percentage of the load is seen to be carried at lower load applications. It is believed that this is caused by ballast rearrangement during initial load seating. This is all reaffirmed by the R2 relationship values of 0.44, 0.89, 0.74, and 0.99 for test series #1 through #4, respectively. Figure 5.9, 5.10 and Figure 5.11 shows how these tests varied by load application.

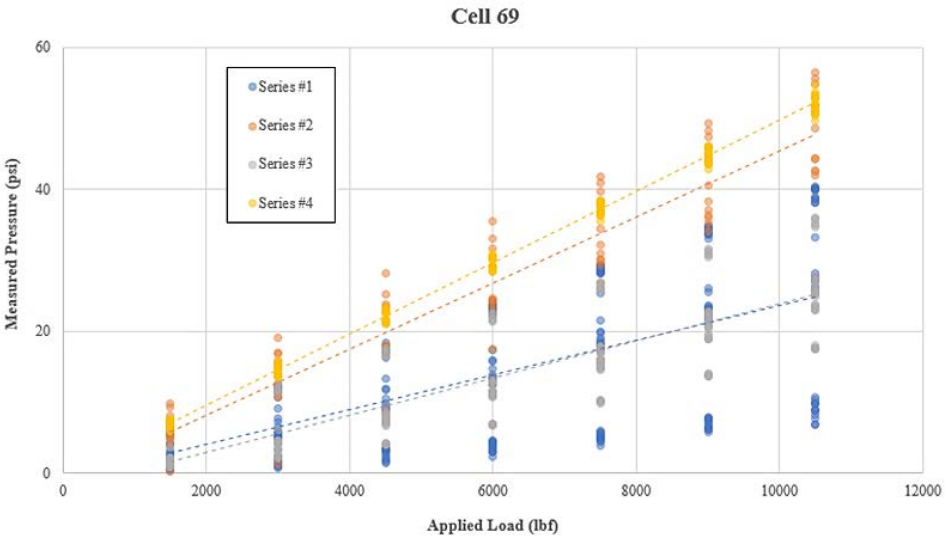

Figure 5.9 Applied Load and Measured Pressure Response for Cell 69

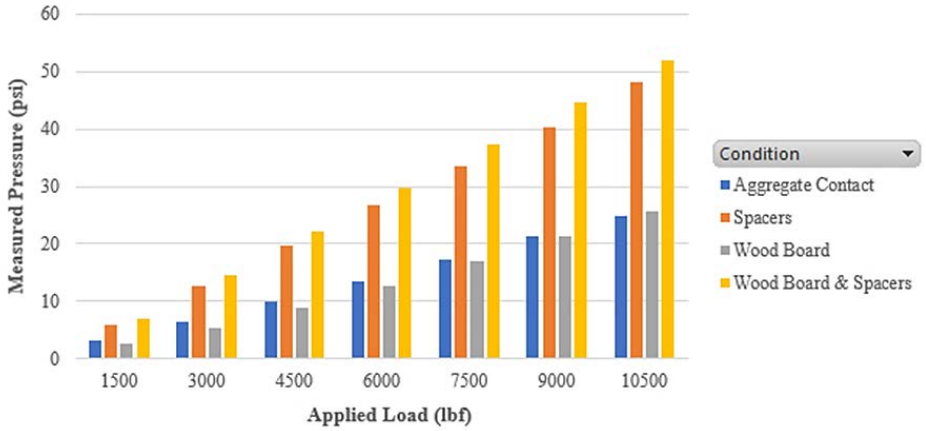

Figure 5.10 Arrangement Variations for Cell 69 via Measured Pressure

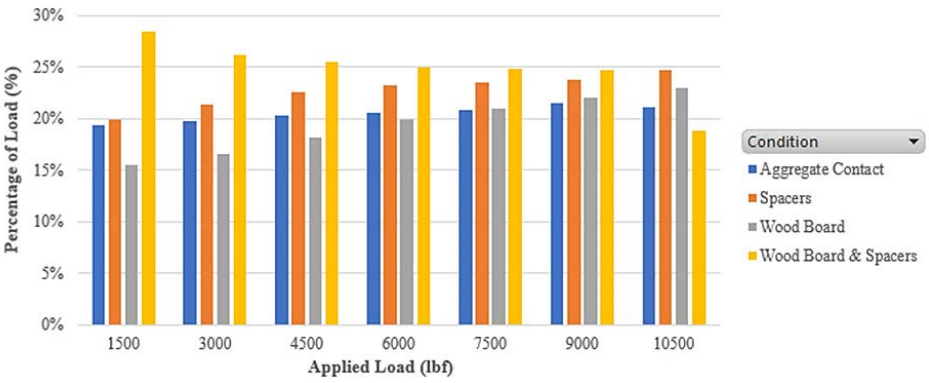

Figure 5.11 Arrangement Variations for Cell 69 via Load Percentage

Cell 70, which was placed directly below the rail seat and the load application, is interesting to analyze because the load percentage for each arrangement is fairly consistent, although each arrangement varies. However, there is a the drop in load percentage between the full aggregate contact condition and the spacer interfaced condition. This reaffirms the conclusion stated prior that the ballast unevenness affecting cell 68 in particular directly correlated to the high spot located at the rail seat. In this case, the load carried at cell 70 dropped 8% between test series #1 and #2, and approximately 2% to 4% of that load was transferred to the adjacent cell locations. This was also verified by high correlations that exist between the measured pressures at cell 70 and the machine applied loads for each arrangement condition. These R^2 relationship values are 0.75, 0.96, 0.94, and 0.98, for series #1 through #4, respectively. Figures 5.12, 5.13 and 5.14 show the variations between series of tests for cell 70. Figure 5.12 in particular shows the linear relationships derived for the R^2 values stated for cell 70.

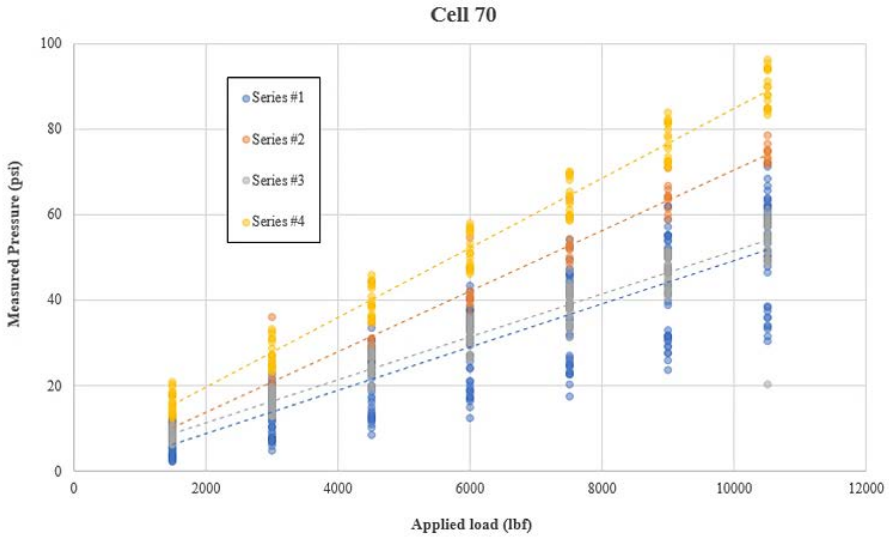

Figure 5.12 Applied Load and Measured Pressure Response for Cell 70

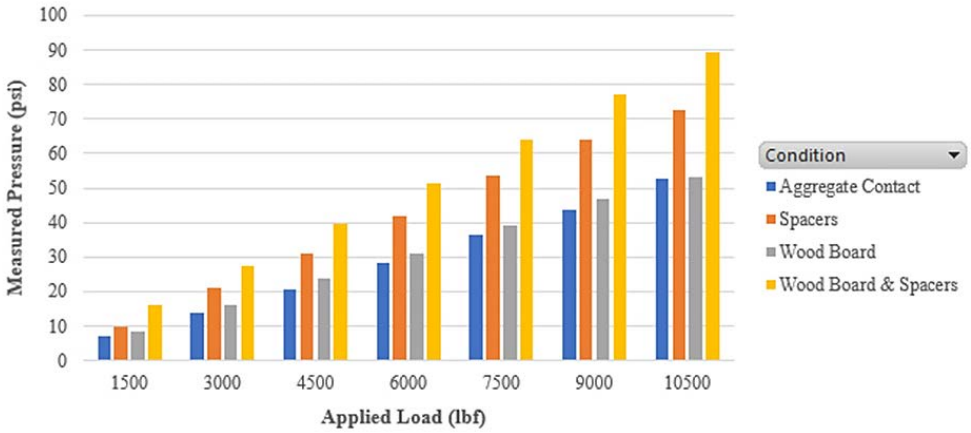

Figure 5.13 Arrangement Variations for Cell 70 via Measured Pressure

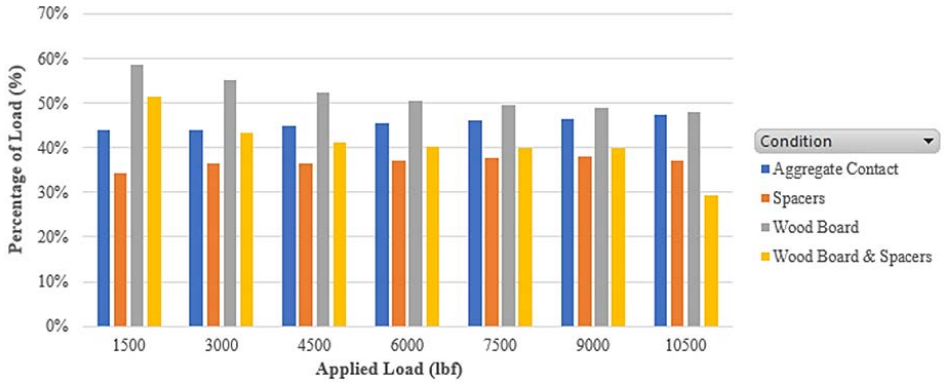

Figure 5.14 Arrangement Variations for Cell 70 via Load Percentage

Cell 71, which was positioned at the end of the crosstie, showed similar results as cell 69 as they were both positioned approximately the same distance from the load application. Very little variation occurred for this between series as R2 values for series #1 through #4 are 0.78, 0.85, 0.93, and 0.96, respectively. Load percentage at this location was found to be typically 25-30%. Figure 5.15 presents the linear relationships that derived the R^2 values stated for this location, and Figures 5.16 and 5.17 detail the variations in pressure and load percentage by arrangement and load application.

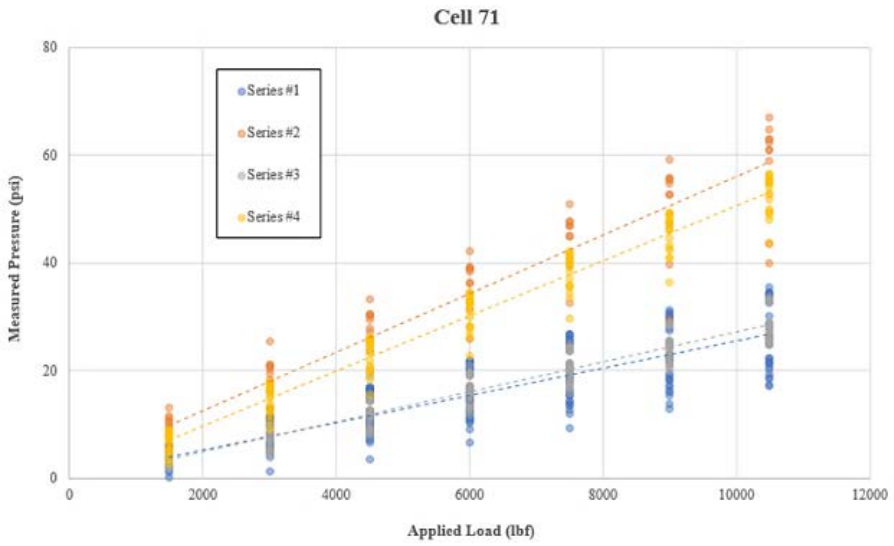

Figure 5.15 Applied Load and Measured Pressure Response for Cell 71

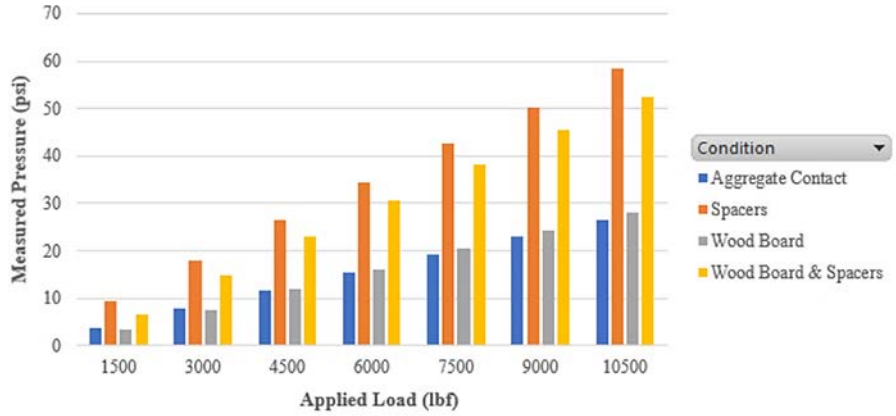

Figure 5.16 Arrangement Variations for Cell 71 via Measured Pressure

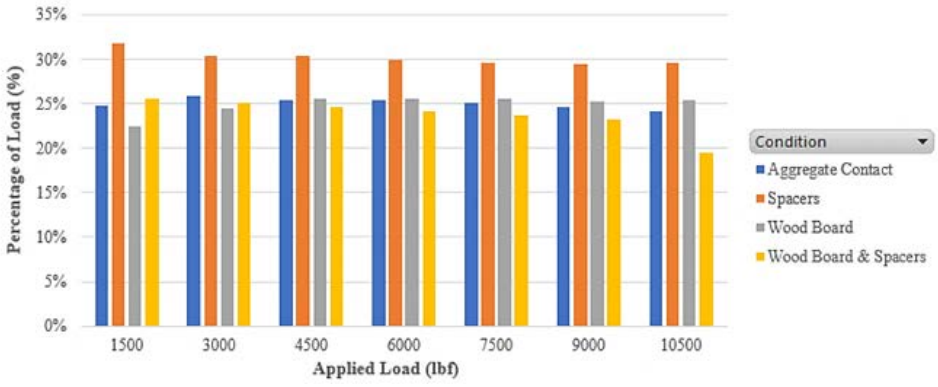

Figure 5.17 Arrangement Variations for Cell 71via Load Percentage

Measured Distributions

To illustrate the data for each arrangement, a series of graphs were created to show the relative distribution along the effective length of the crosstie. This was performed for half-tie sections (55-inches, 1.4 m) in terms of measured pressure response and load percentage. In addition, symmetry was used across the centerline axis to represent the relative distribution along the entire 102-inch (2.6 m) crosstie section.

For Series #1, where full aggregate contact was made with the ballast bed and the instrumented crosstie section, the distributions shown in Figures 5.18, 5.19 and 5.20 were calculated.

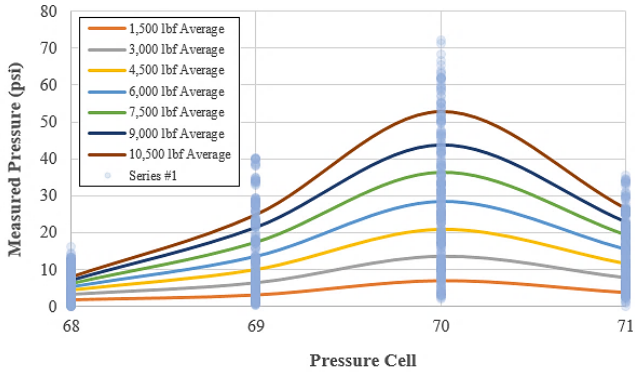

Figure 5.18 Applied Load Distribution of Pressure via Series #1

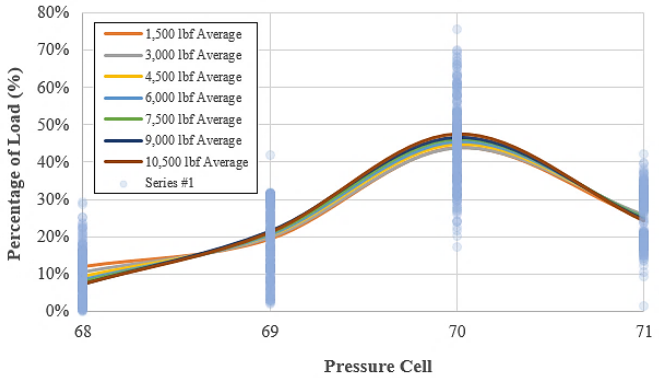

Figure 5.19 Applied Load Distribution of Load Percentage via Series #1

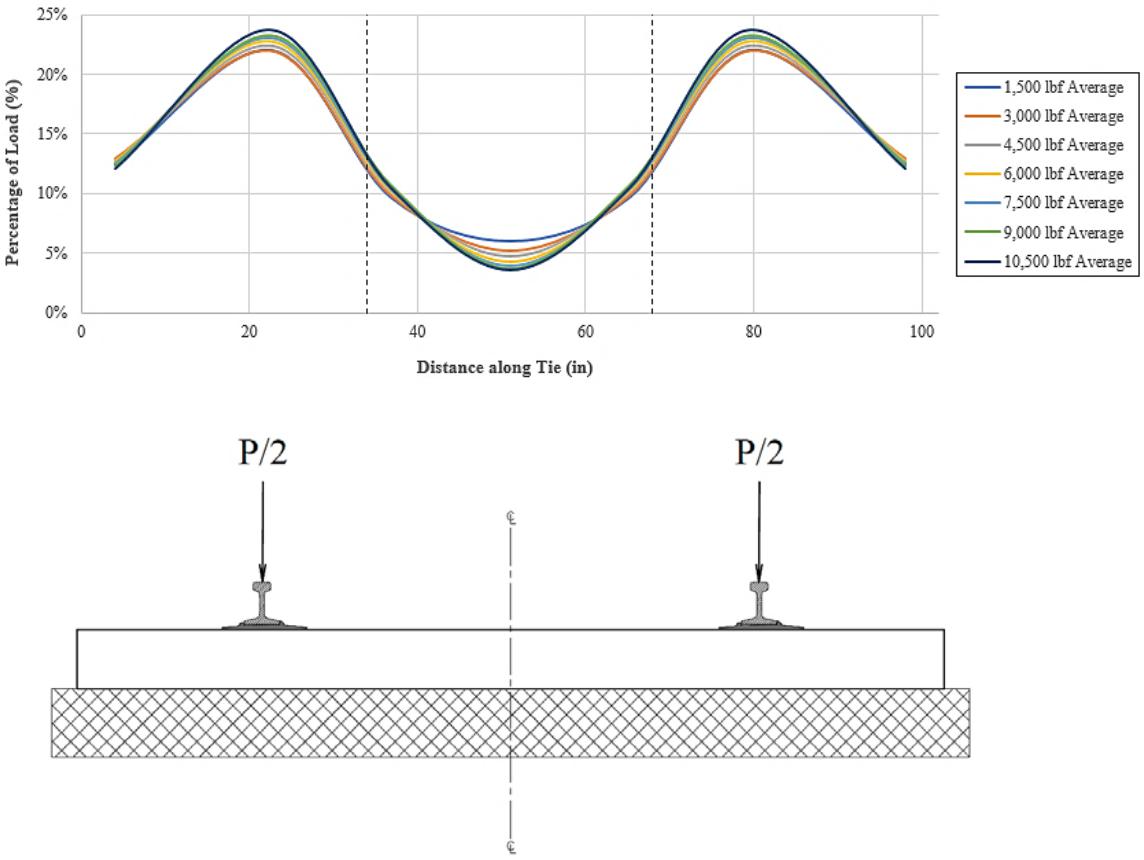

Figure 5.20 Assumed Distribution Along Full Length of Crosstie via Series #1

Based on the load distribution assumption, p/2, included in figure 5.20, the average percentage of load that would be expected at the crosstie-ballast interface, directly below the rail seat, would be approximately 24% of the pressure applied along the entire footprint of the crosstie-ballast interface. If direct measurements are taken at the crosstie-ballast interface, directly below the rail seat in the track, the amount of pressure at other critical locations along the tie can be calculated. As an example, if 30 psi was recorded directly below the rail seat, no more than 5 psi would be expected at the centerline of the track.

It is also interesting to note the dashed lines shown in the top portion of Figure 5.20. These represent the outer-thirds of each end of the crosstie. Assuming this recommendation

would indicate that the load bearing percentages on the crosstie below 12-13% are not considered or negligible for design purposes. Although small on a percentage basis, they should be considered as they can subsequently contribute to center bound failure.

For Series #2, the same type of calculations were performed, and are presented in Figures 5.21, 5.22, and 5.23.

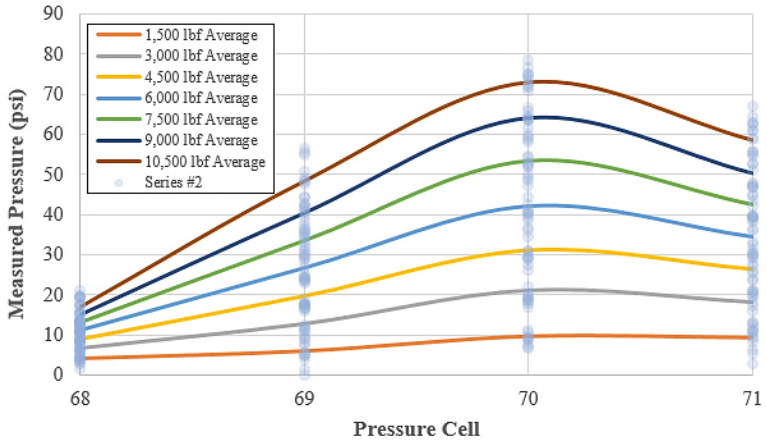

Figure 5.21 Applied Load Distribution of Pressure via Series #2

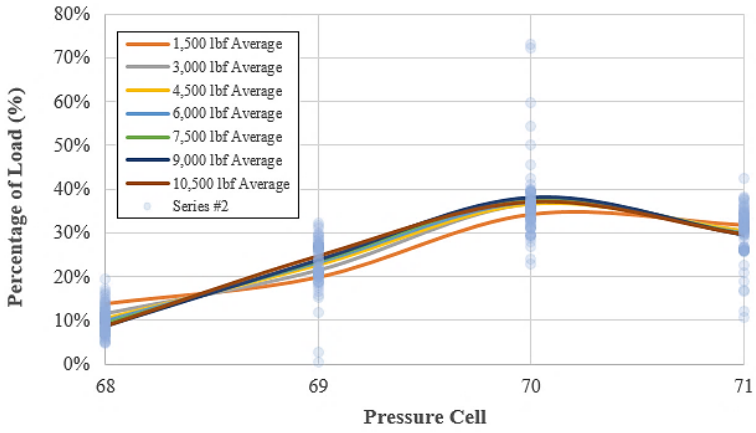

Figure 5.22 Applied Load Distribution of Load Percentage via Series #2

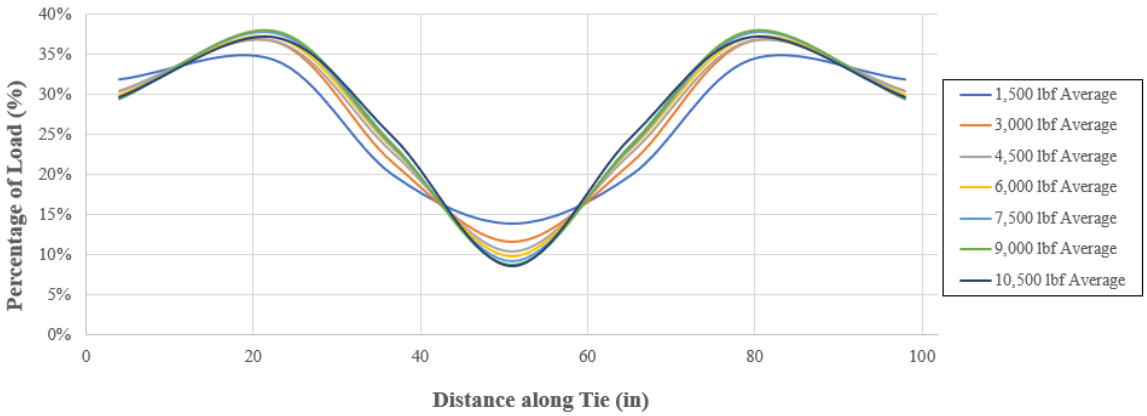

Figure 5.23 Assumed Distribution Along Full Length of Crosstie via Series #2

For this series, the percentage of load expected under the rail seat would be approximately 18%. Using the Series #1 example already presented, this would equate to approximately 7 psi at the centerline of the track. It's also important to note that a higher load percentage was measured on the ends of the crosstie (approx. 15-16%).

For Series #3, the same procedure was performed for a condition considered to possess a more uniform ballast bed; results are shown in Figures 5.24, 5.25, and 5.26.

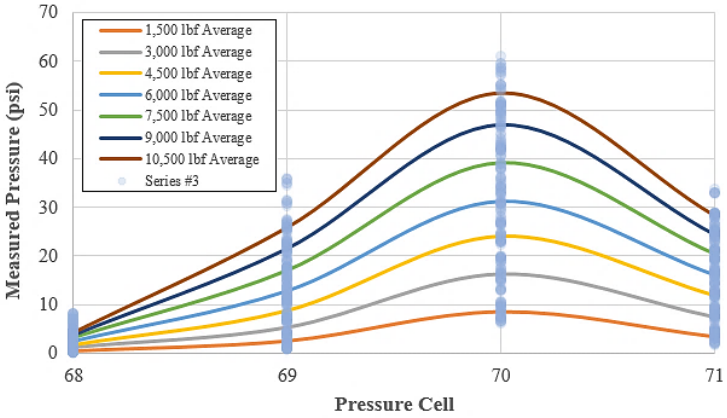

Figure 5.24 Applied Load Distribution of Pressure via Series #3

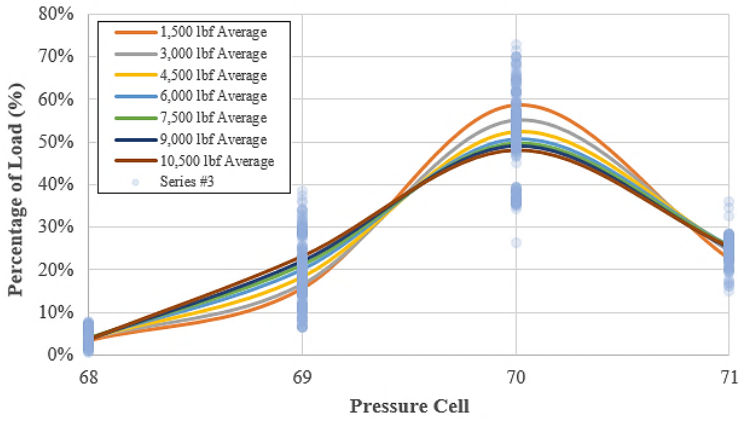

Figure 5.25 Applied Load Distribution of Load Percentage via Series #3

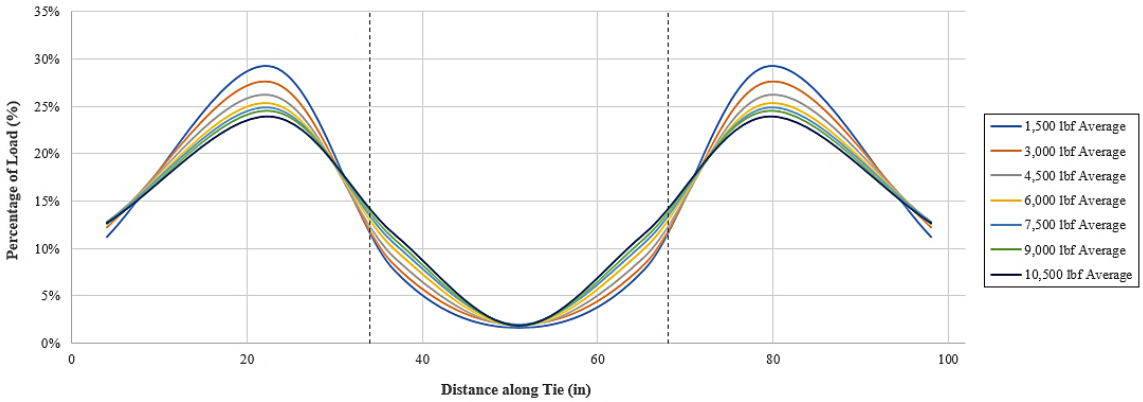

Figure 5.26 Assumed Distribution Along Full Length of Crosstie via Series #3

For this series, the results compared favorably to series #1 in terms of percentages, but a lower concentration at the centerline is observed. This is to be expected for uniform trackbeds. In this case, the rail seat is expected to transmit around 26% of the pressure to the ballast. Using the example described prior, this would account to approximately 2 psi at the centerline of the track.

The same procedure was used to evaluate the relative pressure distribution for Series #4, which was an arrangement consisting of the total load concentration on the pressure cells with a uniform trackbed. These are shown in Figures 5.27, 5.28, and 5.29.

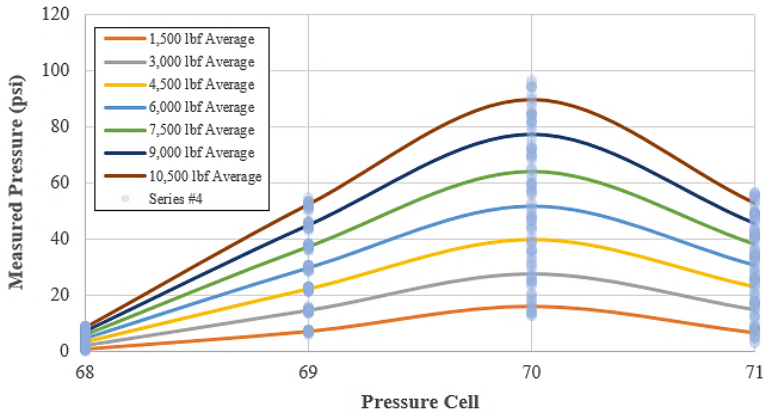

Figure 5.27 Applied Load Distribution of Pressure via Series #4

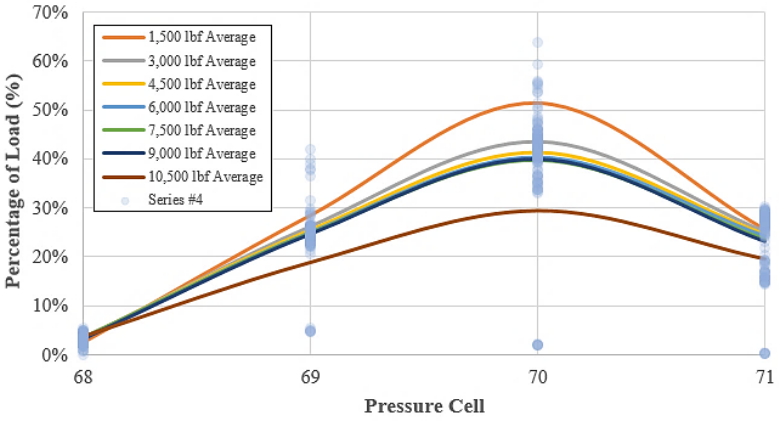

Figure 5.28 Applied Load Distribution of Load Percentage via Series #4

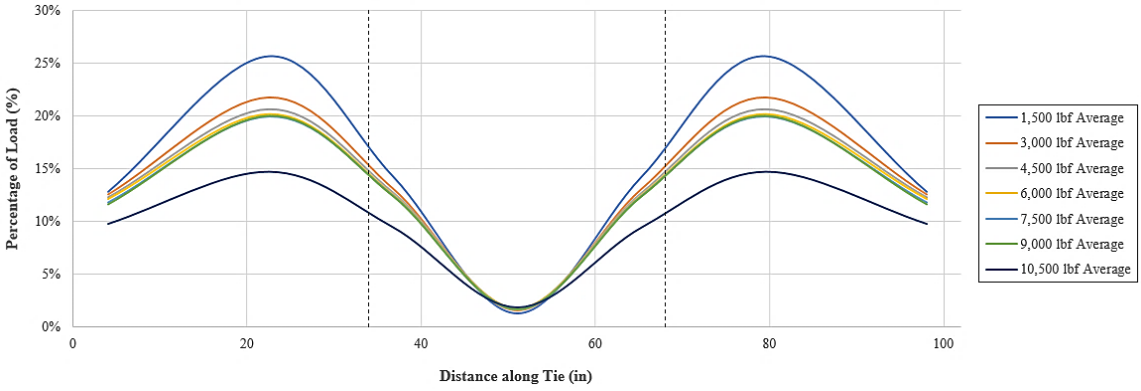

Figure 5.29 Assumed Distribution Along Full Length of Crosstie via Series #4

This series compared favorably with what was seen in series #2, but similar to what was seen in series #3. Less load concentration is seen at the centerline, which should be expected for well consolidated and uniform trackbeds. In this case, approximately 20% of the pressure at the rail seat was transmitted to the ballast. This would equate to approximately 3 psi at the centerline of the track.

An overall chart presenting the average load percentages for each particular cell and each particular test is included in Appendix F. In addition, the example calculations mentioned in this chapter are included in Appendix F.

Additional Evaluations

In addition to evaluating the arrangements described previously, a series of tests were performed to evaluate the effect that load application rate has on the pressures and load percentages at the crosstie-ballast interface.

Load application rates of 0.1 in/min (2.54 mm/min), a standard used for previous tests, 0.2 in/min (5.08 mm/min), and 0.3 in/min (7.6 mm/min) were selected. Arrangement #1 with the crosstie and cells directly in contact with the ballast was also selected as a baseline to identify any variations. The results of those tests are shown in Figures 5.30, 5.31, and 5.32.

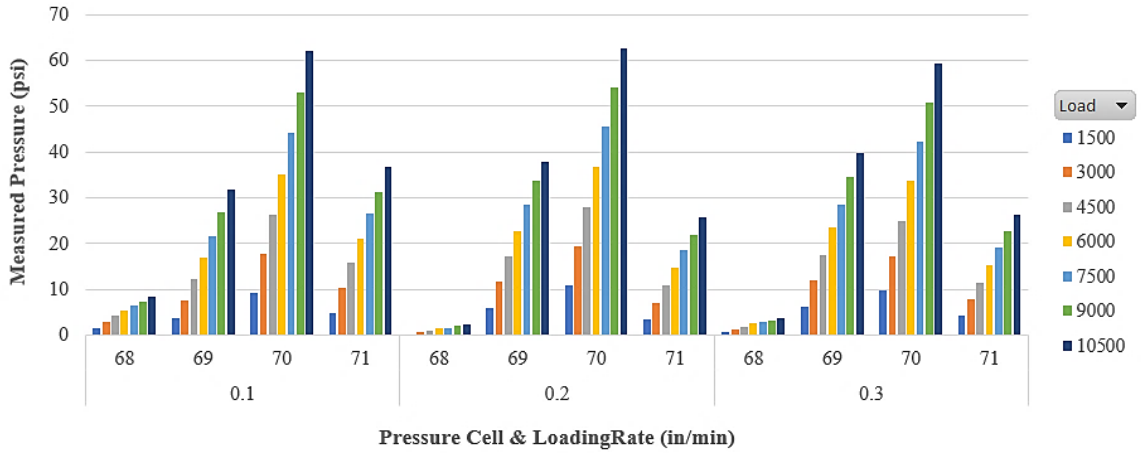

Figure 5.30 Load Rate Variations for Each Cell and Load Application via Pressure

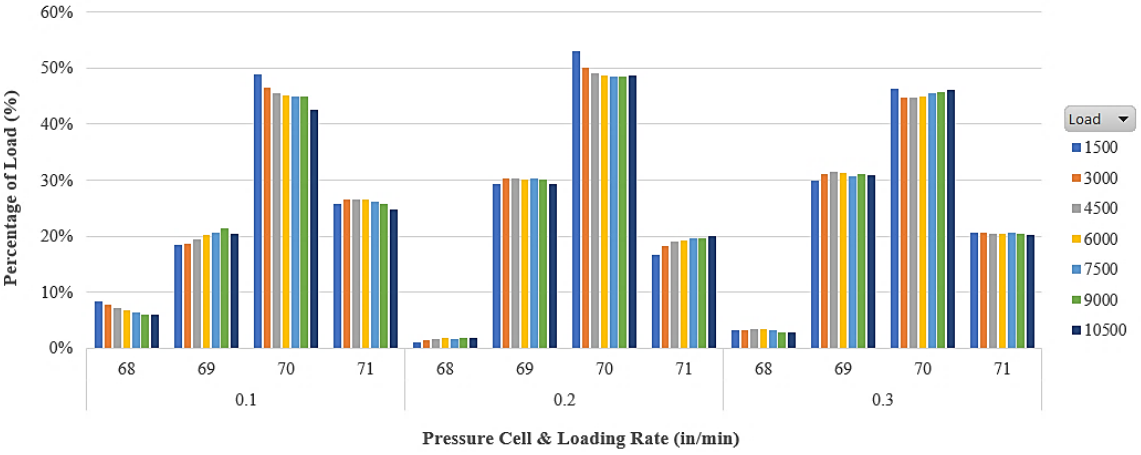

Figure 5.31 Load Rate Variations for Each Cell and Load Application via Percentage

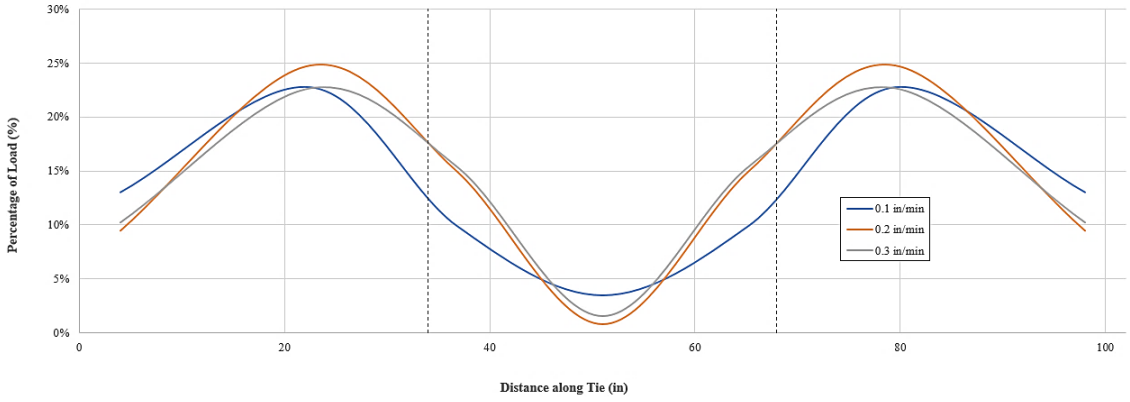

Figure 5.32 Assumed Distribution Along Full Length of Crosstie for Each Load Rate

These results indicate that there exists little to no change exists on the pressure distribution along the footprint of the crosstie for various load rates. It can be noticed that the pressures and load percentage obtained for cell 68 varies slightly, but this change is inherently related to the ballast surface variability between the 0.1 in/min and the 0.2/0.3 in/min tests. The pressures and load percentage for cell 68 actually increase after the 0.2 in/min test, thus reaffirming the fact that the ballast bed levelness and density change frequently for this condition.

Based on the information presented in this chapter, one can notice that the support conditions beneath a crosstie can greatly influence the overall magnitude and distribution of pressures along the footprint of the crosstie. Therefore, it is imperative that these findings considered for in-track testing procedures. Chapter 6 outlines the procedures and presents the results of in-track testing conducted based on the procedures and findings from laboratory tests.

CHAPTER 6. IN-TRACK PRESSURE MEASUREMENTS

Based on the successful and accurate results of laboratory calibration testing using the routing procedure described previously, research was conducted to assess the applicability of this method for measuring in-track pressures. The site subsequently selected to perform this evaluation was at Mascot, TN.

Mascot, TN Test Site

The Mascot, TN test site is located on a tangent section of a Norfolk Southern (NS) mainline track approximately 20 miles (30.2 km) east of Knoxville, TN. The track consists of 136 RE continuous welded rail secured with cut spike fasteners to timber crossties. Crossties are positioned at approximately 20-inch (50.8 cm) center-to-center spacing and each crosstie is box anchored. The track support at this site consists of standard NS mainline granite ballast on a well-seasoned roadbed. NS personnel reported that the area has a long record of stable roadbed/trackbed behavior requiring minimal track maintenance. The most recent timber and surfacing procedure was completed in November of 2015.

As alluded to previously, the test site is positioned on a horizontal tangent section with a 0.25% vertical grade which is eastbound ascending. The track annually carries approximately 37 million gross tons (MGT) of traffic, with a maximum train speed of 45 mph (72 km/hr).

All east-west bound trains passing through Knoxville, TN traverse this test site. A wayside automatic equipment identification (AEI) reader adjacent to the test site

documents the passing train consist. In addition, through trains that pass over Wheel Impact Load Detector (WILD) sites west of Knoxville at either Ebenezer, TN or Flatrock, KY pass this site as well. The data from the WILD permits subsequent comparisons of the crosstie-ballast pressures versus wheel-rail impact loads, which will be discussed in greater detail in Chapter 7. Figure 6.1 contains an aerial view of the test site, and two photos depicting the on-site conditions.

Figure 6.1 Mascot, TN Test Site

Instrumented Crosstie Installation

In order to place instrumented crossties into the track at this site, special precaution was made in protecting the electrical components using thin metal plates to cover the transducer housing. Waterproof electrical boxes were used adjacent to the track to store the instrument wiring (as was discussed in Chapter 3). Fortunately, NS provided the equipment and personnel necessary to install the series of instrumented crossties. The crew took extreme care to avoid damage to the instrumented crossties during the installation process. Figure 6.2 illustrates the handling (a) and placement (b) of the instrumented ties.

Figure 6.2 Handling and Placement of Instrumented Crossties

The instrumented crossties were also immediately tamped and a testing procedure similar to what was used during laboratory calibration was used. Initially only the instrumented crossties were tamped, but after some initial testing, fifteen approach crossties on either side of the test section were also tamped to provide uniform ballast consolidation on the approaches and within the test area. Figure 6.3 shows the NS crew tamping the test site after installation.

Figure 6.3 Tamping the Test Section

The entire installation consisted of inserting eight instrumented crossties into the trackbed. Four of those crossties were instrumented with a pressure cell directly under one rail seat. As for the other four crossties, two of them were instrumented with cells below both rail seats, and the others instrumented only at the centerline. Figure 6.4 illustrates and labels the location and identification for each particular cell.

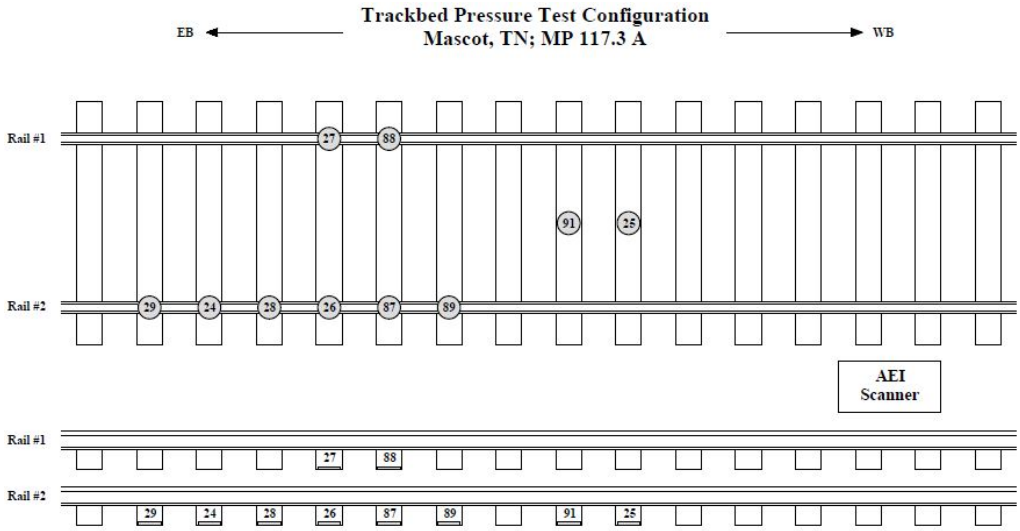

Figure 6.4 Pressure Cell Locations

Data Acquisition

Using the data acquisition equipment described previously, eight cells are connected directly to a data logger for simultaneous and dynamic logging at 2 kHz (2,000

samples/second). This sample rate allows for adequate sampling of wheel impacts as the wheels traverse the test section encompassing a full revolution of a 33-inch (83.8 cm) diameter wheel. In addition to recording pressures, the following information was obtained for each test train.

- Train Number
- Lead Locomotive Number
- Time
- Type of Train
- Number of Locomotives
- Number of Axles
- Direction of Travel
- Gallons of Fuel
- Speed of Train
- Length of Train
- Tonnage of Train
- Number of Cars

Using this information, several relationships were derived for particular pressure behavior. Figure 6.5 presents a schematic for the testing procedure used at the Mascot, TN test site. Note that in addition to the 12 Vdc power station used to power the data logger, an extra 12 Vdc battery is positioned adjacent to the testing equipment. This is required for in-track testing as time between tests can vary from several minutes to several hours, thus the battery of the laptop computer may need to be charged. The extra battery can also serve as a backup for the existing power station.

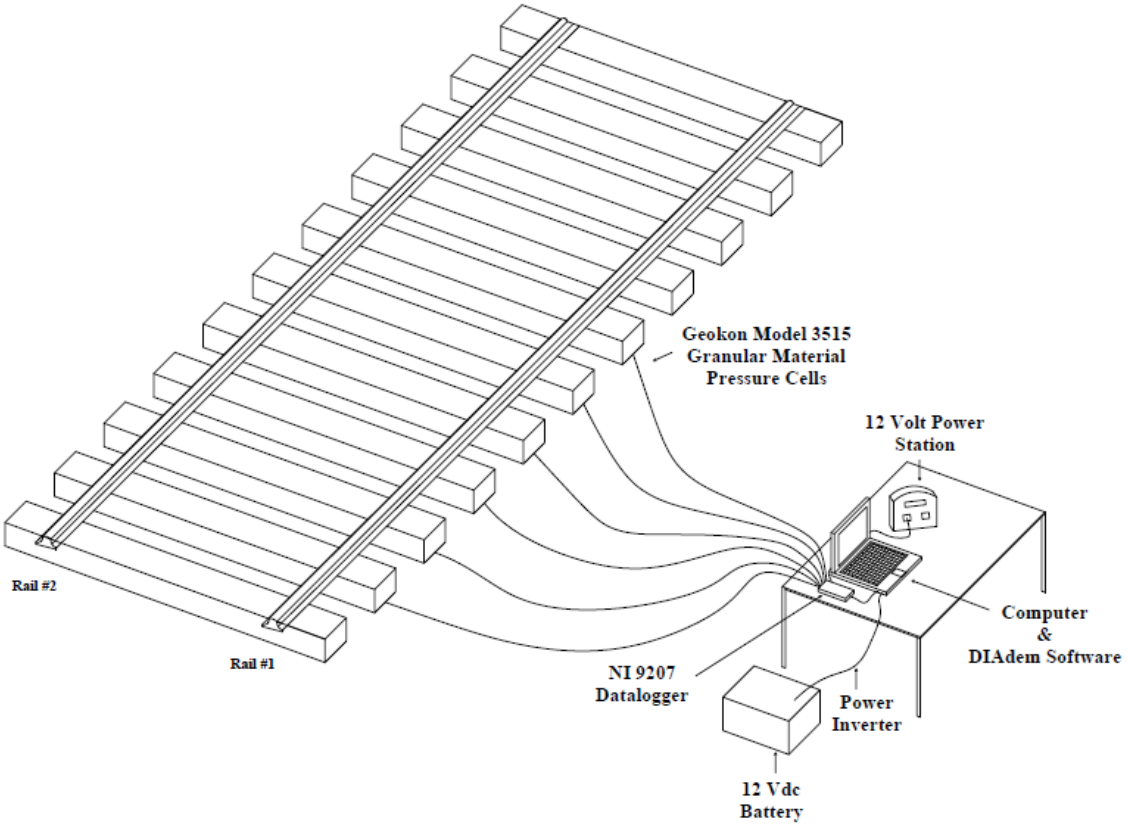

Figure 6.5 Data Acquisition Setup for In-Track Testing

Various Pressure Data Measurements

Based on the testing procedure outlined previously, the dynamic pressure measurements of a revenue train can be recorded and analyzed in greater detail. Figure 6.6 shows the pressure recording of a typical mixed train with heavy and light axle loads.

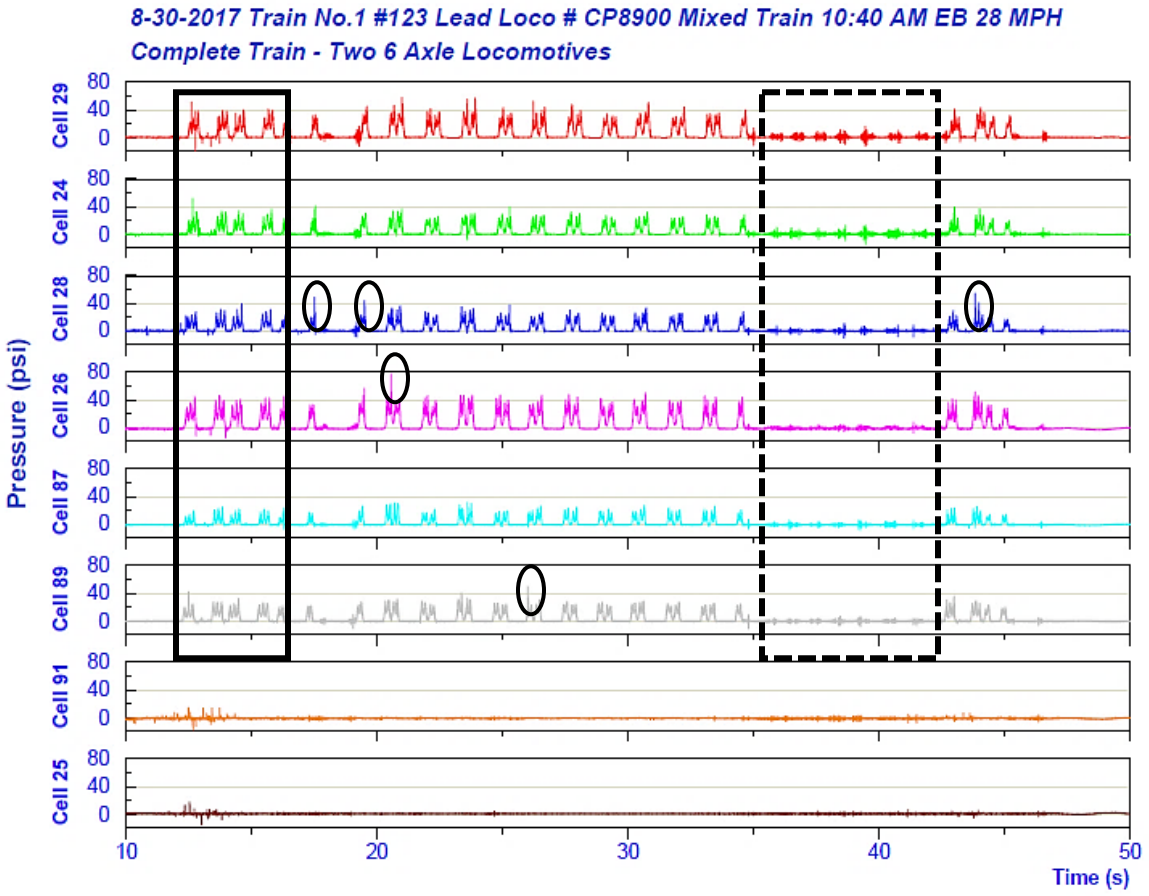

Figure 6.6 Typical Pressure Reading of a Revenue Train

As noted in Figure 6.6, there are a considerable amount of unique characteristics and behaviors based on the interaction at the wheel-rail interface. The first being the distinct signature of the two 6-axle locomotives that lead the train consist (outlined with a solid black rectangle). Each of the twelve axles can be seen clearly and are typically associated with a magnitude of 30 psi (206.8 kPa). There is also an inherent shift among all pressure cell readings as noted in the enlarged lead locomotive in Figure 6.7.

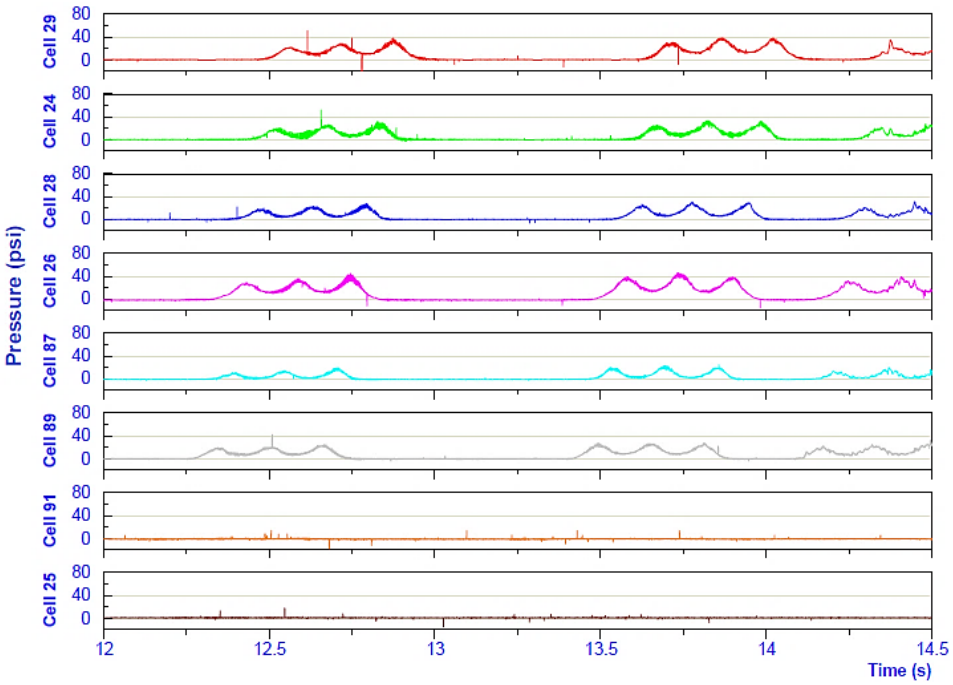

Figure 6.7 Enlarged Scale of Lead Locomotive

This shift is due to the amount of time it takes for an axle to traverse a particular crosstie to the adjacent crosstie. The local maximum of each pressure signature denotes the instance in time when an axle is directly over an instrumented tie. In the case of the example shown in Figure 6.7, the revenue train was moving in an east-bound direction since the lead axle of the lead locomotive registered pressure on Cell 89 before any of the other instrumented ties.

Another unique characteristic noted in Figure 6.6 is the distinctive signatures of heavily loaded freight cars (timeframe of 20-35 seconds), and empty/lightly loaded freight cars (highlighted with a dashed line rectangle). For heavily loaded freight cars, each of the four axles of an individual car can be clearly identified (similar to the locomotives), and the pressure magnitudes for a particular axle is typically in the range of 20-30 psi (137.9-206.8 kPa), depending on the loading and car type. A significant difference between car types can be noted in Figure 6.8, where a series of flex-van articulated intermodal train cars

traversed the test site. For a typical mixed or unit revenue train, the signatures of each axle for a particular car remain consistent, as the load is distributed equally on each axle. However, in the case of a series of articulated intermodal cars, the shared truck portion (highlighted with a solid black rectangle) typically registers pressures much lower than those not shared (dashed line rectangle). Those trucks and axles that are not shared, actually behave similar to that of a locomotive, with axle pressure equal if not exceeding those of a locomotive (30-40 psi, 206.8-275.8 kPa). This is an interesting behavior to acknowledge as these more frequent and heavy axle loads can lead to more frequent maintenance activities.

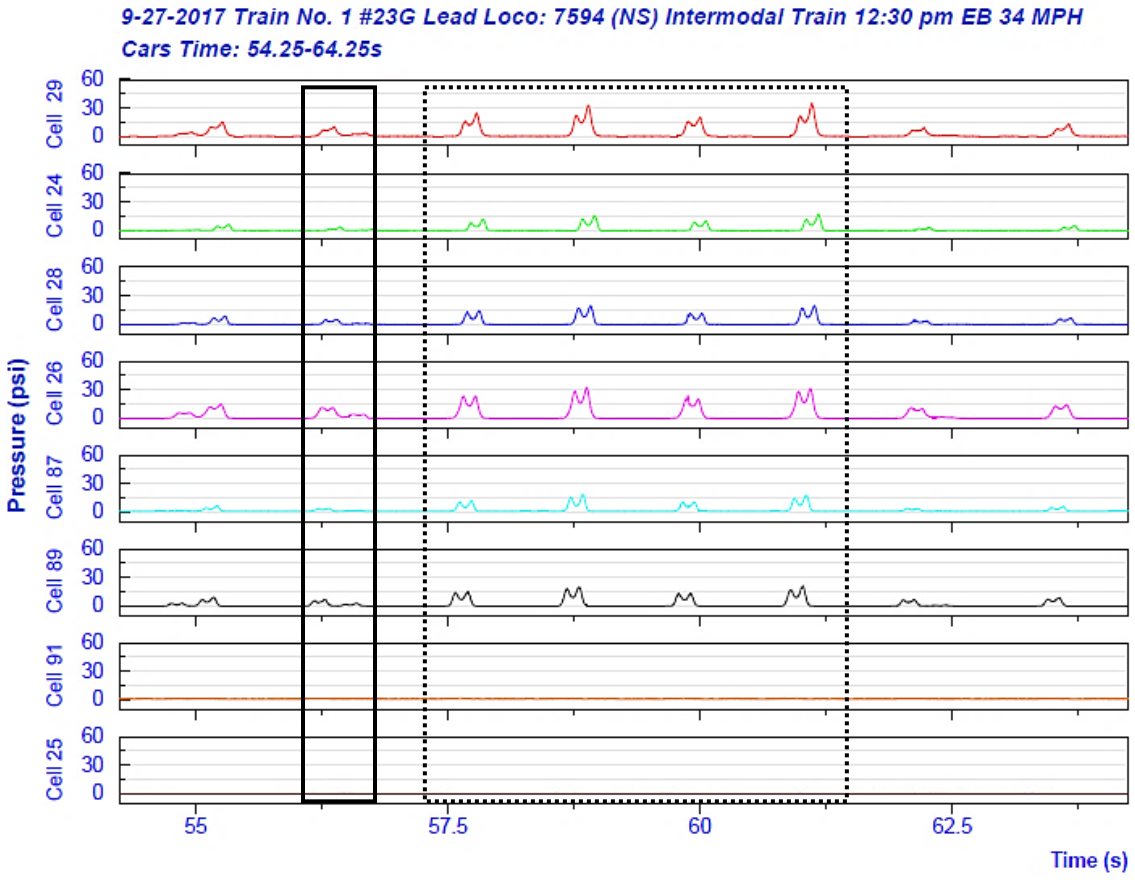

Figure 6.8 Typical Series of Intermodal Cars

Examining the signature of an empty/lightly loaded series of freight cars (shown in Figure 6.6), it is difficult to identify the axles as they pass over the instrumented ties. The magnitude of the pressure signature that can be seen is only in the range of 0-3 psi (0-20.7 kPa), which is negligible. In addition to the low magnitudes, inherent noise and/or vibration registers with these empty/light loads, which tends to suggest that these cars vibrate and shift a considerable amount during travel.

In addition to the characteristics already described, the behavior of wheel irregularities can also be noticed while recording tie/ballast pressures. These wheel irregularities, commonly referred to as wheel flats, are indicated by large spikes of pressure at a split-second instant of time (highlighted with black ovals in Figure 6.6). These wheel irregularities have been observed to increase the pressure of a particular axle by several orders of magnitude and can range from 50-100 psi (344.7-689.5 kPa) depending on the severity of the wheel irregularity. As can be noticed in Figure 6.6, the same wheel irregularity is typically only registered on one or two cells as only one complete wheel revolution is recorded. A schematic showing the span of ties needed for one complete wheel revolution is shown in Figure 6.9. The black and red dots represent the ends of the revolving wheel set.

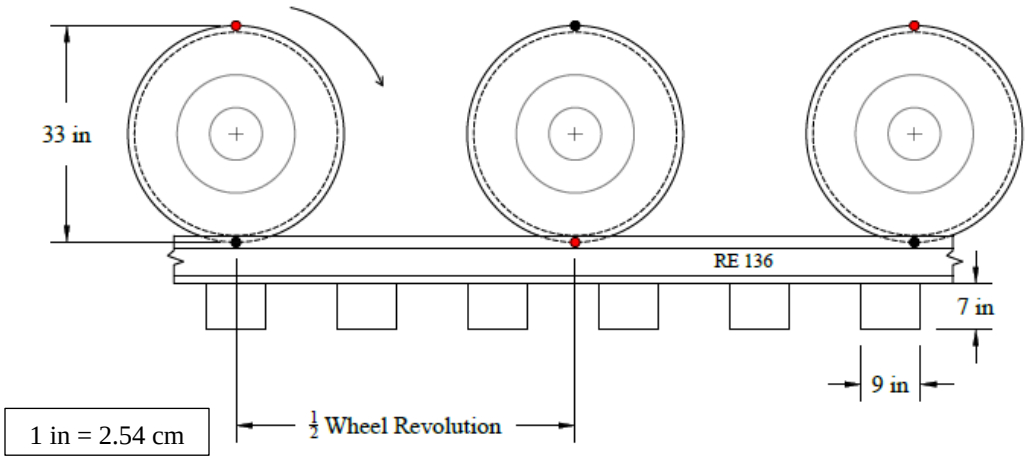

Figure 6.9 One Wheel Revolution over Test Section

Although somewhat insignificant, it is also important to note the behavior of the pressure cells located at the centerline of the track. As can be noted in Figures 6.6-6.8, the pressures recorded at the tie/ballast interface at the centerline of the track structure (Cells 91 and 25) register pressures in the range of 0-2 psi (0-13.8 kPa) and are not subject to change over time. Due to these low readings and based on the fact that there are no discernable wave signatures at the centerline, it is hard to quantify any relationships or other unique characteristics at this location. Thus, the relationships discussed in the following section will be based on the pressure cell readings under the rail seat.

Pressure Relationships Over Time

Since establishing a methodology to record the crosstie-ballast pressures of revenue trains, several tests and maintenance procedures have been performed over the span of nearly two years to describe the typical behavior and pressure magnitudes at the tie/ballast interface. This span of time consisted of nineteen different testing days, with a total of 58 revenue trains recorded. Of those 58 revenue trains, 42 were designated as mixed freight,

and 8 of them were of the intermodal variety. The other 8 trains measured consisted of a few empty unit coal, loaded unit coal, rail, and auto trains. The complete listing of trains observed over this time can be found in Appendix G. In addition, an example recording of each train type is included in Appendix H.

To describe the behavior at the crosstie-ballast interface over this span of time, Figure 6.10 was created, which graphically represents the average and range of pressures for locomotives that traversed the test section on each test date. In addition, the graphic denotes when a specific type of maintenance activity was performed, such as tamping or surfacing. Each test date is labeled with a letter for simplicity; Table 6.1 provides a guide for the actual test date that corresponds to each letter.

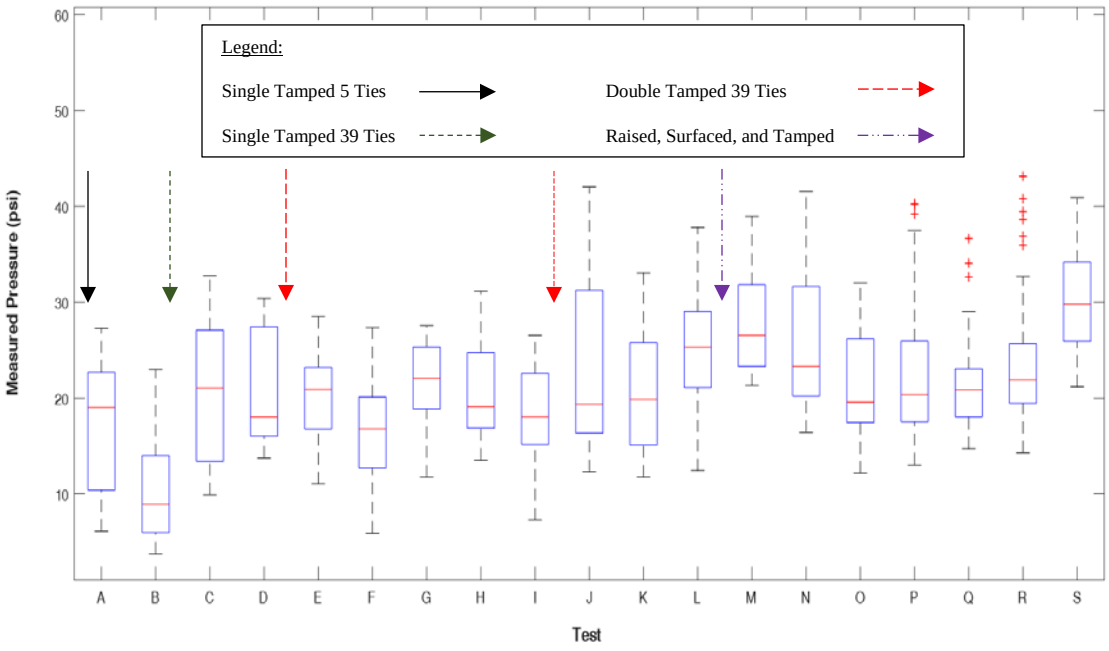

Figure 6.10 Average and Range of Pressures Measured at Mascot, TN

Table 6.1 Legend for Test Dates

A	B	C	D	E	F	G	H	I	J
9/26/16	10/12/16	10/26/16	11/7/16	11/28/16	12/15/16	4/13/17	4/27/17	4/28/17	6/26/17
K	L	M	N	O	P	Q	R	S	
6/27/17	8/7/17	8/8/17	8/30/17	9/27/17	11/3/17	2/9/18	3/9/18	6/25/18	

Although measurements are seen to fluctuate a minor amount over time, the pressure cells do indicate that for typical locomotives (33,000 lbf wheel load), the pressures transmitted at the crosstie-ballast interface are in the range of 20-30 psi (137.9-206.8 kPa) on average, and usually do not exceed 40 psi (275.8 kPa). This is an interested fact to note as trackbeds are designed with the assumption that the load transmission at this interface is in the range of 65 psi (448.2 kPa) for timber crossties.

Although interesting, it is important to note some potential reasons for the pressure fluctuations that are potentially skewing these results. The first being the maintenance procedures deployed over the span of these tests. As mentioned previously, when the first series of instrumented ties were installed, only the instrumented ties were tamped. This procedure, as shown in Figure 6.10, actually caused non-uniform ballast settlement which reduced the pressures transmitted to the crosstie-ballast interface for the ensuing test sequence. After this was observed, 15 approach ties on either side of the test section, along with the ties within the test section (39 total), were single tamped to provide a more uniform trackbed. After this sequence, pressures did increase, but then dropped off slightly in the following test sequence. A double-tamping procedure was then used at two different instances, but results were still variable. Due to this variability, the track was actually given a raise and was surfaced accordingly to make certain that the ballast throughout the entire test section was uniformly consolidated. After the surfacing procedure, results were more consistent over the concluding seven test sequences.

In addition to the concern for ballast uniformity, temperature has also been considered to have an effect on the recorded pressures. Figure 6.11 compares the reported ambient temperature (Weather Underground, 2018) and the average locomotive pressure

for each revenue train. Based on the figure, there does seem to be a slight trend in some instances due to temperature, such as the decrease in pressure during test sequence “F” (12/15/2017) with a decrease in temperature, but the trend is not consistent. As an example, between test sequences “P” and “Q”, there is a significant drop in temperature, but the pressures remain relatively constant. When performing a regression analysis between the average pressure and temperature readings, no relationship was apparent. Thus, variations in temperature may not have an effect. Based on the manufactures’ cell specifications relating to temperature discussed in Chapter 3, there should be negligible effects due to temperature.

Figure 6.11 Average Pressure Compared to Ambient Temperature

One of the limitations of this study is the fact that much of the information, specifically in regards to relative car weights is unknown, which makes it difficult to provide substantial justification for the trends presented in this chapter. Even though most locomotives are assumed to have a wheel load of 33,000 lbs (146.7 kN), some of the variation in pressures presented previously may be due to the actual variation in wheel loads among locomotives. This is where the utilization of Wheel-Impact Load Detector

data can and will be useful to perform direct wheel for wheel correlations between wheel/rail forces and tie/ballast pressure. This will be discussed in greater detail in Chapter 7.

CHAPTER 7. WHEEL IMPACT LOAD DETECTOR (WILD) RELATIONSHIPS

As alluded to in the previous chapter, data produced by Wheel Impact Load Detectors (WILD) can provide researchers with the opportunity to directly compare the loads applied to the wheel-rail interface with the pressures transmitted to the crosstie-ballast interface. With the ability to directly compare these two datasets, the data acquired through this study at the crosstie-ballast interface can be more adequately justified.

Development of the Wheel Impact Load Detector

The undesirable effects of wheel/rail impact loadings on the track and supporting structure have been considered and evaluated for many years. A primary reason for the virtual demise of jointed rail track for mainline trackage was to eliminate the need of incorporating joints every 39 ft (11.9 m). The impact forces that ensued from the wheels having to traverse the open section of the rail at the joint resulted in impact forces on the track and support structure with attendant settlement of the track in the vicinity of the joint. The individual rails became misaligned vertically across the joint and the wheels added additional impact forces and accelerated wear at the rail ends. This also increased impact forces and settlement of the track and support structure. Railroad track maintenance forces routinely raised and surfaced the track in the joint areas to reduce impact forces at the joints. This was particularly the prevailing situation when marginal quality trackbed support layers were often the norm, and when coupled with inadequate drainage, the trackbed provided less than desirable structural support.

Technological advances beginning in the mid-1900s to produce continuously welded rail (CWR) resulted in the advancement of installing rail without joints which was

subsequently widely adopted as a standard for mainline track. A smoother and much improved ride quality ensued with greatly decreased impact forces at the wheel/rail interface. This in turn reduced track maintenance efforts and costs, which extended the life of the rail and track components.

Although the adoption of CWR for mainline, high tonnage rail lines eliminated the primary source of wheel-rail impact forces, it alone did not completely eliminate impact forces. An additional source of impact forces was due to imperfections in the wheel tread contact surface as it rolled along the rail. These were typically flat spots, but also included imperfections in the steel, resulting in "rough" spots on the tread surface. The impact forces resulted in higher stresses in the wheel and the rail that could result in damage to the rail cars and lading and damage to the track and support structure.

The technology for continuously measuring contact forces, including normal and added impact forces due to wheel imperfections, was developed in 1983. Salient Systems (recently became a wholly owned subsidiary of LB Foster Company) was involved with the early development and applications of this technology. The incorporation of wayside wheel impact load detectors (WILDs) began in 1984 and by 1995 more than sixty systems had been installed in North America and Europe by Salient Systems (LB Foster - Salient Systems, 2018).

The incorporation of WILDs is considered a standard practice for major railroads. These are strategically placed at selected locations throughout the system in order to routinely measure and evaluate the presence and severity of wheels producing high impact forces at the wheel/rail interface. Wheels having imperfections exceeding specified limits

are detected, inspected, tracked, removed based on specified criteria, and replaced with new wheels based on industry standards (Wiley & Elsaleiby, 2011) & (Wiley & Elsaleiby, 2012).

WILD Measurement Procedure and Output

A Wheel Impact Load Detector (WILD) consists of a series of individual strain gauges mounted on the neutral axis of web of the rail for a consecutive series of cribs for measuring vertical rail strain in order to calculate wheel loads (Van Dyk, Dersch, Edwards, Ruppert, & Barkan, 2014). WILD sites are located on tangent track where lateral to vertical load ratios are typically less than 0.1. The track and support consists of premium size rail on concrete ties overlying a typical thickness of premium ballast supported by a well compacted thickness of subballast, typically hot-mix asphalt, and a well-compacted subgrade. This will reduce sources of variations within the track structure due to geometry and support conditions irregularities.

A WILD site normally involves about 200 to 250 ft (61 to 76 m) long section of track. This contains the track measurement zone, that is typically 50.5 ft (15.4m) long, and transitions on each end. The rail is instrumented at various intervals to capture each single wheel's rotation at least two times. Peak loadings, which include impact, as well as nominal or average loadings are collected at 25 kHz frequency. The static wheel load is estimated by filtering the average or nominal forces from the peak forces by using an algorithm that analyzes variability along the site.

The Peak wheel load is simply the highest recorded measurement from the strain gauge closest to the impact. It is the maximum impact force and is used for analyzing impacts for loaded cars and locomotives at a constant speed. For a given defect, the PEAK

will tend to increase with vehicle weight and/or speed. The Association of American Railroads issues industry standards (criteria for repairs) for WILD alarms. The minimum alert threshold is 65 kips (290 kN). The Dynamic Impact is the difference between the Peak Load and the Nominal Load. This term is useful for analyzing intermediately loaded vehicles, but there are no industry threshold standards based on Dynamic Impact. The Peak Load divided by the Nominal Load is the Ratio or Impact Factor. It is useful for analyzing empty or lightly loaded vehicles. Although there is no alert threshold for Ratio, it is observed that once the ratio becomes higher than 3, it is likely that the vehicle will exceed the established Peak threshold when heavily loaded. These relationships are shown in Figure 7.1.

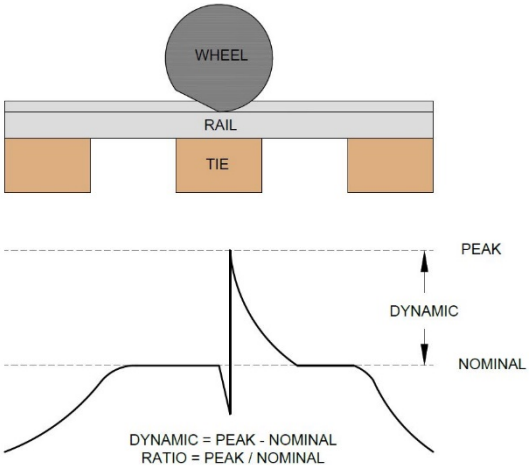

Figure 7.1 WILD Output Relationships

The Salient WILD design, being the initial type developed in the 1980s, is the most widely used system in the world today, with more than 200 installed worldwide to date. Over 90% of the WILD systems in the U.S. are Salient products. These evaluate millions of wheels per day throughout the international railway systems that detect and alarm when excessive wheel vertical impacts occur, so that the defective wheels are identified for inspection, tracking, treatment, and subsequent removal as standards dictate. A view of a

Salient Mk-III WILD used to gather data for this study is shown in Figure 7.2. This represents one of NS's fifteen WILDs designed and installed by Salient Systems.

Figure 7.2 Typical Salient Mk-III WILD Installation

The instrumented zone for the measurement of vertical forces exerted by each wheel of a passing train consists of a series of strain gage load circuits, micro-welded directly to the neutral axis of the rail. Signal processors, housed in a nearby enclosure, analyze the data to isolate wheel tread irregularities. If any wheel generates a force that exceeds a customer configured alarming threshold, a report identifies that wheel for subsequent action. Depending on operating procedures, multiple alarm thresholds can be configured. The reports are distributed in real-time to interested parties such as rail traffic control centers and vehicle repair shops.

WILDs are considered a strategic device for the protection of rail infrastructure. High impacting wheels can dissipate on the order of 25 horsepower each, degrading track, ballast and bridge structures, while reducing bearing and other vehicle component lives. Over time, the repetitive load cycles of defective wheels may result in rail fractures.

Pressure Data Conversion

WILD data is produced in an axle domain with loads (nominal, peak) in its corresponding range. This format allows maintenance crews to directly identify wheel defects for downstream remedial action. WILD reports are also based on a format that describes cars in an A or B-end category, and re-orients them for the convenience of engineering and maintenance crews. In order to perform direct wheel-for-wheel comparisons with trackbed pressures, NS and LB Foster (Salient Systems) provided WILD reports that eliminated the re-orientation procedure. Even with that however, pressure measurements at the crosstie-ballast interface are recorded in a frequency domain, complicating with WILD produced data.

Relating the trackbed crosstie-ballast interfacial pressures with the WILD force measurements required conversion of the recorded pressure data from a real-time/frequency domain to an axle domain. This was perfromed using a combination of bandwidth filtering and a simple waveform peak algorithm using MATLAB. The bandwidth filter (approx. 60 Hz) enabled production of a smooth wheel (nominal pressure) model of each axle (as shown in Figure 7.3).

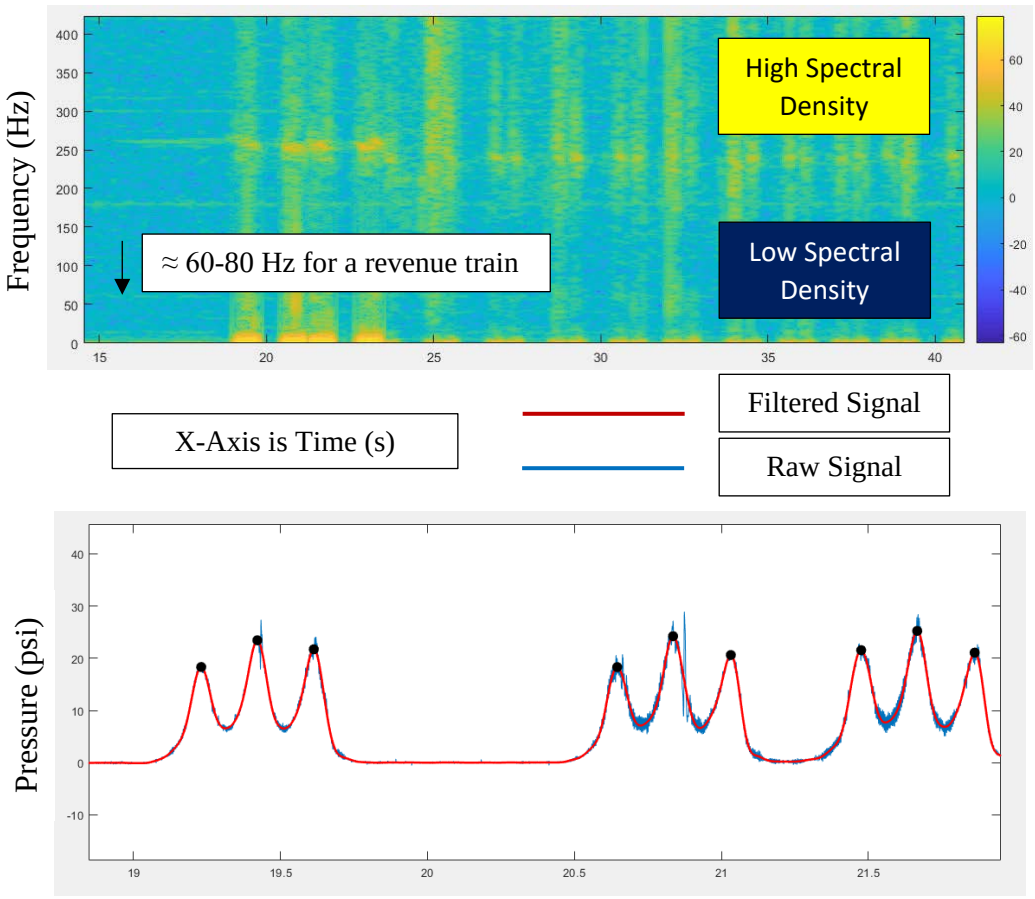

Figure 7.3 Modeling the Nominal Pressure of a Revenue Train

A simple script could then locate, pick off, and tabulate the corresponding pressure for each axle (included in Appendix I). Wheel irregularities and empty loads still required manual attention/quality control, as the corresponding wave signatures could not be easily modeled (as shown in Figure 7.4).

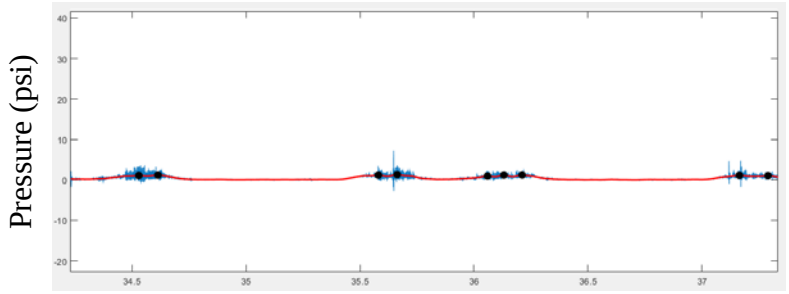

Figure 7.4 Empty Load Discrepancies

Signal analyzing software such as DIAdem (produced by National Instruments), so that a user can easily trace the signal, addressed these irregularities. From the processed data, nominal and peak pressure values were produced in an axle domain for direct WILD comparisons. Dynamic pressure and pressure ratio parameters, similar to those reported by WILDs, were also calculated.

Relationships between WILD and Tie/Ballast Pressure Measurements

To examine the relationships between crosstie-ballast interfacial pressures and WILD parameters, each axle of eight revenue trains was aggregated together and compared. This dataset is comprised of two coal trains (one empty, one loaded), four mixed freight (three loaded, one empty), and two intermodal trains, which provided ample coverage of the diverse types of trains.

To perform these comparisons, three different methodologies were used. The first presented individual axles with reported measurements for each individual pressure cell. The second methodology considered the average measurements of each particular car for each individual pressure cell. The third method contained the average value for each particular car, considering all pressure cells. The average value derived for each car, considering all six pressure cells averaged together, provided the most favorable relationships for each WILD parameter. This average reduces the variability between individual pressure measurements due to track levelness/position. Figure 7.5 highlights the relationships between each WILD parameter and each corresponding tie/ballast pressure variable. Appendix J provides the same relationships for the first two dataset methodologies.

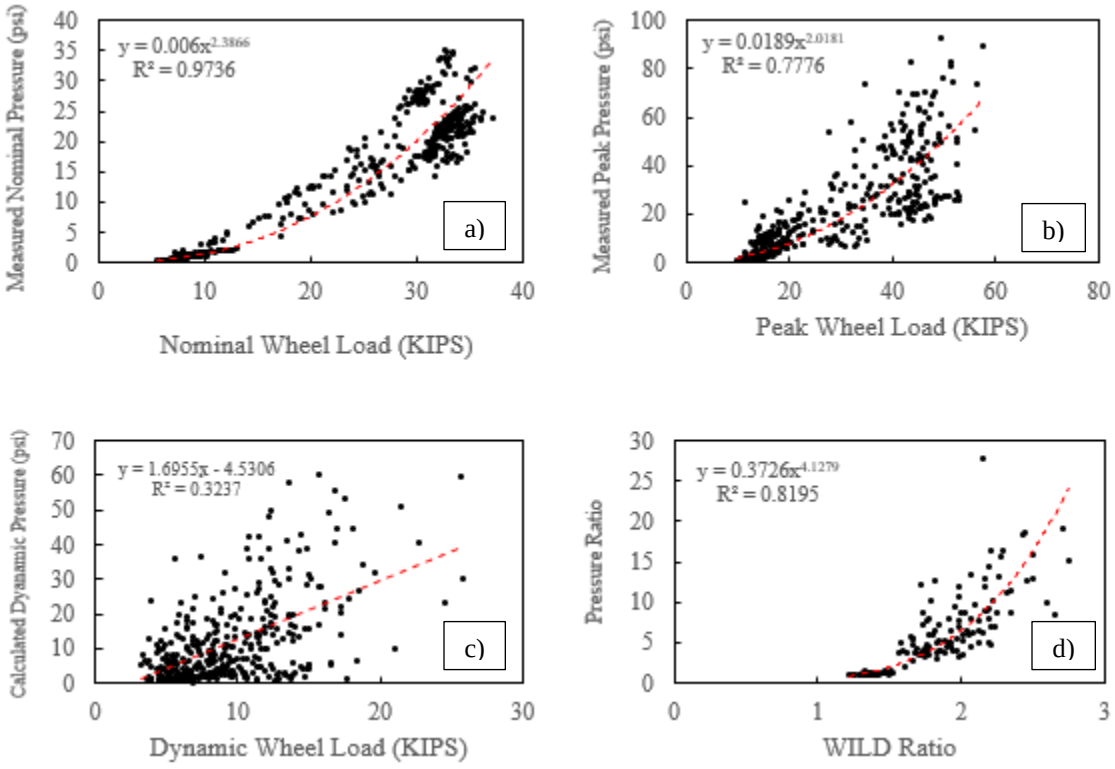

Figure 7.5 Relationships between WILD and Tie/Ballast Pressure Measurement Parameters

Nominal wheel loads measured at the wheel/rail interface relate very well to the corresponding nominal crosstie/ballast interfacial pressures. The two appeared linked in a power relative manner with an R-squared value of 0.97, as shown in Figure 7.5a. Based on the power regression relationship, an increase 50% in Nominal loading at magnitudes less than 10 kips (44 kN) results in an 81% increase in Nominal ballast pressure. However, at higher load magnitudes a 15% increase in Nominal loading results in only a 31% increase in ballast pressure. This suggests that higher Nominal wheel loads do in fact affect the track substructure significantly, but decrease in severity at higher load magnitudes.

With regard to WILD Peak loadings, shown in Figure 7.5b, a similar trend is seen as a 50% increase in Peak wheel/rail loading at lower magnitudes (less than 20 kips (89 kN)) results in a 75% increase in the transmitted ballast pressure. However, a 17% increase in Peak loading at higher load magnitudes (60 kips (267 kN)), results in only a 31% increase in the pressures transmitted to the tie/ballast interface. This is significant in that ballast degradation rates are increased substantially, but also seem to decrease in severity at higher load magnitudes.

Dynamic wheel loads, shown in Figure 7.5c, did not indicate a strong relationship ($R^2 = 0.32$). This is interesting since a strong relationship was found between absolute peak magnitude and measured peak pressure values. This could be attributed to the variable position along the rail of the wheel impact, which may not always fall directly above the instrumented crosstie. If each impact was at the same location above the instrumented crosstie, a stronger relationship might be apparent.

WILD Ratio, shown in Figure 7.5d, exhibited a much stronger relationship ($R^2 = 0.82$). This suggests that the relative magnitude increase between nominal and peak wheel loads and pressures does follow a trend. This dataset shows that an approximate 20% increase in the WILD Ratio results in a 60% increase in the calculated Pressure Ratio.

CHAPTER 8. SUMMARY FINDINGS, CONCLUSIONS AND SUGGESTED FUTURE RESEARCH

The primary objectives of this study were to: 1) continue a laboratory series of test using controlled and measured loadings to further develop, calibrate, and determine the applicability of Granular Material Pressure Cells for accurately measuring timber crosstie-ballast interfacial pressures, and 2) install a series of the cells, imbedded in consecutive crossties directly under the rail, in a revenue track to quantify pressures developed at the crosstie-ballast interface for various wheel loadings and train operations.

Repeated laboratory test and calibrations (Chapter 4), using known loading conditions, revealed that these pressure cells accurately and consistently measured crosstie-ballast interfacial pressures. Additional laboratory tests (Chapter 5) were conducted using a one-half length crosstie positioned on a similar length of simulated trackbed support to determine the relative magnitudes and distributions of pressures transmitted to the crosstie-ballast interface along the length of the crosstie for typical applied wheel loadings. The subballast and ballast layers were pre-compacted to represent a seasoned track support system. Pressure distributions along the one-half length crosstie indicated that ballast pressures directly below the rail seat account for 23 to 28 percent of the rail seat load. Pressures in the crosstie areas to either side (the crosstie end and the mid-point between the rail and crosstie center) each account for 10 to 12.5 percent of the load. Pressure at the crosstie center normally accounts for less than 2.5 percent of the applied load.

In-track crosstie-ballast interfacial pressure tests (Chapter 6) were obtained at a test site on an NS Railway well-maintained mainline just east of Knoxville, TN. The cells were

attached to and recessed within the bottoms of six successive timber crossties below the rail seat and in the center of two crossties. During a period of twenty-one months, crosstie-ballast interfacial pressures were periodically measured for numerous revenue freight trams traveling on a mainline at prevailing speeds. Nominal maximum static wheel loadings ranged from 6,000 lbf (27 kN) for empty freight cars to 36,000 lbf (161 kN) for locomotives and loaded cars.

Measured pressures at the crosstie-ballast interface ranged from 20 to 30 psi (140 to 210 kPa) for locomotives and loaded freight cars with smooth wheels producing negligible wheel/rail impacts. Measured crosstie-ballast interface pressures were typically 3 psi (20 kPa) maximum for empty freight cars with smooth wheels. Heavily loaded articulated intermodal car pressure measurements for shared trucks tended to reach nearly 40 psi (280 kPa), actually higher than locomotive-produced pressures. Pressure cells were also installed at the crosstie center where the ballast is typically not tamped or consolidated. The recorded pressures were normally less than 1 psi (7 kPa) for locomotives and loaded freight cars.

Wheel loading parameters (Chapter 7) obtained from nearby wayside wheel impact load detectors (WILDs) were compared to recorded crosstie-ballast interfacial pressure measurements for the same trains traversing the test site. Nominal wheel forces measured at the wheel/rail interface relate very well to the corresponding nominal crosstie-ballast interfacial pressures; linked in a power relationship manner with an R-squared value of 0.97. Increases in peak WILD loadings, either due to heavier wheel loads or increased impacts, relate favorably to increases in recorded trackbed pressures. In particular, peak

wheel loads tend to increase pressures substantially, which can have long-term detrimental effects on the ballast and support layers.

During the course of this study, considerable advancements have been made towards quantifying pressures imparted to the crosstie-ballast interface for a wide range of revenue train traffic. The procedure was initially confirmed in the laboratory using controlled load applications. Further in-track tests confirmed the applicability, accuracy, and repeatability of the measurement procedure. It is desirable to further develop and utilize the procedure. Several topics are suggested for future research studies.

The in-track data was only obtained during the periods that the research team was on-site with data acquisition equipment. Day-long testing sequences were taken at one-to-two month intervals. To more accurately represent the effects of weather and traffic fluctuations, remote sensing capabilities could be employed. More developed algorithms will be needed to quickly process the data.

Pressure measurement data needs to be compared directly with currently obtained track deflection and stress/strain measurements along the crosstie and rail. This type of analysis is particularly important and useful to verify the accuracy of the pressure measurements and to determine how each track component dissipates its respective pressures. Based on the low crosstie-ballast pressure levels noted in this study, it is proposed that the rail actually carries more of the induced loading than commonly assumed.

Laboratory studies should also be expanded to evaluate pressure distribution along the entire length of the crosstie. In this research, a half-length section was used due to the constraints of the laboratory test machine. The effect of the free end of the crosstie may

have slightly influenced the relative distributions measured and calculated, thus the use of two simultaneous static loading rams would more accurately depict typical loading configuration in the track. In addition to static loading, cyclic loading should also be performed on the same laboratory section to better emulate the loading cycles applied to a typical trackbed.

Another area for future study is providing a methodology for assessing wheel impacts more accurately. In this study, the length of the six instrumented ties only provided for one complete wheel revolution; having a test section with twice the number of instrumented ties would provide two complete wheel revolutions. This would be ideal to assess the validity of the magnitudes of recorded pressures. In addition to having more data for verification, an algorithm could be produced to determine the true peak/impact of a wheel irregularity. As was observed, the exact location of the wheel impact is not necessarily known, thus if the wheel impact was not applied directly over the instrumented tie, the measured pressure impacts are most likely not represented accurately. Test results discussed in Chapter 7 indicated that the differential "dynamic" WILD reading does not appear to have a strong relationship with the calculated pressure differential.

This study also focused on timber (wood) crossties; the primary type of crossties Norfolk Southern Railway uses for their tracks. Similar studies could be conducted to assess the behavior of various track conditions with varying crosstie materials. This should include concrete crossties, which are commonly used by the Western U.S. railroads and steel ties crossties, which are becoming more commonly used in yard tracks. Additionally, composites should be evaluated in lieu of recent material polymer improvements.

The trackbed at the Mascot test site consisted of unusually high and consistent quality all-granular support layers historically requiring minimal maintenance to maintain acceptable track support. A similar type of installation should be selected at a historically high-maintenance track site consisting of inherently soft subgrade support and requiring frequent maintenance to restore acceptable support.

A final area for future research is to incorporate in-track pressure measurements to provide recommendations for trackbed design technology. Many of the currently used design guidelines are based on historical analytical analyses and empirical tests and observations. Applying a more data driven approach to trackbed design would not only assist in developing designs that would consider the stability of a trackbed; but could also assist railroad management in incorporating performance-driven decisions assuring more economical maintenance practices and new-construction designs resulting in higher quality extended life track.

APPENDICES

Appendix A – Model 3500 Pressure Cell Technical Specifications

Information given in the following table can be found in the Geokon 3500/4800 Pressure Cell Data Specification Sheet listed in the reference section of this document.

Transducer Type	Semiconductor
Output	Millivolt: 100 mV (10 mV/V) Voltage: 0-5 VDC Current: 4-20 mA (2 wire)
Standard Ranges	100, 250, 400, 600 kPa; 1, 2.5, 6 MPa; 145, 362, 870 psi
Over Range	1.5 x rated pressure
Resolution	Infinite
Accuracy	± 0.25 % F.S.
Linearity	< 0.5 % F.S.
Thermal Effect on Zero	0.05 % F.S.
Typical Long-Term Drift	± 0.02 % F.S./yr.
Cell Dimensions (H x D)	6 x 230 mm (0.25 x 9 in)
Transducer Dimensions (L x D)	150 x 32 mm (6 x 1.25 in)
Excitation Voltage	Millivolt: 10 VDC regulated Voltage: 6.5 – 35 VDC Current: 24 VDC (7-35 VDC)
Excitation Frequency	n/a
Material	Stainless Steel
Temperature Range	-20 °C to +80 °C (-4 °F – 176 °F)

Appendix B – Typical Pressure Transducer Calibration Report

GEOKON 48 Spencer St. Lebanon, N.H. 03766 USA

Pressure Transducer Calibration Report

This Calibration has been Verified/ Validated as of: December 19, 2016

Model Number: 3515-3-2.5 MPa

Serial Number: [redacted]

Pressure Range: 2.5 MPa

Date of Calibration: [redacted]

Temperature: 20.8 °C

†Barometric Pressure: 984.1 mbar

Calibration Instruction: CI-VW Pressure Transducers

Technician: [redacted]

Applied Pressure (MPa)	Gage Reading (mA) 1st Cycle	Gage Reading (mA) 2nd Cycle	Average Gage Reading	Change	Linearity (%FS)	Polynomial Fit (%FS)
0.0	3.993	3.995	3.994		-0.09	0.01
0.5	7.201	7.206	7.204	3.21	0.00	-0.01
1.0	10.407	10.413	10.410	3.21	0.08	0.00
1.5	13.606	13.606	13.606	3.20	0.08	0.01
2.0	16.791	16.792	16.792	3.19	0.02	0.00
2.5	19.966	19.970	19.968	3.18	-0.10	0.00

Linear Gage Factor (G): 0.1565 **(MPa/ mA)** **Regression Zero:** 4.008

Polynomial Gage Factors: A: 6.82E-05 **B:** 0.1549 **C:** -0.6194

Calculated Pressures: **Linear, $P = G(R_1 - R_0)$**

Polynomial, $P = AR_1^2 + BR_1 + C$

Input Voltage: 24 VDC

Wiring Code: See manual for further information.

The above instrument was found to be In Tolerance in all operating ranges.
The above named instrument has been calibrated by comparison with standards traceable to the NIST, in compliance with ANSI Z540-1.

Appendix C – Pressure Recording Software Code Map

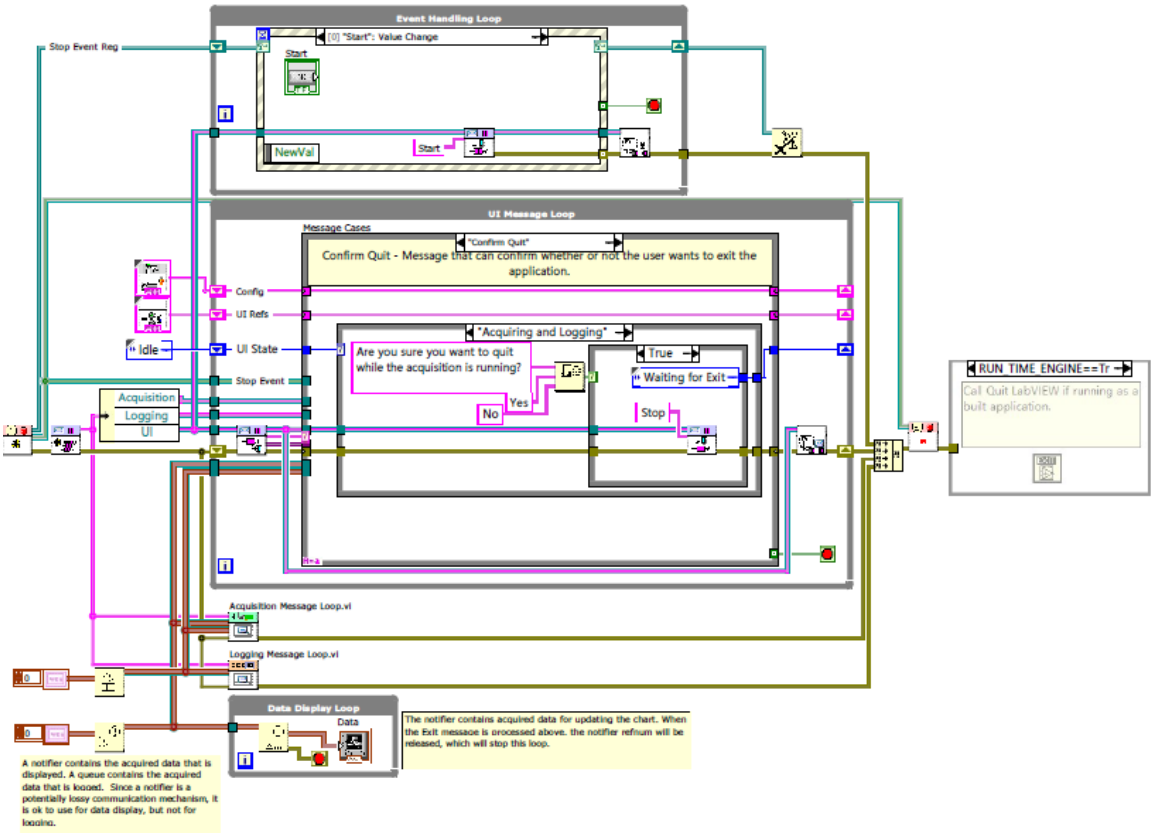
Event Handling Loop
Stop Event Req
[0] "Start": Value Change
Start
NewVal
Start
UI Message Loop
Message Cases
"Confirm Quit"
Confirm Quit - Message that can confirm whether or not the user wants to exit the application.
Config
UI Refs
Idle
UI State
Stop Event
Acquisition
Logging
UI
"Acquiring and Logging"
Are you sure you want to quit while the acquisition is running?
No
Yes
True
Waiting for Exit
Stop
RUN_TIME_ENGINE==Tr
Call Quit LabVIEW if running as a built application.
Acquisition Message Loop.vi
Logging Message Loop.vi
Data Display Loop
Data
The notifier contains acquired data for updating the chart. When the Exit message is processed above, the notifier refnum will be released, which will stop this loop.
A notifier contains the acquired data that is displayed. A queue contains the acquired data that is logged. Since a notifier is a potentially lossy communication mechanism, it is ok to use for data display, but not for logging.

Appendix D – Tabulated Data for Calibration Testing

Test #1 - Repeatability

Cell 88

Machine	Test	*(a)*	*(b)*	*(c)*	*(d)*	*(e)*	*(f)*	AVG (psi)
Applied (lbf)	**Applied (psi)**	**Measured (psi)**	**Measured (psi)**	**Measured (psi)**	**Measured (psi)**	**Measured (psi)**	**Measured (psi)**	
1500	29.8	32.8	31.5	31.1	30.8	30.7	30.8	31.1
3000	59.7	61.7	62.3	61.5	60.7	61.1	60.9	61.1
4500	89.5	92.6	92.2	91.8	89.9	90.2	90.1	90.9
6000	119.4	120.1	118.8	118.1	118.2	118.3	118.1	118.7

Cell 89

Machine	Test	*(a)*	*(b)*	*(c)*	*(d)*	*(e)*	*(f)*	AVG (psi)
Applied (lbf)	**Applied (psi)**	**Measured (psi)**	**Measured (psi)**	**Measured (psi)**	**Measured (psi)**	**Measured (psi)**	**Measured (psi)**	
1500	29.8	30.3	30.5	29.7	29.4	30.1	29.8	30.0
3000	59.7	59.8	60.2	59.1	59.2	58.7	59.1	59.4
4500	89.5	88.7	88.1	87.8	88.1	87.5	87.4	87.9
6000	119.4	114.8	117.6	115.2	114.9	115.5	115.3	115.6

Cell 91

Machine	Test	*(a)*	*(b)*	*(c)*	*(d)*	*(e)*	*(f)*	AVG (psi)
Applied (lbf)	**Applied (psi)**	**Measured (psi)**	**Measured (psi)**	**Measured (psi)**	**Measured (psi)**	**Measured (psi)**	**Measured (psi)**	
1500	29.8	30.7	30.8	30.7	31.1	31.2	30.3	30.8
3000	59.7	60.4	60.7	60.5	60.8	60.9	60.1	60.6
4500	89.5	89.5	90.4	89.8	90.1	89.7	89.8	89.9
6000	119.4	118.6	118.3	118.1	117.8	118.5	118.2	118.3

Cell 87

Machine	Test	*(a)*	*(b)*	*(c)*	*(d)*	*(e)*	*(f)*	AVG (psi)
Applied (lbf)	**Applied (psi)**	**Measured (psi)**	**Measured (psi)**	**Measured (psi)**	**Measured (psi)**	**Measured (psi)**	**Measured (psi)**	
1500	29.8	30.5	31.2	30.1	30.3	30.8	30.6	30.6
3000	59.7	59.8	60.8	59.9	59.7	59.8	59.9	60.0
4500	89.5	88.9	89.5	87.4	87.6	88.7	88.6	88.5
6000	119.4	116.7	115.1	110.5	111.1	112.2	111.8	112.9

Test #2 – Position

Cell Below Solid Tie – Cell 88

Machine	Test	*(a)*	*(b)*	*(c)*	*(d)*	*(e)*	*(f)*	**AVG (psi)**
Applied (lbf)	**Applied (psi)**	**Measured (psi)**	**Measured (psi)**	**Measured (psi)**	**Measured (psi)**	**Measured (psi)**	**Measured (psi)**	
1500	29.8	30.1	29.5	30.2	30.5	29.8	30.2	30.0
3000	59.7	59.2	58.8	58.7	58.8	58.5	59.8	59.1
4500	89.5	86.8	87.1	87.6	87.5	87.1	87.8	87.6
6000	119.4	115.4	114.3	114.7	114.6	114.1	114.8	115.3

Cell within Tie Recess – Cell 88

Machine	**Test**	*(a)*	*(b)*	*(c)*	*(d)*	*(e)*	*(f)*	**AVG (psi)**
Applied (lbf)	**Applied (psi)**	**Measured (psi)**	**Measured (psi)**	**Measured (psi)**	**Measured (psi)**	**Measured (psi)**	**Measured (psi)**	
1500	29.8	32.8	31.5	31.1	30.8	30.7	30.8	31.1
3000	59.7	61.7	62.3	61.5	60.7	61.1	60.9	61.1
4500	89.5	92.6	92.2	91.8	89.9	90.2	90.1	90.9
6000	119.4	120.1	118.8	118.1	118.2	118.3	118.1	118.7

Test #3 – Attachment

No Attachment – Cell 88

Machine	**Test**	*(a)*	*(b)*	*(c)*	*(d)*	*(e)*	*(f)*	**AVG (psi)**
Applied (lbf)	**Applied (psi)**	**Measured (psi)**	**Measured (psi)**	**Measured (psi)**	**Measured (psi)**	**Measured (psi)**	**Measured (psi)**	
1500	29.8	32.8	31.5	31.1	30.8	30.7	30.8	31.1
3000	59.7	61.7	62.3	61.5	60.7	61.1	60.9	61.1
4500	89.5	92.6	92.2	91.8	89.9	90.2	90.1	90.9
6000	119.4	120.1	118.8	118.1	118.2	118.3	118.1	118.7

Screw Attachment – Cell 88

Machine	Test	*(a)*	*(b)*	*(c)*	*(d)*	*(e)*	*(f)*	**AVG**
Applied (lbf)	**Applied (psi)**	**Measured (psi)**	**Measured (psi)**	**Measured (psi)**	**Measured (psi)**	**Measured (psi)**	**Measured (psi)**	
1500	29.8	30.5	30.3	31.2	30.8	30.7	31.5	30.7
3000	59.7	59.8	60.1	61.3	60.9	60.5	60.8	60.4
4500	89.5	89.1	89.4	89.7	89.8	89.4	89.6	89.5
6000	119.4	117.2	117.8	118.1	118.2	117.8	117.7	118.0

Corner Brace Attachment – Cell 88

Machine	**Test**	*(a)*	*(b)*	*(c)*	*(d)*	*(e)*	*(f)*	**AVG**
Applied (lbf)	**Applied (psi)**	**Measured (psi)**	**Measured (psi)**	**Measured (psi)**	**Measured (psi)**	**Measured (psi)**	**Measured (psi)**	
1500	29.8	29.8	30.4	30.6	30.3	30.8	29.6	30.2
3000	59.7	59.5	60.1	60.7	59.8	60.3	60.1	60.0
4500	89.5	88.7	89.5	89.1	90.3	89.7	89.1	89.4
6000	119.4	116.8	117.3	117.2	117.6	117.1	117.4	117.5

Test #4 – Length of Tie Effect on Single Pressure Cell

11-inch Section

Test Machine		**Measured Cell Readings (psi)**							
Applied (lbf)	Applied (psi)	*(a)*	*(b)*	*(c)*	*(d)*	*(e)*	*(f)*	*(g)**	**AVG (psi)**
1500	29.8	28.5	29.6	29.1	30.8	30.1	30.5	28.5	29.6
3000	59.7	56.4	58.8	57.6	59.6	59.2	59.4	56.4	58.2
4500	89.5	84.3	86.5	85.4	87.1	86.7	86.8	83.6	85.8
6000	119.4	112.2	114.8	112.8	115.2	114.3	114.1	111.5	113.6

* repeated test, not considered in calculations

20-inch Section

Test Machine		**Measured Cell Readings (psi)**							
Applied (lbf)	Applied (psi)	*(a)*	*(b)*	*(c)*	*(d)*	*(e)*	*(f)*	*(g)**	**AVG (psi)**
1500	29.8	29.3	28.7	28.6	29.2	28.6	28.8	28.1	28.8
3000	59.7	57.5	56.8	56.2	57.1	56.8	56.3	56.2	56.7
4500	89.5	85.4	84.3	84.1	84.8	83.7	84.4	83.1	84.3
6000	119.4	112.8	111.5	111.1	111.6	110.3	110.8	110.3	111.2

* repeated test, not considered in calculations

30-inch Section

Test Machine		**Measured Cell Readings (psi)**						
Applied (lbf)	Applied (psi)	*(a)*	*(b)*	*(c)*	*(d)*	*(e)*	*(f)*	**AVG (psi)**
1500	29.8	28.5	27.4	28.1	27.8	27.1	27.1	27.7
3000	59.7	56.3	54.6	55.7	55.8	54.5	54.5	55.2
4500	89.5	83.8	82.5	83.3	83.4	82.7	82.7	83.1
6000	119.4	111.4	109.1	110.2	109.8	109.1	109.1	109.8

40-inch Section

Test Machine		**Measured Cell Readings (psi)**						
Applied (lbf)	Applied (psi)	*(a)*	*(b)*	*(c)*	*(d)*	*(e)*	*(f)*	**AVG (psi)**
1500	29.8	26.1	27.8	27.1	26.7	26.5	27.5	27.0
3000	59.7	53.8	55.4	55.5	54.6	54.3	55.7	54.9
4500	89.5	81.8	82.5	82.2	80.5	81.4	81.5	81.7
6000	119.4	109.3	109.1	108.4	106.8	107.5	107.4	108.1

Appendix E – Multi-Cell Testing Data Catalog

Test Date	Loading Condition	Test Name	Number of Tests	Number of Data Points
3/28/2018	Full Aggregate Contact Against Tie and Cells	101	7 (a-g)	184
4/4/2018	Full Aggregate Contact Against Tie and Cells	102	8 (a-h)	224
4/18/2018	Spacers Between Cells and Ballast	201	10 (a-j)	280
5/8/2018	Full Aggregate Contact Against Tie and Cells	301	6 (a-f)	168
5/8/2018[1]	Full Aggregate Contact Against Tie and Cells	302	6 (a-f)	168
5/8/2018[1]	Full Aggregate Contact Against Tie and Cells	303	6 (a-f)	168
5/15/2018	Wood Board Interfacing Tie and Ballast	401	7 (a-g)	196
5/15/2018	Wood Board Interfacing Tie and Ballast	402	6 (a-f)	168
5/15/2018	Wood Board Interfacing Tie and Ballast	403	6 (a-f)	168
5/21/2018	Wood Board Interfacing Tie and Ballast	501	6 (a-f)	168
5/21/2018	Spacers Interfacing Tie and Wood Board; Wood Board Interfacing Spacers from Ballast	502	6 (a-f)	168
5/31/2018	Spacers Interfacing Tie and Wood Board; Wood Board Interfacing Spacers from Ballast	602	6 (a-f)	168
5/31/2018	Spacers Interfacing Tie and Wood Board; Wood Board Interfacing Spacers from Ballast	603	6 (a-f)	168
5/31/2018	Full Aggregate Contact Against Tie and Cells	701	6 (a-f)	168
5/31/2018	Wood Board Interfacing Tie and Ballast	901	6 (a-f)	168

[1]Test 302 was performed with 0.2 in/min loading rate. Test 303 was performed with 0.3 in/min loading rate. All other tests were performed at 0.1 in/min.

Total Number of Data Points:	**2,732**
For Full Aggregate Contact:	1,080
Spacers Interfacing Ballast:	280
Wood Board Interfacing Ballast:	868
Wood Board and Spacers Interfacing Ballast:	504

Picture of Series #1

Picture of Series #3

Appendix F – Overall Load Percentages for Each Agreement and Pressure Cell

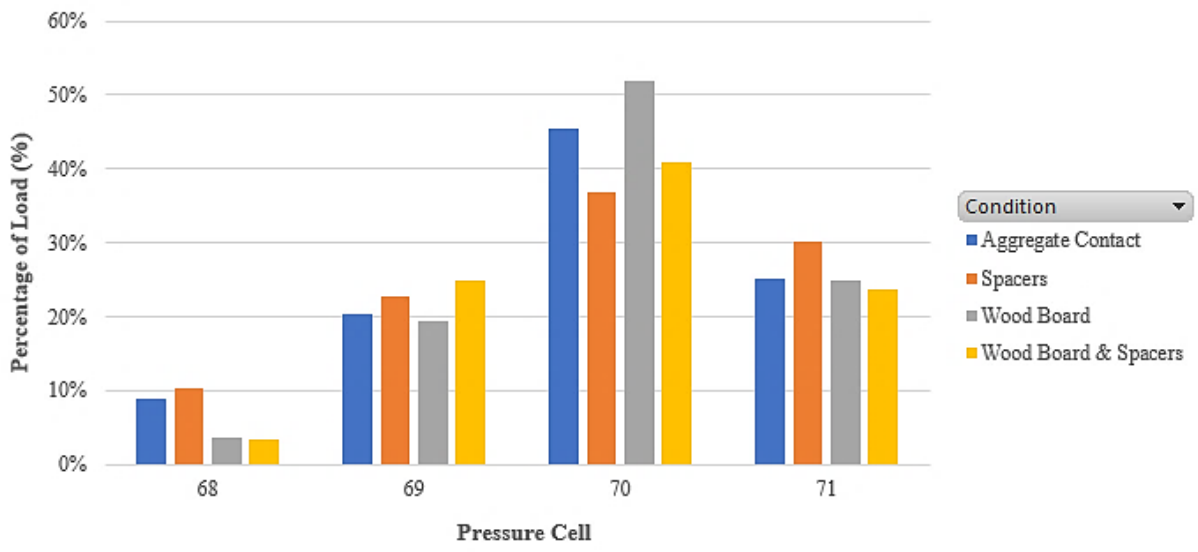

Example Calculations:

Series #1

Given: 30 psi rail seat tie-ballast pressure
24% of load varied by rail seat
4% of load carried by centerline

Solution: 30/24% = P/4% → P = 5 psi

Series #2

Given: 30 psi rail seat tie-ballast pressure
18% of load varied by rail seat
4% of load carried by centerline

Solution: 30/18% = P/4% → P = 7 psi

Series #3

Given: 30 psi rail seat tie-ballast pressure
26% of load varied by rail seat
2% of load carried by centerline

Solution: 30/26% = P/2% → P = 2 psi

Series #4

Given: 30 psi rail seat tie-ballast pressure
20% of load varied by rail seat
4% of load carried by centerline

Solution: 30/24% = P/2% → P = 3 psi

Appendix G – Revenue Train Catalog

Rows highlighted did not record locomotives correctly

Date	*Test Train*	*Train #*	*Lead Loco*	*Time*	*Type*	*Locomotives*	*Direction*	*Speed*	*Length*	*Tonnage*	*Cars*
9/26/2016	1	163	9411	12:24 PM	Mixed	4 Six-Axle	WB	25	-	-	36
9/26/2016	2	799	5142	1:42 PM	Empty Coal	1 Four-Axle 1 Six-Axle	EB	25	-	-	130
Notes: Train 163: The five instrumented ties (six cells) were installed earlier in the day. After installing the ties, one train passed prior to tamping the ties. Train 799: NS 8636 trailing. The five instrumented ties (six cells) were installed earlier in the day. After installing the ties, one train passed prior to tamping the ties.											
10/12/2016	1	23G	3623	11:15 AM	Intermodal	3 Six-Axle	EB	25	8727	-	46
10/12/2016	2	16T	9048	11:30 AM	Mixed	3 Six-Axle	EB	25	4100	-	62
10/12/2016	3	135	2714	12:20 PM	Mixed	3 Six-Axle	WB	25	8100	-	147
10/12/2016	4	163	8891	1:08 PM	Mixed	6 Six-Axle 1 Four-Axle	WB	25	6400	-	89
Notes: Train 23G: NS 7608 Trailing. 12 auto cars on front – very smooth ride. Remaining cars are container cars, many are articulated with 5 individual cars. Train 16T: NS 9245, NS 3608. Several empty loads about halfway. Maybe 2 or 3 empties near the rear. Most cars were loaded. Train 135: NS 8727, NS 2511. Lot of empty cars. Several empty coal cars on rear. Train 163: The track was tamped after this train. This included tamping the test ties plus 15 ties on both ends and the ties between test ties. Attempting to obtain equal track stiffness throughout the area. No other tests today. Will wait for two weeks to test. Cell 27 did not record on this day											
10/26/2016	1	134	7024	10:17 AM	Mixed	3 Six-Axle	EB	25	5163	-	81
10/26/2016	2	16T	9253	12:45 PM	Mixed	3 Six-Axle	EB	25	4160	6621	63
10/26/2016	3	163	7651	1:32 PM	Mixed	5 Six-Axle	WB	25	5300	7100	86
10/26/2016	4	132	8391	2:00 PM	Mixed	3 Six-Axle	EB	25	5810	11580	101
10/26/2016	5	202	7648	2:38 PM	Intermodal	3 Six-Axle	EB	25	8085	6396	46
Notes: Train 163: Some flat wheels											
11/7/2016	1	163	9595	11:08 AM	Mixed	3 Six-Axle	WB	34	2139	1796	33
11/7/2016	2	165	9426	1:03 PM	Mixed	3 Six-Axle	WB	25	4440	4548	77
11/7/2016	3	135	CP 8632	2:00 PM	Mixed	4 Six-Axle	WB	26	5100	3671	91
Notes: Train 165: This data is bad, no use in processing. Go on to train 3. Train 135: Last train tested today. Use trains 1 and 3. Will likely re-tamp and surface track before next tests.											
11/28/2016	1	27V	9943	11:30 AM	Auto	2 Six-Axle	WB	38	5542	3049	57
11/28/2016	2	135	9359	12:50 PM	Mixed	6 Six-Axle	WB	34	1800	1268	20
11/28/2016	3	16T	BNSF 4803	2:43 PM	Mixed	3 Six-Axle	EB	28	4271	6703	67
Notes: Train 27V: Some flat wheels Train 16T: Last Train											
12/15/2016	1	817	8077	10:22 AM	Empty Coal	4 Six-Axle	WB	35	6000	6000	120
12/15/2016	2	135	2590	12:22 PM	Mixed	2 Six-Axle	WB	32	2557	1710	33
12/15/2016	3	163	7597	1:55 PM	Mixed	4 Six-Axle	WB	38	6799	10122	114
12/15/2016	4	202	UP 7219	2:10 PM	Intermodal	3 Six-Axle	EB	32	7328	5551	42
Notes: Train 817: Did not record locomotives, just the empty cars. This was the first train for this date. Train 135: Had 5 loaded and 28 empty. Trailing Loco # = 9647 Train 202: Several of the cars were articulated, so Number of Cars is a bit deceiving. This was the last of the four trains for this date.											

Date	*Test Train*	*Train #*	*Lead Loco*	*Time*	*Type*	*Locomotives*	*Direction*	*Speed*	*Length*	*Tonnage*	*Cars*
4/13/2017	1	134	2616	11:35 AM	Mixed	3 Six-Axle	EB	31	4100	5801	?
4/13/2017	2	15T	6769	1:13 PM	Mixed	3 Six-Axle	WB	32	4990	2885	?
4/13/2017	3	23G	7690*	1:52 PM	Auto	3 Six-Axle	EB	36	6200	6400	24

Notes:

* 8085 was on the rear
Train 23G was through train, likely went over one of the WILDs. It had 15 autos, ~ 84 container cars, and 1 loco on rear. We missed recording the head locos and possibly a few of front end cars. Did get most of train including the rear loco.
Train 134 cell 29 did not record, was repaired for the following two trains.

4/27/2017	1	134	9908	11:23 AM	Mixed	3 Six-Axle	EB	31	4784	7859	82
4/27/2017	2	132	8958	11:49 AM	Mixed	3 Six-Axle	EB	32	4130	8230	71
4/27/2017	3	16T	9364	1:44 PM	Mixed	3 Six-Axle	EB	39	3354	4719	51

Notes:

Not sure if any of these were through trains that passed over WILDs at Flat Rock or Ebenezer. (However, train 918 the following day was a loaded rail train probably coming from Atlanta, so would likely have passed over Ebenezer.)

4/28/2017	4	918	2801	10:14 AM	Rail Train	1 Six-Axle	EB	32	1664	2340	30
4/28/2017	5	165	9233	11:50 AM	Mixed	3 Six-Axle	WB	40	2509	1834	42
4/28/2017	6	135	4509 (UP)	12:26 PM	Mixed	6 Six-Axle	WB	33	1870	1380	24

Notes:

Trains 1, 2, and 3 on 4-27, Trains 4, 5, and 6 on 4-28. Train 918 had 1 loco, 1 box car, CWR rail cars, and 1 box car. Train 135 had two UP locos in lead.

6/26/2017	1	135	1061	12:23 PM	Mixed	2 Six-Axle	WB	35	3008	2034	56
6/26/2017	2	163	3639	2:40 PM	Mixed	4 Six-Axle	WB	23	2782	2600	41
6/27/2017	3	162	9682	11:17 AM	Mixed	3 Six-Axle	EB	37	3059	5361	49
6/27/2017	4	16T	7028	1:48 PM	Mixed	3 Six-Axle	EB	36	5700	9075	88

Notes:

Not sure if any of these were through trains that passed over WILDs at Flat Rock or Ebenezer. I understand that the two EB trains on the 27th did pass over Ebenezer; however, a block may have been set off or picked up at Knoxville, so the consists may have changed. Not sure about the 26th trains.

8/7/2017	1	917	6769	11:09 AM	Rail Train	2 Six-Axle	EB	26	1600	N/A	30
8/7/2017	2	135	9408	2:30 PM	Mixed**	2 Six-Axle	WB	27	5296	32000	103
8/7/2017	3	23G	8027	2:45 PM	Container	2 Six-Axle*	EB	39	5050	5600	?***

Notes:

* One Pushing
** Mainly Empty Coal Hoppers
*** Some Articulated

8/8/2017	1	163	2715	1:45 PM	Mixed	3 Six-Axle	WB	24	3300	4520	54

Notes:

Recorded pressures made during tamping/surfacing process. Test Train # 1 was first train over test site following the tamping/surfacing conducted about one hour earlier. Only train measured. Will wait about three weeks for follow-up testing after three weeks of train traffic.

8/30/2017	1	123	8900 (CP)	10:40 AM	Mixed	2 Six-Axle*	EB	28	1464	2035	23
8/30/2017	2	16T	1084	12:24 PM	Mixed	3 Six-Axle	EB	28	3740	5853	54
8/30/2017	3	134	1103	1:16 PM	Mixed	4 Six-Axle	EB	33	2810	5507	46

Notes:

* Plus one CP loco pushing, the 3rd car from the rear
Surfaced track on August 8th, no trackwork since.

Date	Test Train	Train #	Lead Loco	Time	Type	Locomotives	Direction	Speed	Length	Tonnage	Cars
9/27/2017	1	23G	7594	12:30 PM	Intermodal	2 Six-Axle*	EB	34	6239	7090	33
9/27/2017	2	202	8710	2:40 PM	Intermodal	3 Six-Axle	EB	35	8035	6333	42

Notes:

* Plus one NS loco pushing form the rear
Train 1 & 2 had 3010 and 2900 gal of fuel, respectively.
Surfaced track on August 8, no trackwork since then

11/3/2017	1	162	9668	2:08 PM	Mixed	3 Six-Axle	EB	10-20	2503	4664	39
11/3/2017	2	15T	9631	3:46 PM	Mixed	2 Six-Axle	WB	22	5487	3721	83
11/3/2017	3	819	8174	5:10 PM	Empty Coal	2 Six-Axle	WB	20	5317	2605	102
11/3/2017	4	134*	9458	5:35 PM	Mixed	4 Six-Axle	EB	40	2560	4999	41

Notes:

Train 162 -- Might have been through train, not sure which WILD data
Train 15T – Likely was a through train, likely have Flatrock WILD data
Train 819 – Through train to Birmingham, should have Ebenezer WILD data
* Train 134 – Reported 41 cars, we counted 45 -- was questioned, was relying on the subsequent AEI Reader (adjacent MP 117.4A), should convert to 45. Also, cars #1 - # 31 came in Knoxville on Train # 162 on 31st of October – see Les Hall's e-mail to follow, likely these 31 cars went over a WILD on the 31st, so maybe just use these 31 cars for WILD/Pressure comparisons – Train 162 for WILD and Train 134 for Pressure. Train 134 originated in Knoxville, but had first 31 cars from block off of Train 162 (10/31).

2/9/2018	1	165	9486	8:12 AM	Mixed	2 Six-Axle	WB	38	5364	4355	88
2/9/2018	2	098	7719 (BNSF)	10:14 AM	Mixed	1 Six-Axle	EB	39	696	419	11
2/9/2018	3	16T	7600	10:35 AM	Mixed	3 Six-Axle	EB	32	1365	1796	18
2/9/2018	4	163	8350	11:05 AM	Mixed	3 Six-Axle	WB	35	6313	11000	99
2/9/2018	5	162	6790	12:56 PM	Mixed	3 Six-Axle	EB	45	6313	10949	99

Notes:

It was reported that Trains 165, 16T and 162 either set off or picked up block(s) of cars at Knoxville, doubtful that WILD data will match. Will forward e-mail from Les Hall in this regard. Not sure about 098 (very doubtful); possibly 163 may have stayed intact, likely the only one if any of the five trains stayed intact. Note that the ambient temperatures varied from 27 to 50 F. Temperatures for each test were: 27, 34, 34, 41, and 50.

Date	Test Train	Train #	Lead Loco	Time	Type	Locomotives	Direction	Speed	Length	Tonnage	Cars
3/9/2018	1	15T	1075	9:35 AM	Mixed	4 Six-Axle	WB	35	3454	1883	49
3/9/2018	2	710	9553 (PRLX)	10:50 AM	Unit Coal	3 Six-Axle	WB	31	5800	13880	100
3/9/2018	3	23G	7052 (BNSF)	12:10 PM	Intermodal	2 Six-Axle	EB	33	6200	7542	34

Notes:

15T was not a through train, later set out rear 12 cars at Sevier, picked up 76 cars on rear, not sure which WILD it later traversed
710 was loaded, later supposedly went over Ebenezer WILD
23G was long intermodal train, had several of the multi-pacs, so total number of cars substantially greater than 34, had 1 6-axle loco pusher on rear, had supposedly went over Flatrock WILD
Surfaced track on August 8, 2017 no trackwork since then

6/25/2018	1	16T	8083	10:35 AM	Mixed	3	EB	31	4794	8817	92
6/25/2018	2	23G	1056	1:26 PM	Intermodal	3*	EB	5-40**	9061	8975	42
6/25/2018	3	123	9075	2:03 PM	Mixed	3	EB	28	4918	8913	86

Notes:

*The third loco was located mid-train
** Started from stop within sight distance, thus variable speed across test area. Number of cars also variable. Over 100 flat cars observed.
Surfaced track on August 8, 2017 no trackwork since then
[After the Revenue Train Tests, the FRA Test Car DOTX 218 conducted Run-Through Tests at variable speeds (40, 30, 20, 10 and ~2 mph) with corresponding pressure measurements recorded trackside) and Static Tests at variable loadings on Tie 11 (E) @ 3, 10, 15, 20 & 22 kips and Tie 6 (C) @ 22 & 10 kips (abbreviated) with corresponding pressure measurements and vertical deflection measurements recorded trackside]

Appendix H – Various Revenue Train Measurements

Example of a Mixed Freight Train

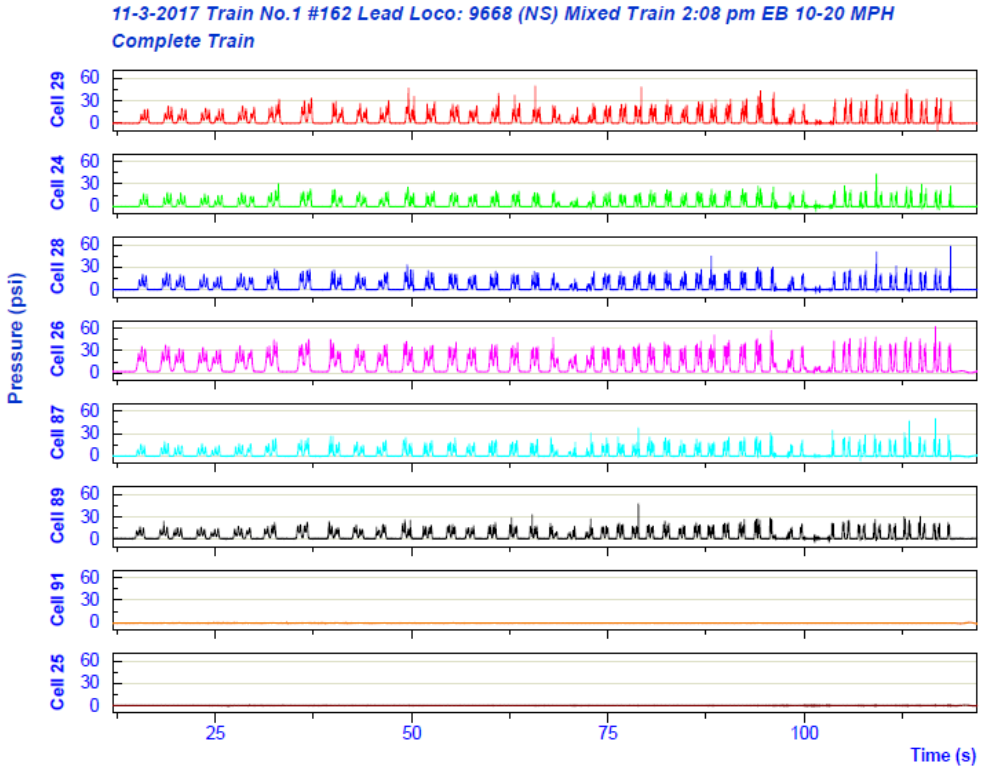

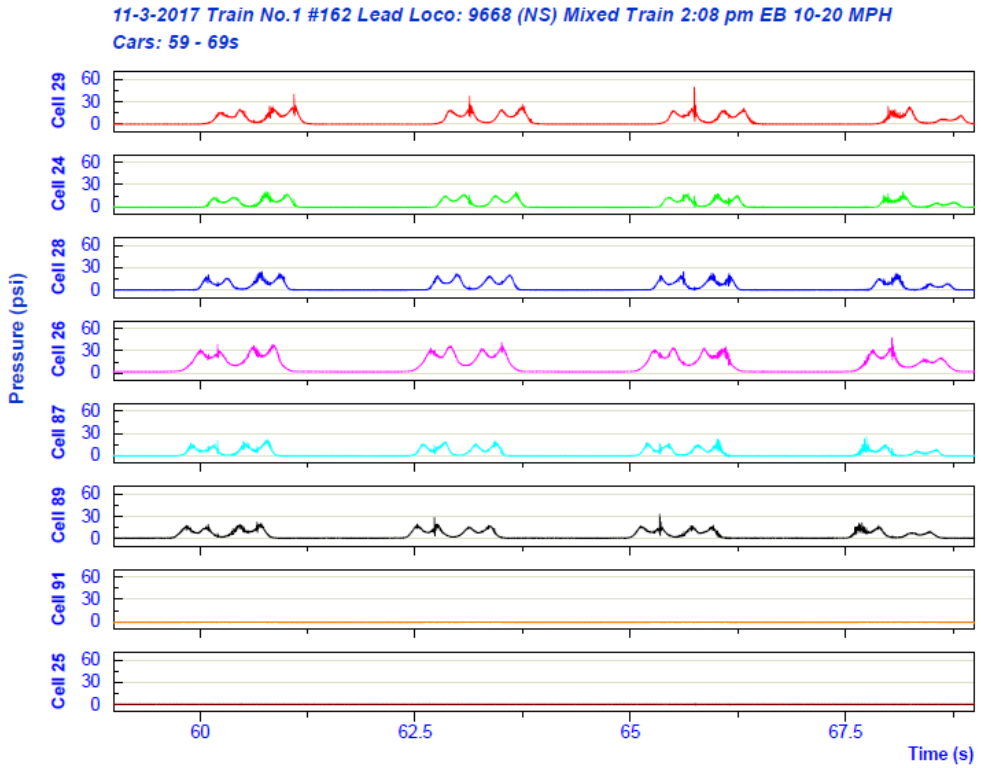

Example of an Intermodal Freight Train

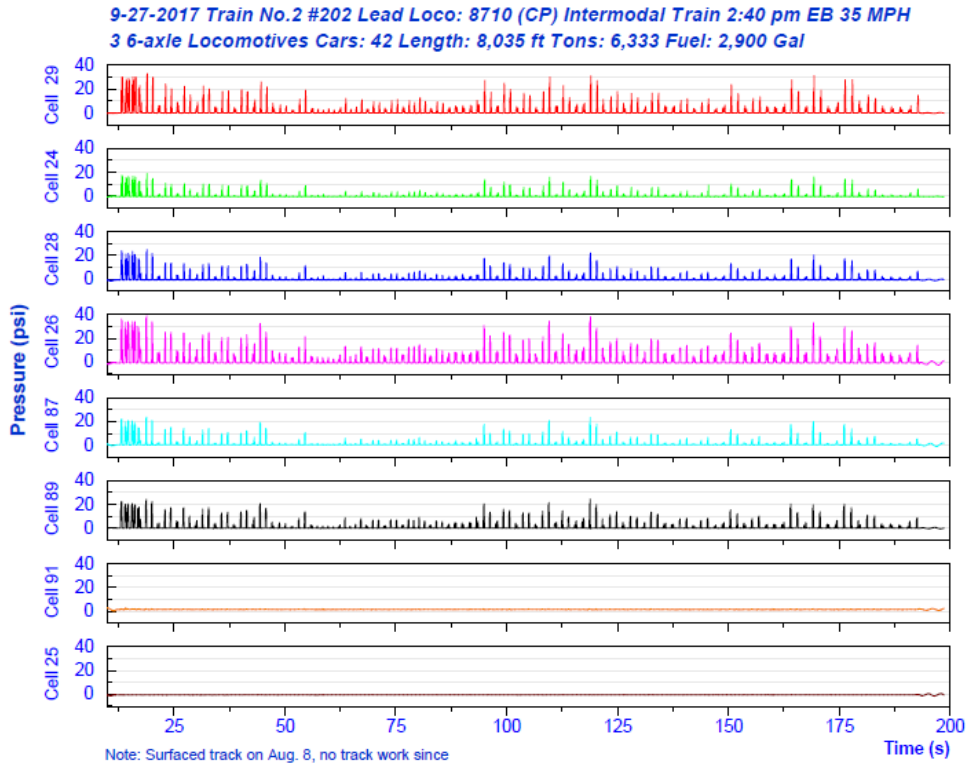

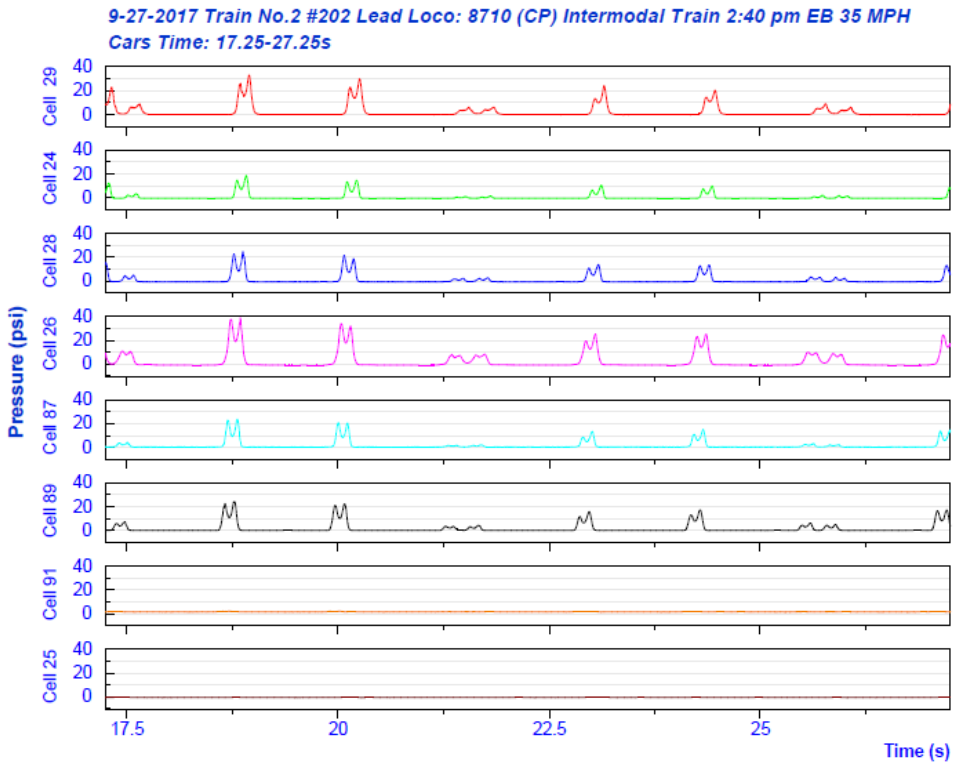

Example of a Rail Train

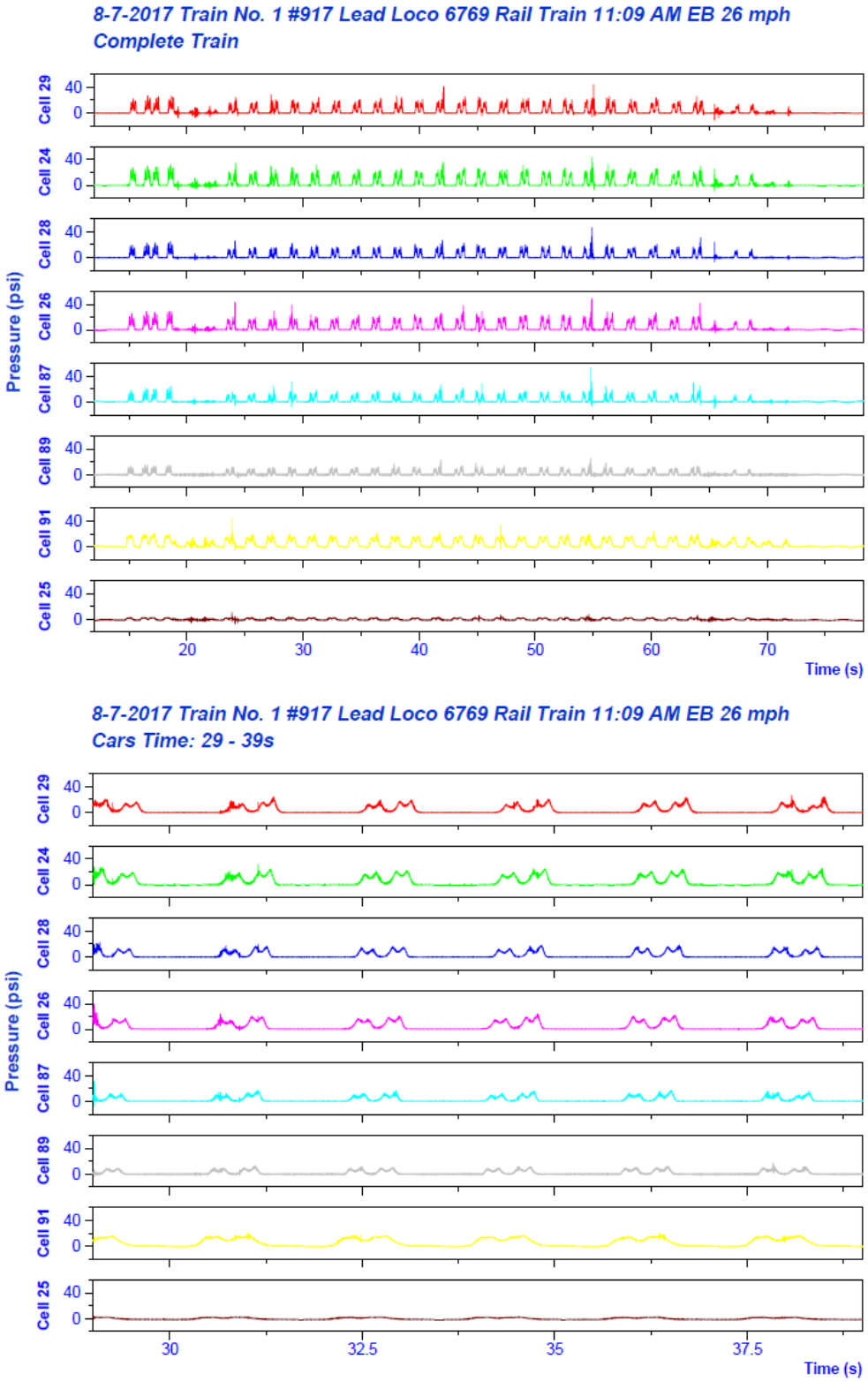

Example of an Auto Train

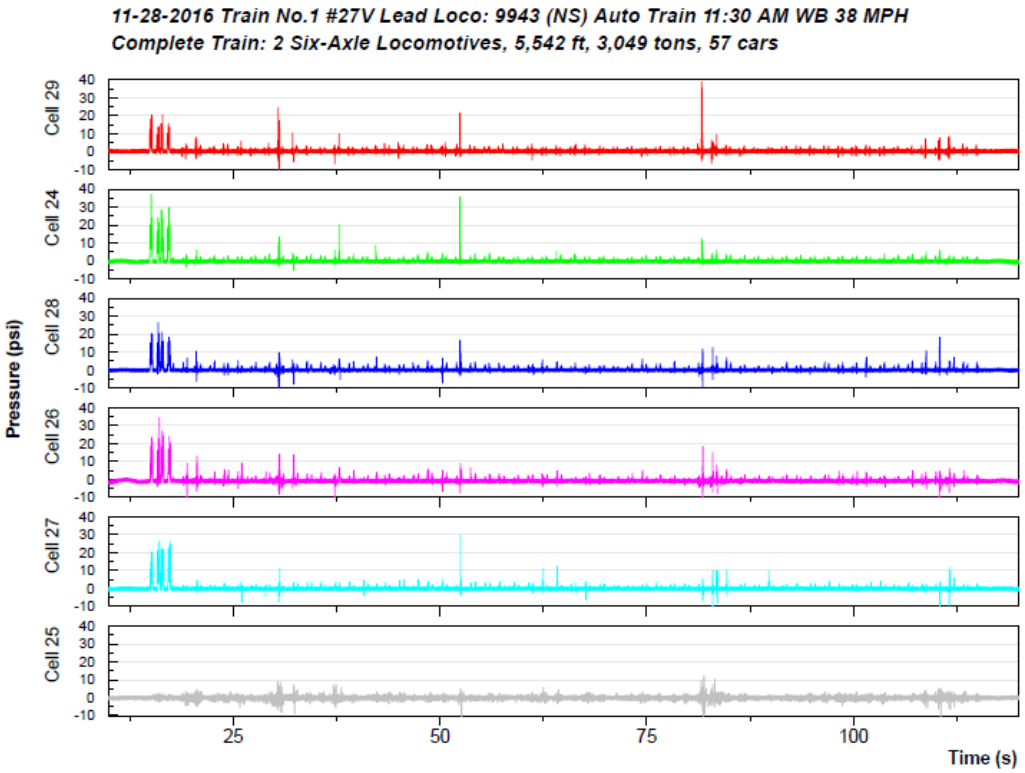

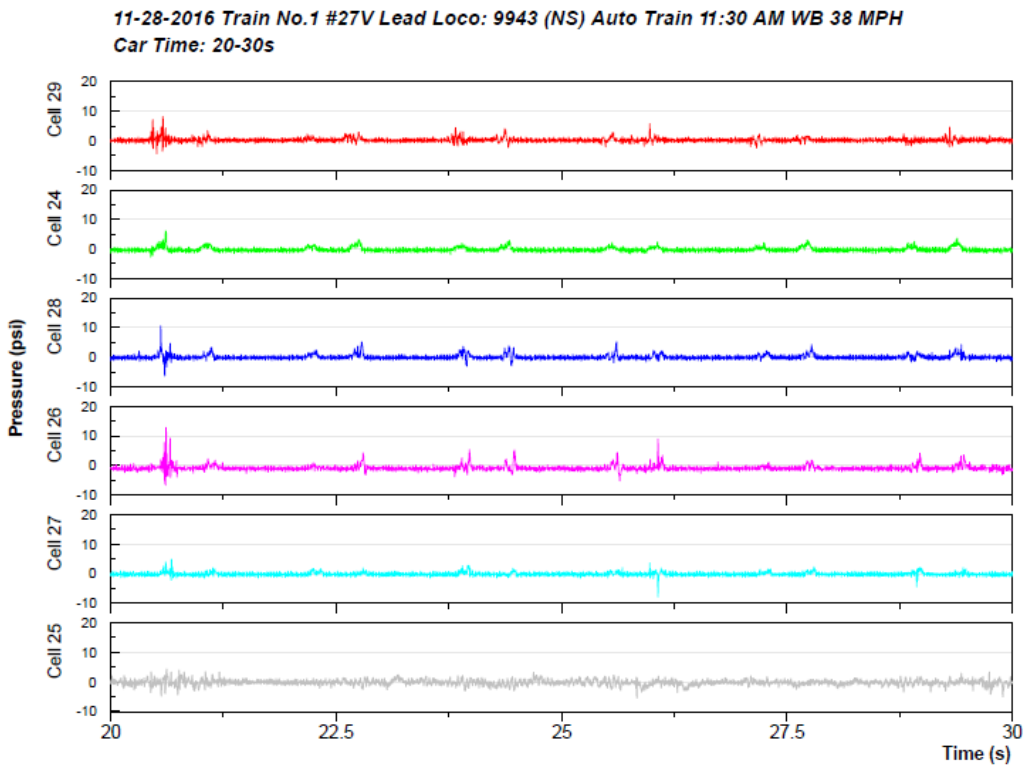

Example of a Unit Coal Train

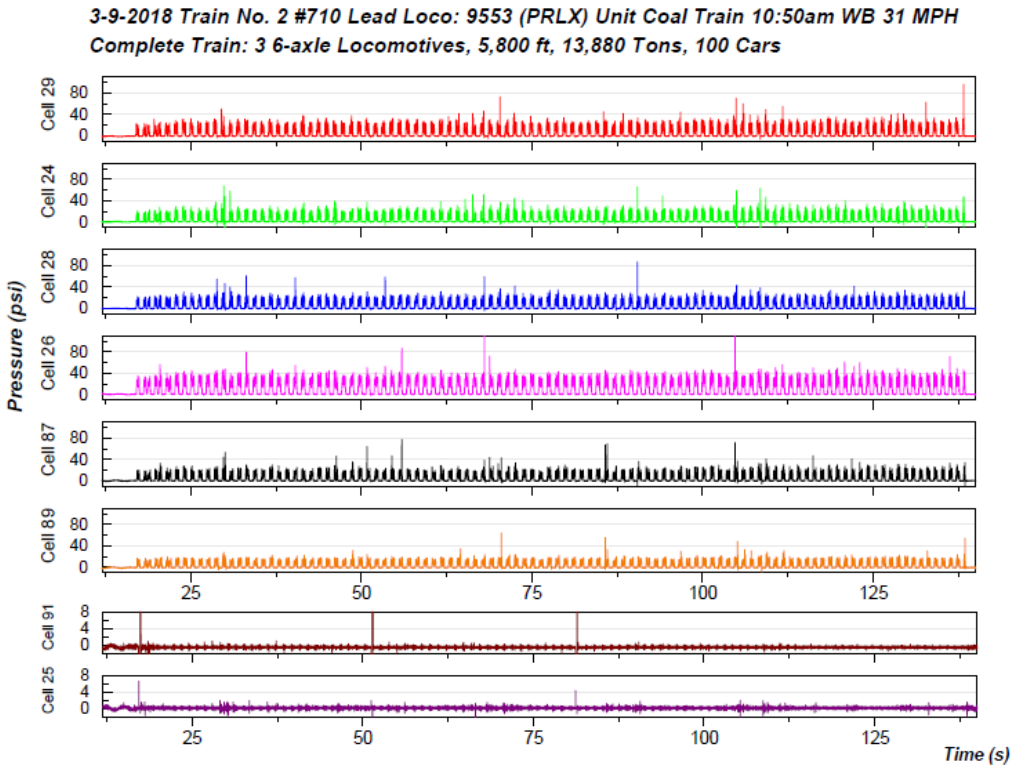

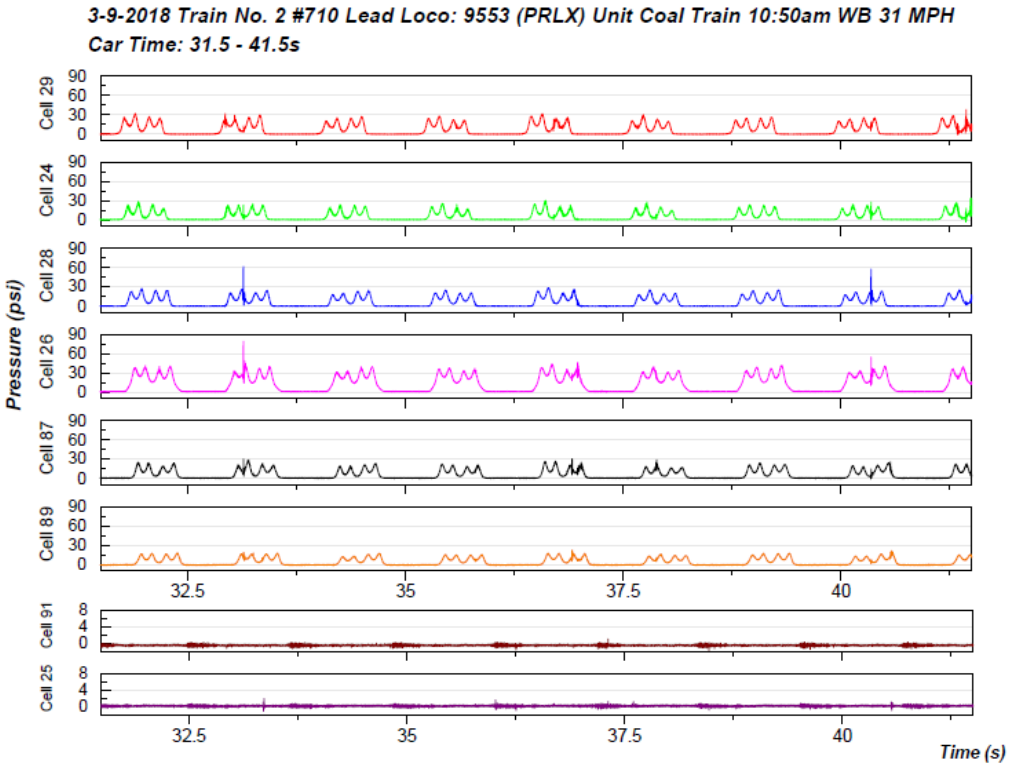

Example of an Empty Coal Train

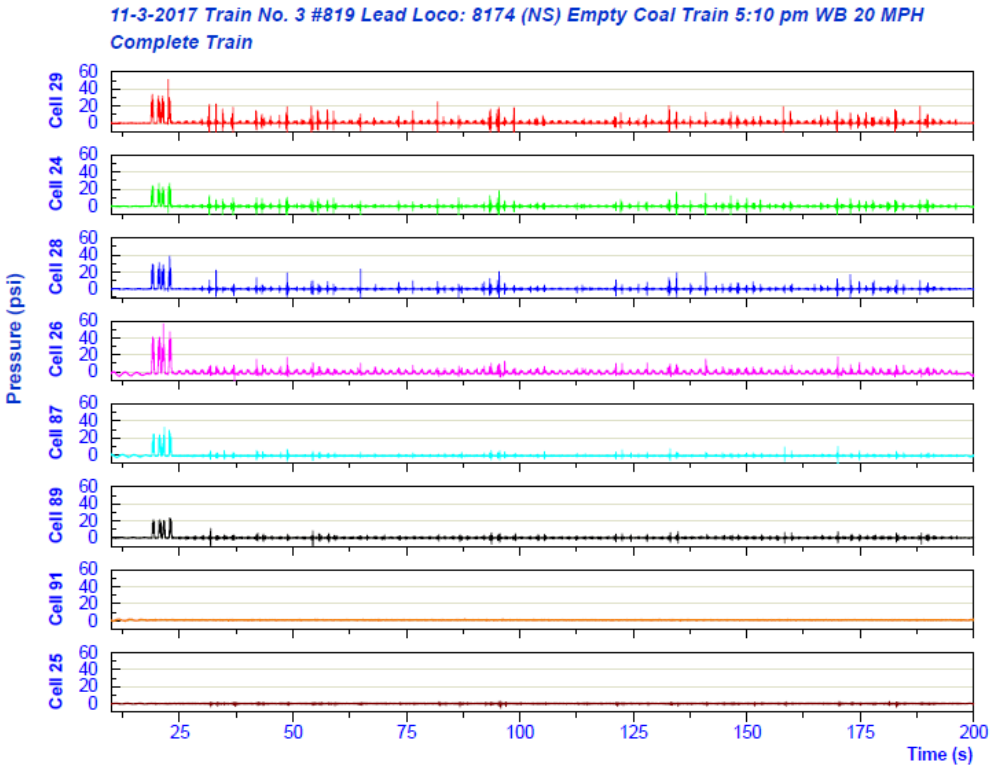

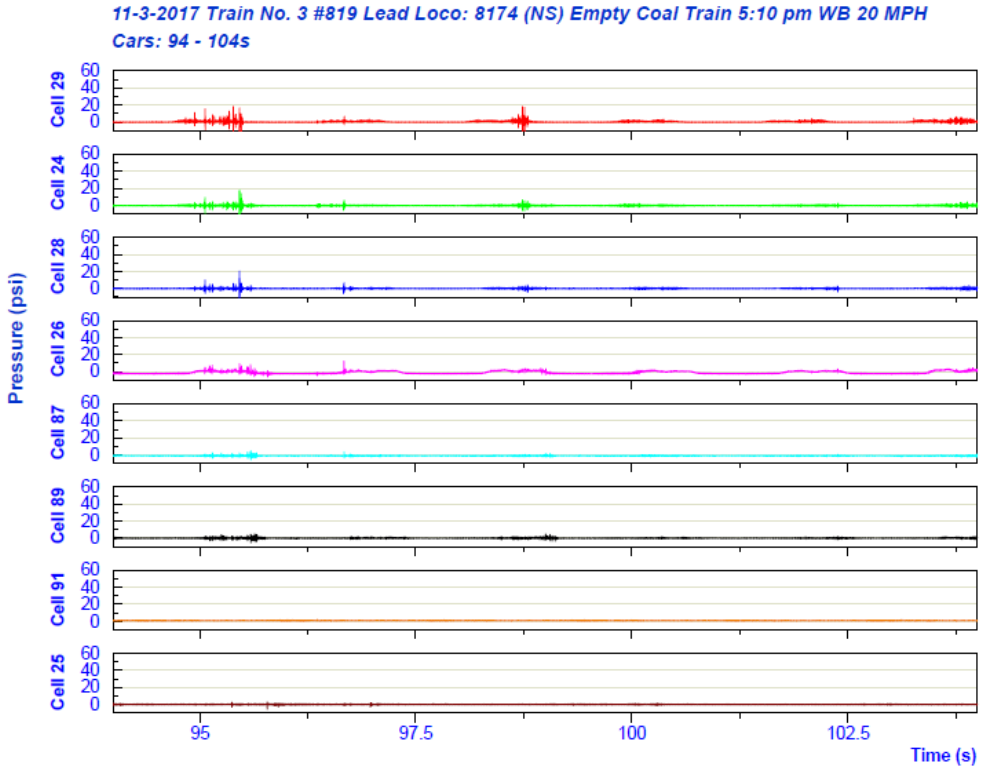

Appendix I – Nominal Tie/Ballast Pressure Modeling Script for Revenue Trains

```
%Welcome to Program Load in the pressure data. The filepath can be
%found by opening the properties of the specific file. Make sure to use
%forward slashes instead of the standard backslash.
disp('Welcome')
prompt ='Please enter train name and date ';
x=input(prompt,'s');
trainname= (x);
prompt = 'Enter the path:';
x = input(prompt,'s');
addpath(x);
Train1=xlsread(x);
disp('Please wait...')
%Define your variables. In this case, we need to define the signal of
%each pressure cell and the corresponding time domain.
c29 = Train1(:,1);  % Cell 29
c24 = Train1(:,2);  % Cell 24
c28 = Train1(:,3);  % Cell 28
c26 = Train1(:,4);  % Cell 26
c87 = Train1(:,5);  % Cell 87
c89 = Train1(:,6);  % Cell 89

% Cell 91 and Cell 25 are the 7th and 8th columns, but do not provide
% significant results to look at.
% Sample Rate is 2000/sec. Each table entry is a sample.
time = [0:length(Train1)-1]/2000;

run=1; %will run the first test
while run==1
    prompt ='Please enter Cell(c29,c24,c28,c26,c87,c89) ';
    x=input(prompt);
    cell=(x);

    % Then, if you want to plot the raw signal output, one must define a
    % new figure and call out the variables needed to be displayed.
    f1=figure;                                  % Creates a new figure

    plot(time,cell);                          % Creates the plot. Can be found in
    % a new window.
    title(trainname);                           % Add title to the figure
    xlabel('Time (s)');                       % Add x-axis label
    ylabel('Pressure (psi)');                 % Add y-axis label
    % Next, a spectrogram needs to be developed to determine the
    % appropriate filter to model the signal. The [s,f,t] function returns
    % a spectrogram at the cyclical frequencies specified in f
    % (x,window,noverlap,f,fs). In other words, a fourier trasnform is
    % performed and a heatmap is created to see the most dominant
    % frequencies.
    f2=figure
    [S,F,T] = spectrogram(cell,hamming(1024),1024-128,2048,2000);
    title(trainname);                           % Add title to the figure
    imagesc(T,F,10*log10(abs(S)));axis('xy');colorbar
```

```
    % Based on the spectrogram, the most dominant energy/frequency is seen
    % at 80 Hz. This will be the frequency used to filter the signal. Most
    % trains are between 60 and 80 Hz.
    % Develop a bandwidth filter at 80 Hz
    prompt ='Enter bandwidth(typ. between 60 Hz and 80Hz)';
    x=input(prompt);
    bandwidth=(x);
    b = fir1(512,[bandwidth/4000]);
    %Hz has to be divided by twice
    % the sample rate
    nflow = filtfilt(b,1,cell);
    % The filtfilt function passes through
    % the signal twice
    specs=0;
    size1=0;
    while specs<1
        while size1<1
            %Get Min Peak Distance
            prompt ='MinPeakDistance(Typ .1)?';
            x=input(prompt);
            MinPeakDistance= (x);

            %Get Min Peak Height
            prompt ='MinPeakHeight(Typ 1)?';
            x=input(prompt);
            MinPeakHeight= (x);

            %Get Min Peak Prominence
            prompt ='MinPeakProminence(Typ .4)?';
            x=input(prompt);
            MinPeakProminencet= (x);


            f3=figure
            plot(time,cell);

            hold on;                                    % Need to define this to↙
superimpose the
            % filtered signal
            plot(time,nflow,'r','Linewidth',1.5);   % Plot the filtered signal

            % Now, we need to mark the axle pressures

            [pv,pl] = findpeaks(nflow,2000,'MinPeakDistance',↙
MinPeakDistance,'MinPeakHeight',MinPeakHeight,'MinPeakProminence',MinPeakProminencet);

            % The function above will need to be played with for each train as
            % speed varies. Don't spend too much time on this. Typically 95% of the
            % heavy vehicles will be loacted. Only about 50-60% of the empty cars
            % do.
```

```
            plot(pl,pv,'xk','MarkerSize',10);          % Plot to see where these peaks are↙
located.

            size (pv)                                  % Check to see how many↙
peaks/axles. In this case
            % these are 134 reported. Most likely more need to be added afterwards.

            prompt ='Does number of peaks look right?(1=yes 0=no)';
            x=input(prompt);
            size1= (x);
        end
        % Define the csv to export

        % Time column for each peak
        prompt ='Please enter value(2=c29,3=c24,4=c28,5=c26,6=c87,7=c89) ';
        x=input(prompt);
        u=(x);
        [p(:,u), p(:,1)] = findpeaks(nflow,2000,'MinPeakDistance',↙
MinPeakDistance,'MinPeakHeight',MinPeakHeight,'MinPeakProminence',MinPeakProminencet);

        % Pressure Value for each peak

        [v(:,u), v(:,1)] = findpeaks(nflow,2000,'MinPeakDistance',↙
MinPeakDistance,'MinPeakHeight',MinPeakHeight,'MinPeakProminence',MinPeakProminencet);

        % Check to see you have the correct matrix dimensions
        size (v)

        prompt ='Are matrix dimension correct? Save csv file?(1=yes 0=no)';
        x=input(prompt);
        specs= (x);
    end

    % Create CSV
    prompt ='Please Name excel sheet(end with .csv or will fail) ';
    x=input(prompt,'s');
    cellname=(x);
    csvwrite(cellname,v)

    % CSV file is written in the folder you are currently working in.
    % Retrive and adjust as needed.

    prompt ='Would you like to run a different cell (1=yes 0=no)';
    x=input(prompt);
    run=(x);
end
```

Appendix J – Extended WILD/Tie-Ballast Pressure Relationships

Method 1 – Per Axle Per Pressure Cell

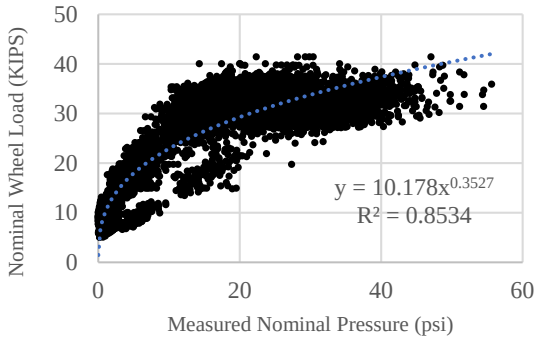

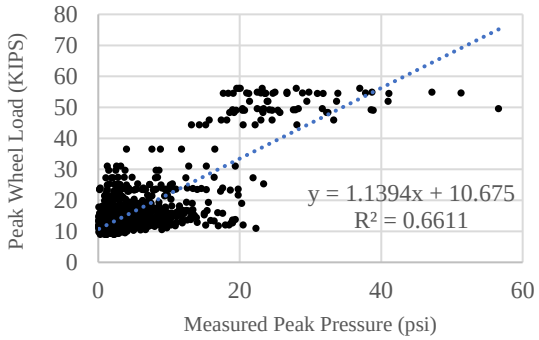

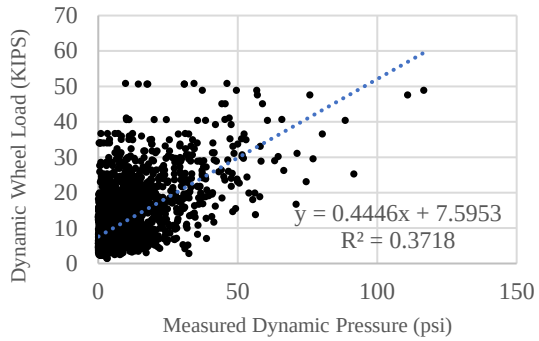

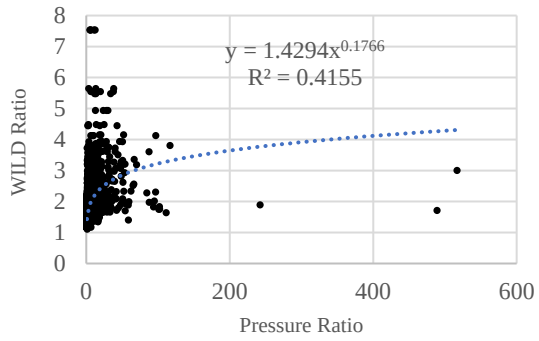

Method 2 – Average Per Car and Per Pressure Cell

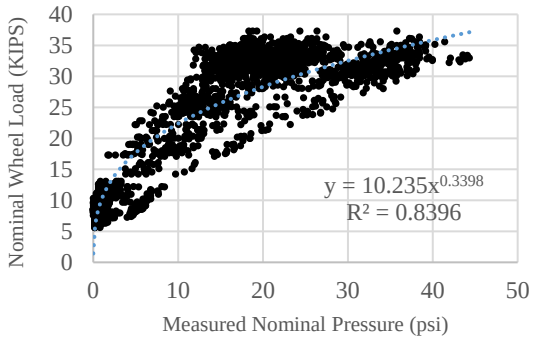

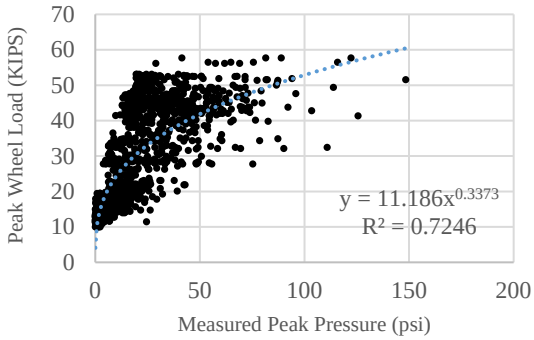

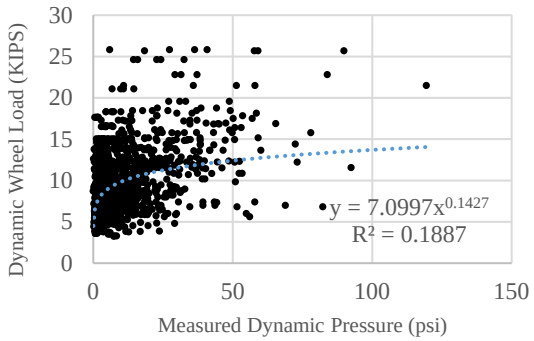

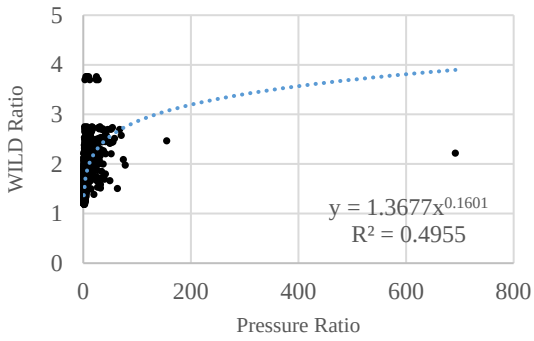

REFERENCES

Aikawa, A. (2013). Determination of Dynamic Ballast Characteristics Under Transient Impact Loading. Electronic Journal of Structural Engineering(1), 18.

Anderson, J. (2006). MSCE Thesis: Asphalt Pavement Pressure Distributions Using TEKSCAN Measurement System. Lexington: University of Kentucky.

AREMA. (2018). Manual for Railway Engineering. Lanham, Maryland: American Railway Engineering and Maintenance of Way Association.

Armstrong, J. H. (2008). The Railroad: What it is, What it Does (5th ed.). Ohmaha, NE, United States: Simmons-Boardman Books, Inc.

Askarinejad, H., Barati, P., Dhanasekar, M., & Gallage, C. (2018). Field Studies on Sleeper Deflections and Ballast Pressure in Heavy Haul Track. Australian Journal of Structural Engineering, 19(2), 96-104. doi:10.1080/13287982.2018.1444335

Atalar, C., Das, B. M., Shin, E. C., & Kim, D. H. (2001). Settlement of geogrid-reinforced railroad bed due to cyclic load. 15th International Conference on Soil Mechanics and Geotechnical Engineering, 3, pp. 2045-2048. Istanbul.

Geokon. (2017). Model 3500 Series Instruction Manual. Lebanon, NH.

Grabe, P. J., Clayton, C. R., & Shaw, F. J. (2005). Deformation Measurement on a Heavy Haul Track Formation. International Hevay Haul Association.

Hay, W. W. (1982). Railroad Engineering (2nd ed.). New York, NY: John Wiley & Sons.

Heath, D. L., Shenton, M. J., Sparrow, R. W., & Waters, J. M. (1972). Design of Conventional Rail Track Foundations. Institute of Civil Engineering, (pp. 251-267).

Indraratna, B. (2011). Advanced Rail Geotechnology - Ballasted Track. London: Taylor & Francis Group.

Indraratna, B., & Ngo, T. (2018). Ballast Railroad Design: SMART-UOW Approach. London: CRC Press: Taylor & Francis Group.

Indraratna, B., Nimbalkar, S., Christie, D., Rujikiatkamjorn, C., & Vinod, J. (2010). Field Assessment of the Performance of Ballasted Rail Track with and without Geosynthetics. Journal of Geotechnical and Environmental Engineering, 136(7), 907-917.

Kerr, A. (2003). Fundamentals of Railway Track Engineering. Omaha, NE: Simmons-Boardman Books, Inc.

Lamas-Lopez, F., Cui, Y.-J., Calon, N., Costa, S., De Oliverira, M. P., & Zhang, T. (2016). Track-bed Mechanical Behavior Under the Impact of Train at Different Speeds. Soils and Foundations: The Japanese Geotechnical Society.

Lampo, R. (2014). Summary of Current State of Practice for Composite Crossties. International Crosstie and Fastening System Symposium. Urbana, UL: United States Army Corps of Engineers.

LB Foster - Salient Systems. (2018). WILD Product Sheet. Pittsburgh, PA. Retrieved from http://www.lbfoster-salientsystems.com/pdf/LBF_Wild_Product_sheet_LOWRES.pdf

Li, D., & Selig, E. T. (1998). Method for Railroad Track Foundation Design I: Development & II: Applications. Journal of Geotechnical Engineering, ASCE, 124(4), 316-322; 323-329.

Li, D., Hyslip, J., Sussmann, T., & Chrismer, S. (2016). Railway Geotechnics. Boca Raton, FL: CRC Press: Taylor & Francis Group.

Liu, Q., Lei, X., Rose, J. G., & Purcell, M. L. (2017). Pressure Measurements at the Tie-Ballast Interface in Railroad Tracks Using Granular Material Pressure Cells. Joint Rail Conference. Philadelphia, PA.

McHenry, M. T. (2013). MSCE Thesis: Pressure Measurement at the Ballast-Tie Interface of Railroad Track Using Matrix Based Tactile Sensors. Lexington, KY: University of Kentucky.

McHenry, M. T., & Rose, J. G. (2012). KTC-12-02/FR 136-04-6F: Railroad Subgrade Support and Performance Indicators - A Review of Available Laboratory and In-Situ Testing Methods. Lexington, KY: Kentucky Transportation Center.

McHenry, M. T., Brown, M., LoPresti, J., Rose, J. G., & Souleyrette, R. (2015). Use of Matrix-Based Tactile Surface Sensors to Asses Fine-Scale Ballast-Tie Interface Pressure Distribution in Railroad Track. Transportation Research Record.

Mundrey, J. S. (2017). Railway Track Engineering (5 ed.). Alapakkam: McGraw Hill Education (India).

Purcell, M. L. (2017). MSCE Research Report: Measurement of In-Situ Track Pressures at the Ballast-Tie Interface Under Service Loads. Lexington: Unpublished.

Raymond, G. P. (1978). Design for Railroad Ballast and Subgrade Support. Journal of the Geotechnical Enginering Division, ASCE, 104(GT1), 45-49.

REB. (2000). Basic Principles of Track Maintenance. Omaha, Nebraska: Railway Education Bureau.

Rose, J. G., & Stith, J. C. (2004). TEKSCAN Sensors - Rail/Sleeper Interface Pressure Measurements in Railway Trackbeds. Railway Engineering. London.

Rose, J. G., Clarke, D. B., Liu, Q., & Watts, T. J. (2018). Application of Granular Material Pressure Cells to Measure Railroad Track Tie/Ballast Interfacial Pressures. Transportation Research Record(2671), 10.

Rose, J. G., Purcell, M. L., & Liu, Q. (2016). Suitability of Earth and Granular Materials Pressure Cells for Measuring Railway Trackbed Tie/Ballast Interfacial Pressures. Joint Rail Conference. Columbia, SC.

Rose, J. G., Souleyrette, R. R., McHenry, M., Greenwell, T., Peng, X., Brown, M., & LoPresti, J. (2015). Tie-Ballast Interaction. National University Rail Center.

Sadeghi, J. M. (2008). Experimental Evaluation of Accuracy of Current Practices in Analysis and Design of Railway Track Sleepers. Canadian Journal of Civil Engineering, 35, 881-893.

Salem, M. T. (1966). PhD Dissertation: Vertical Pressure Distribution in the Ballast Section and on the Subgrade Beneath Statically Loaded Ties. Urbana: University of Illinois.

Selig, E., & Waters, J. (1994). Track Geotechnology and Substruture Management. London: Thomas Telford Publications.

Shenton, M. J. (1975). Deformation of railway ballast under repeated loading conditions. Symposium held at Princeton University (pp. 387-404). In Kerr: Railroad Track Mechanics and Technology.

Stith, J. C. (2005). MSCE Thesis: Railroad Track Pressure Measurements at the Rail/Tie Interface Using TEKSCAN Sensors. Lexington: University of Kentucky.

Talbot, A. (1940). Stresses in Railroad Track - The Talbot Reports. Washington, D.C.: American Railway Engineering Association.

US Army Corps of Engineers. (2000). TI 850-02: Railroad Design and Rehabilitation. Washington.

Van Dyk, B. J., Dersch, M. S., Edwards, J. R., Ruppert, C. J., & Barkan, C. P. (2014). Load Characterization Techniques and Overview of Loading Enviornment in North America. Transportation Research Record: Journal of the Transportation Research Board, No. 2448, 80-86.

Walker, L. (2002). MSCE Thesis: Evaluations of Hot-Mix Asphalt Underlayments in Railroad/Highway At-Grade Crossings. Lexington: University of Kentucky.

Weather Underground. (2018). Historical Weather. Retrieved from https://www.wunderground.com/history

Wiley, R., & Elsaleiby, A. (2011, March). TD-11-007: A Review of Wheel Impact Measurement Variation. Technology Digest.

Wiley, R., & Elsaleiby, A. (2012, June). TD-12-2012: Industry-wide Wheel Impact Measurement Variation. Technology Digest.

VITA

Travis James Watts was born in Lexington, Kentucky. His parents are James and Saundra Watts. His elementary and secondary education was completed in Nicholasville, Kentucky. Upon graduating from East Jessamine High School in May of 2013, he enrolled at the University of Kentucky that fall where he received a Bachelor of Science Degree in Civil Engineering in May of 2017. He began work on his Master's Degree in Civil Engineering in the Fall of 2017, selecting the thesis MSCE program option. Portions of this thesis have been co-authored by Travis as Development of a Laboratory Test Method for Measuring Trackbed Pressure at the Tie/Ballast Interface in the Proceedings of the Transportation Research Board – 2018 Annual Meeting Online and Application of Granular Material Pressure Cells to Measure Railroad Track Tie/Ballast Interfacial Pressures in the 2018 Transportation Research Record: Journal of TRB. He has also co-authored Relationships Between Wheel/Rail Surface Impact Loadings and Correspondingly Transmitted Tie/Ballast Impact Pressures for Revenue Train Operations in the Proceedings of the 2018 Joint Rail Conference. Additionally, he has co-authored three National University Rail Center (NURail) reports containing portions of this thesis. As of November of 2018, Travis has also co-authored In-Track Crosstie/Ballast Interfacial Pressure Measurements and Comparisons with WILD Measurements, which will be included in the Proceedings of the Transportation Research Board – 2019 Annual Meeting Online and In-Track Measurements of Crosstie-Ballast Interfacial Pressure Magnitudes and Distributions with Varying Train Operational Conditions, which will be included in the Proceedings of the 2019 ASCE Transportation and Development Conference. As a testament to the work Travis has completed in his time as a Master's Student at the University of Kentucky, he

was also named the National University Rail Center's Student of the Year for the year 2018. This honor will be presented to him at the 2019 Transportation Research Board Annual Meeting in Washington, D.C.